

# REVIEW OF MESOSPHERIC TEMPERATURE TRENDS

G. Beig,<sup>1</sup> P. Keckhut,<sup>2</sup> R. P. Lowe,<sup>3</sup> R. G. Roble,<sup>4</sup> M. G. Mlynczak,<sup>5</sup> J. Scheer,<sup>6</sup> V. I. Fomichev,<sup>7</sup> D. Offermann,<sup>8</sup> W. J. R. French,<sup>9</sup> M. G. Shepherd,<sup>10</sup> A. I. Semenov,<sup>11</sup> E. E. Remsberg,<sup>12</sup> C. Y. She,<sup>13</sup> F. J. Lübken,<sup>14</sup> J. Bremer,<sup>14</sup> B. R. Clemesha,<sup>15</sup> J. Stegman,<sup>16</sup> F. Sigernes,<sup>17</sup> and S. Fadnavis<sup>1</sup>

Received 30 October 2002; revised 9 May 2003; accepted 14 July 2003; published 22 October 2003.

[1] In recent times it has become increasingly clear that releases of trace gases from human activity have a potential for causing change in the upper atmosphere. However, our knowledge of systematic changes and trends in the temperature of the mesosphere and lower thermosphere is relatively limited compared to the Earth's lower atmosphere, and not much effort has been made to synthesize these results so far. In this article, a comprehensive review of long-term trends in the temperature of the region from 50 to 100 km is made on the basis of the available up-to-date understanding of measurements and model calculations. An objective evaluation of the available data sets is attempted, and important uncertainly factors are discussed. Some natural variability factors, which are likely to play a role in modulating temperature trends, are also briefly touched upon. There are a growing number of experimental results centered on, or consistent with, zero temperature trend in the mesopause region (80–100 km). The most reliable data sets show no significant trend but an uncertainty of at least 2 K/decade. On the other hand, a majority of studies indicate negative trends in the lower and middle mesosphere with an amplitude of a few degrees (2–3 K) per decade. In tropical latitudes

the cooling trend increases in the upper mesosphere. The most recent general circulation models indicate increased cooling closer to both poles in the middle mesosphere and a decrease in cooling toward the summer pole in the upper mesosphere. Quantitatively, the simulated cooling trend in the middle mesosphere produced only by CO<sub>2</sub> increase is usually below the observed level. However, including other greenhouse gases and taking into account a “thermal shrinking” of the upper atmosphere result in a cooling of a few degrees per decade. This is close to the lower limit of the observed nonzero trends. In the mesopause region, recent model simulations produce trends, usually below 1 K/decade, that appear to be consistent with most observations in this region. *INDEX TERMS*: 1610 Global Change: Atmosphere (0315, 0325); 1630 Global Change: Impact phenomena; 0350 Atmospheric Composition and Structure: Pressure, density, and temperature; 0342 Atmospheric Composition and Structure: Middle atmosphere–energy deposition; 0325 Atmospheric Composition and Structure: Evolution of the atmosphere; *KEYWORDS*: temperature trends, thermal shrinking, mesosphere, greenhouse gases

*Citation*: Beig, G., et al., Review of mesospheric temperature trends, *Rev. Geophys.*, 41(4), 1015, doi:10.1029/2002RG000121, 2003.

## 1. INTRODUCTION

[2] The detection of global change signals in the upper part of the atmosphere (above the stratopause) is a

topic of current interest. At the end of the 1980s it became obvious that systematic variations of lower atmospheric properties should be accompanied by associ-

<sup>1</sup>Indian Institute of Tropical Meteorology, Pune, India.

<sup>2</sup>Service d'Aeronomie, Institut Pierre Simon Laplace, Verrieres-Le-Buisson, France.

<sup>3</sup>Centre for Research in Earth and Space Technology, University of Western Ontario, London, Ontario, Canada.

<sup>4</sup>High Altitude Observatory, National Center for Atmospheric Research, Boulder, Colorado, USA.

<sup>5</sup>Radiation and Aerosol Branch, NASA Langley Research Center, Hampton, Virginia, USA.

<sup>6</sup>Instituto de Astronomia y Fisica del Espacio, Ciudad Universitaria, Buenos Aires, Argentina.

<sup>7</sup>Department of Earth and Atmospheric Science, York University, Toronto, Ontario, Canada.

<sup>8</sup>Physics Department, University of Wuppertal, Wuppertal, Germany.

<sup>9</sup>Atmospheric and Space Physics Group, Australian Antarctic Division, Tasmania, Australia.

<sup>10</sup>Centre for Research in Earth and Space Science, York University, Toronto, Ontario, Canada.

<sup>11</sup>Obukhov Institute of Atmospheric Physics, Russian Academy of Science, Moscow, Russia.

<sup>12</sup>Atmospheric Sciences Research, NASA Langley Research Center, Hampton, Virginia, USA.

<sup>13</sup>Physics Department, Colorado State University, Fort Collins, Colorado, USA.

<sup>14</sup>Leibniz-Institute of Atmospheric Physics, K hlungborn, Germany.

<sup>15</sup>Instituto Nacional de Pesquisas Espaciais, Sao Jose dos Campos, Brazil.

<sup>16</sup>Meteorologiska Institutionen, Stockholms Universitet, Stockholm, Sweden.

<sup>17</sup>University Courses on Svalbard, Longyearbyen, Norway.

ated variations in the upper regions, the mesosphere and thermosphere. Unlike the lower atmosphere, there are not many routine measurements in the mesosphere, since they are considered to be of no value in operational weather forecasting. However, during the last decade, there has been an ever growing impetus for temperature trend investigations in this region, now that it has been established that the secular increases in greenhouse gases at the ground should have a substantial impact on the radiative-chemical-dynamical equilibrium of the middle atmosphere.

[3] The analysis of systematic changes in temperature in the mesosphere and lower thermosphere has not been as comprehensive as in the lower atmosphere. The stratospheric temperature trend is now better understood, and a comprehensive review of trends based on the stratospheric temperature trend assessment has been published by *Ramaswamy et al.* [2001]. The limited availability of data sets and the comparatively short length of data records have been the major constraints for mesospheric trend analysis. Nevertheless, during the past decade a number of studies have been carried out, and possible long-term trends in mesospheric temperatures have been reported. Most of these studies have attributed these trends to anthropogenic forcing from the ground. If sustained, the observed apparent changes in temperature and the resulting hydrostatic contraction could have future consequences for the ionosphere, atmospheric drag on space vehicles, and possibly effects on lower atmospheric climate.

[4] This review concentrates on long-term changes of temperature in the 50- to 100-km region based on the published results. We discuss the lower thermosphere only as an upper boundary rather than in its own right. For convenience, the whole region from 50 to 100 km is referred to as the mesosphere and lower thermosphere (MLT) region. The region from 50 to 80 km will be referred to as the “mesosphere,” and the region from 80 to 100 km will be referred to as the “mesopause region.” In addition, parts of the mesosphere are referred to as the “lower mesosphere” (50–70 km) and the “upper mesosphere” (70–80 km).

[5] We should make clear the definition of “long-term trend” that is used here. Earlier model predictions of greenhouse cooling led one to believe that the atmosphere should cool slowly, as the greenhouse gases build up. Thus a monotonic decline in temperature would be expected with a more or less linear trend over a period of time. However, as we will discuss in section 5, the trend itself appears to be variable in the MLT region. It has been common practice to analyze the data with a term that varies monotonically with time. The linear regression coefficient is what is referred to as “long-term trend.” All the data, which span a decade or the length of a solar cycle, are considered eligible for trend detection in this review and are discussed.

[6] In the past a number of authors have discussed global change and temperature in relation to observa-

tions or models [e.g., *Roble*, 1995; *Thomas*, 1996; *Golitsyn et al.*, 1996; *Danilov*, 1997]. A brief status report of observational and model results for temperature trends in this region was presented recently by several authors [e.g., *Chanin*, 1993; *Danilov*, 1997; *Akmaev and Fomichev*, 1998; *Beig*, 2000a, 2000b; *Beig*, 2002]. The results reported by individual groups so far indicated no cooling to strong cooling trends in mesospheric temperatures during the past few decades in annual mean temperature data. The initial results of *Clancy and Rusch* [1989], based on the SME satellite data, indicated two extreme ranges of heating and cooling in the mesosphere. These conclusions are, however, not significant for decadal timescales, as they were based on very short series of data. The first trend results based on a sufficiently long series of rocketsonde measurements were reported from Russia [*Kokin et al.*, 1990; *Kokin and Lysenko*, 1994] and revealed moderate to strong cooling trends (up to  $\sim 10$  K/decade) for the mesosphere. *Taubenheim et al.* [1990, 1997], *Bremer* [1997, 1998], *Gadsden* [1990, 1997, 1998], and *Serafimov and Serafimova* [1992] have reported a possible cooling in the ionosphere based on analyses of the long base of ionospheric observations. These ionospheric data provide rough estimates corresponding to a broad altitude range, and most authors derived a negative trend for this region. *Lastovicka* [1994] has inferred long-term trends in planetary wave activity from radio wave absorption data. Results reported by *Lübken* [2000, 2001] for mesospheric temperature, using rocket grenade and falling sphere data, report no discernable trend during summer. A number of papers dealing with long-term changes and trends in MLT temperature have recently been published in a special issue of the journal *Physics and Chemistry of the Earth* (“Long Term Changes in the Atmosphere,” 2002). A detailed analysis of all these results indicates that trends may vary with latitude. This requires additional study and is addressed further in this review.

[7] A prerequisite for trend study is a detailed knowledge of the variations due to natural sources [*World Meteorological Organization (WMO)*, 1995, 1999]. Natural variations arising on decadal and longer timescales may also play a significant role in long-term trend calculations. One of the major sources of decadal natural variations in the atmosphere is the 11-year solar activity cycle [e.g., *Brasseur and Solomon*, 1986]. There are several theoretical [*Brasseur*, 1993; *Wuebbles et al.*, 1991] and observational [*Hood et al.*, 1991; *Hood*, 1997] studies that suggest that periodic changes during the solar cycle should affect the chemical composition and thermal structure of the middle atmosphere. The solar cycle influence on temperature is a major factor that may hamper trend detection if not filtered properly [*Beig*, 2002]. There is a well-known discrepancy between theoretical and observed solar variability effects on temperature. Hence it is essential to address such natural causes while discussing long-term trends, which is attempted in this article.

[8] Until recently, no attempt has been made to synthesize trend results or discuss rigorously the status of mesospheric temperature trends in an organized manner. The main reason for this is that the reported results were so diverse and mutually inconsistent. In 1998 an international workshop held in Moscow on cooling and sinking of the middle atmosphere was dedicated to this aim. In 1999 the first international workshop “Long-term Changes and Trends in the Atmosphere (LT-ACT’99)” was held at Pune, India, with the aim of considering the issue of mesospheric temperature trends in detail. Partly as a result of LT-ACT’99, the debate on global change signals in the upper part of the atmosphere has intensified. Subsequently, the International Association of Geomagnetism and Aeronomy (IAGA), an association of the International Union of Geodesy and Geophysics, has taken the initiative in forming a working group, in 1999, under the auspices of IAGA, the International Commission for Middle Atmosphere, and the Planetary Scale Mesopause Observing System, a project of the Scientific Committee on Solar-Terrestrial Physics. This working group has constituted the Mesospheric Temperature Trend Assessment (MTTA) panel, with the objective of dealing with issues related to mesospheric temperature trends. It was decided that the first step for the MTTA would be to make available a consolidated review of mesospheric temperature trends, with a view to outlining the current status by synthesizing all the published results for both observations and modeling. Another intention was to assess similarities and differences in the various data sets and to identify issues to be taken up as the next step in MTTA activities. This review paper is based on the MTTA report that attempted to achieve the first objective.

[9] We start with our present understanding of the different processes concerning mesospheric temperature variations in section 2. The brief description of each technique for the measurement of MLT temperature and the uncertainties associated with each technique are discussed in section 3. Details of all data sets and analysis methods are also included. In section 4 we will briefly discuss all those natural and episodic factors of variability like solar influences, volcanic effects, tidal effects, the quasi-biennial oscillation (QBO), the El Niño–Southern Oscillation (ENSO), etc., which are capable of affecting the correct detection of long-term temperature trends. The core of the paper is contained in section 5, where observed long-term trends in the MLT region are discussed. In addition to the zonal annual mean, seasonal and regional trends we also discuss short-term differences and fluctuations. Section 6 gives details of the results of temperature trend model simulations. Simulations of the past few decades and of doubled- $\text{CO}_2$  scenarios are discussed. This section also includes results from a few recent global models for evaluating global change. Wherever possible, discussion and possible interpretation of the observed results are also briefly included. An attempt has also been made to understand the similarities

and differences in various results based on physical processes. A brief summary of observed and model results and principal conclusions on MLT temperature trends will be given in section 7. Finally, an outlook on future directions of research is presented (section 8).

## 2. MESOSPHERIC ENERGY BALANCE: CURRENT ASSESSMENT

[10] The energy budget of the terrestrial mesosphere is a frontier of research in the atmospheric sciences. A fundamental difference between the mesospheric energy budget and that in the lower atmospheric regions is the primary mesospheric heating and cooling mechanisms that involve processes far removed from local thermodynamic equilibrium (LTE). The factors contributing to energy balance have been studied extensively beginning with *Murgatroyd and Goody* [1958] who made the first computation of the mesospheric energy balance and considered nonlocal thermodynamic equilibrium (non-LTE) effects in their computation of radiative cooling by carbon dioxide. They also recognized the importance of chemical potential energy and exothermic chemical reactions as sources of heat and purposely limited the altitude range of their calculation to below 90 km to avoid large errors in the computed heating rates. Shortly thereafter, *Kellog* [1961] postulated that the warm winter mesopause was at least partially maintained by energy release from exothermic reactions involving atomic oxygen transported from the thermosphere. *Hines* [1965] discussed the role of viscous dissipation of internal gravity waves in the energy balance. *Shved* [1972] discussed the role of airglow in reducing the amount of energy available for heat in solar energy deposition and exothermic reactions. These pioneering studies provided the direction for our contemporary understanding of the heat balance of the mesosphere.

[11] In the past decade, there has been great advancement in the knowledge of many of these processes. For example, we currently believe that exothermic chemical reactions generate more heat in the upper mesosphere than is provided directly by solar radiation [*Mlynczak and Solomon*, 1993]. We also believe that radiative emission and cooling by carbon dioxide ( $\text{CO}_2$ ) is governed primarily by collisional energy transfer from atomic oxygen [*Rodgers et al.*, 1992] and that the  $\text{CO}_2$  molecule is a variable species in the upper mesosphere [*Lopez-Puertas and Taylor*, 1989]. Airglow has been shown to significantly reduce the efficiencies of both solar heating and exothermic reactions [*Mlynczak and Solomon*, 1993]. Dynamical processes including gravity waves and turbulence are clearly important for the heat budget of the upper atmosphere [*Ebel*, 1984; *Lübken*, 1997]. Because of the non-LTE nature of the radiative heating and cooling and chemical heating processes, meticulous and accurate laboratory measurements of the rates of non-LTE energy transfer processes are also required before we can model the mesosphere with certainty.

[12] To date, there is no data set from which the mesospheric energy budget can be confidently derived on a global basis, and thus we know very little concerning the relative importance of the various sources and sinks of energy and their overall role in determining the structure and variability of the mesosphere. We do not even know basic properties, such as, if the mesosphere is in global mean radiative equilibrium on monthly to seasonal timescales, as is the stratosphere [Mlynczak et al., 1999]. However, the major radiative, chemical, and dynamical processes that govern the energy balance in the mesosphere are thought to be well known. Analysis of the energy budget produced by the extended Canadian Middle Atmosphere Model (CMAM) [Fomichev et al., 2002] revealed radiative processes to be dominant throughout the middle and upper atmosphere. Fomichev et al. found two atmospheric regions where the energy balance is relatively simple. The first lies in the altitude region between the tropopause and 70 km, where the atmosphere is close to radiative equilibrium on a monthly and globally averaged basis. The second region lies above 130 km in the thermosphere. Here the strong extreme ultraviolet solar heating is primarily balanced by molecular diffusion. The pattern is considerably more complicated in the mesosphere and lower thermosphere region between 70 and 120 km. Although radiative processes still dominate here, other mechanisms, such as dynamical and chemical heating, provide a substantial contribution to the energy budget. However, it should be noted that any model estimations inherit some limitations and our knowledge of atmospheric processes should always be tested by observations. It is anticipated that the recently launched Thermosphere-Ionosphere-Mesosphere Energetics and Dynamics (TIMED) Mission, and the significant ground-based program that accompanies it, will provide this essential understanding of the energy budget of this critical region of Earth's atmosphere.

## 2.1. Principles of Energy Conservation in the Mesosphere

[13] In order to evaluate the energy balance in the mesosphere we must consider input of solar and terrestrial radiation, input of energy associated with dynamical phenomena, output of energy in the form of infrared and airglow emission, storage of energy in latent chemical form, conversion of energy, and energy transport. These processes are not new or different, especially the radiative phenomena, and are considered in almost any study of atmospheric energetics.

[14] Shown in Figure 1 is a diagram indicating the major flows of energy in the mesosphere. Solar energy (primarily electromagnetic radiation, but particle inputs cannot be totally neglected in the upper mesosphere) is absorbed by  $O_2$ ,  $O_3$ , and  $CO_2$ . The wavelengths that are absorbed range from the ultraviolet Lyman  $\alpha$  at 121.5 nm absorbed by  $O_2$  to the mid infrared at 4.3  $\mu m$  absorbed by  $CO_2$ . Listed in Table 1 are the primary

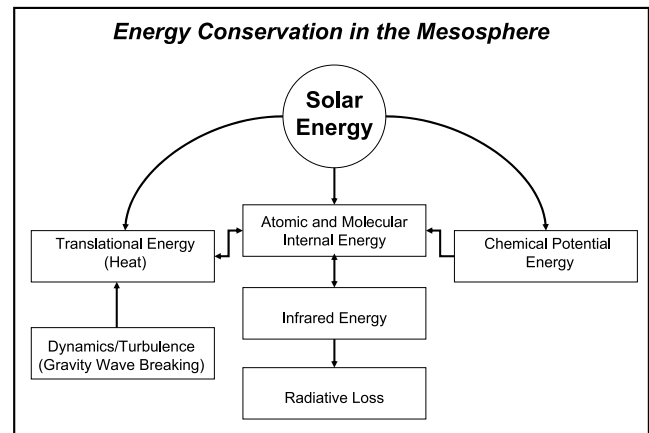


Figure 1. Energy conservation in the mesosphere

absorption features relevant to solar radiative energy inputs in the mesosphere.

[15] As indicated in Figure 1, absorbed solar energy may be initially apportioned into three pools: translational energy (heat), internal energy of electronically or vibrationally excited photolysis product species, and chemical potential energy. The latter is defined as the solar energy used to break chemical bonds and thus dissociate the absorbing species. Listed in Table 2 are the fractions of absorbed energy apportioned to each of the three pools immediately upon photolysis of ozone and molecular oxygen.

[16] For the main absorption bands of  $O_3$  and  $O_2$  in the mesosphere most energy initially shows up as chemical potential energy or internal energy and not as heat. Consequently, the heating rate primarily depends on the disposition of the energy in the chemical and internal energy pools. The chemical potential energy, primarily carried by atomic oxygen, may not be realized until quite some time after the original photon deposition because of the long chemical lifetime of O above  $\sim 75$  km, allowing for significant transport of energy to occur through atomic oxygen transport. An evaluation of the energy balance in the mesosphere must account explicitly for the production, transport, and conversion of chemical energy.

Table 1. Primary Absorbers, Features, and Wavelength Ranges of Solar Radiation Absorption in the Mesosphere

Absorber	Feature	Wavelength Range
$O_3$	Hartley band	203–305 nm
	Huggins band	305–397 nm
	Chappuis band	397–850 nm
$O_2$	Schumann-Runge continuum	130–175 nm
	Schumann-Runge bands	175–200 nm
	Herzberg continuum	200–240 nm
	Lyman $\alpha$	121.5 nm
$CO_2$	atmospheric band	762 nm
	middle infrared bands	2.0, 2.7, and 4.3 $\mu m$

**Table 2. Initial Disposition of Energy Absorbed by Ozone and Molecular Oxygen**

	Heat, %	Chemical Potential, %	Internal Energy, %
<i>Ozone</i>			
Hartley band	13	24	63
Huggins band	76	24	0
Chappuis band	76	24	0
<i>Oxygen</i>			
Schumann-Runge continuum	1	72	27
Schumann-Runge band	24	76	0
Lyman $\alpha$	30	50	20

[17] The energy in the internal energy pool has essentially two fates. It may be physically quenched to heat through collisions, or it may be radiated in the form of airglow emission, primarily from  $O_2(^1\Delta)$  and  $O_2(^1\Sigma)$ , and also  $CO_2$  at 4.3  $\mu\text{m}$ . This emission significantly reduces the amount of energy available for heat thus giving a heating efficiency substantially less than 1.0. In addition, exothermic reactions and recombination may form excited product species (such as  $OH(v)$ ), which may radiate some of the original chemical potential energy before it is physically quenched to heat, thus reducing the chemical heating efficiency. Detailed models of production and loss of excited product species are required to accurately assess the heating due to solar and chemical processes. A complete description of the deposition and conversion of solar (and chemical) energy to heat and radiation is given by *Mlynczak and Solomon* [1993].

[18] Radiative cooling in the mesosphere is driven primarily by non-LTE processes in the carbon dioxide molecule. Often the process of radiative cooling involves the consideration of complex radiative exchange between atmospheric layers, as indicated by the vertical double arrow in Figure 1. Cooling by ozone (9.6  $\mu\text{m}$ ) and water vapor (6.3  $\mu\text{m}$  vibration-rotation bands and the far infrared rotational bands) is important in the lower mesosphere. In the lower thermosphere the cooling eventually transitions from  $CO_2$ -dominated to that dominated by the NO molecule in the vibration-rotation bands at 5.3  $\mu\text{m}$ . Note that the fine structure lines of atomic oxygen in the far-infrared bands are also important in lower thermospheric cooling. With the exception of the far-infrared  $H_2O$  and possibly the atomic oxygen lines, non-LTE occurs and must be considered in evaluating the cooling rates.

## 2.2. Current Assessment of Mesospheric Heat Balance

[19] In this section we will review the status of knowledge of the major energy budget terms. For more detail, see *Mlynczak* [2000] for calculations of many of the processes that are based on observations made by the

SME experiment that observed temperatures and airglow emissions in the mesosphere in the 1980s.

### 2.2.1. Solar Heating Rates

[20] The computation of solar heating rates requires knowledge of the solar irradiance, the absorber amount, and the absorption cross section for each absorber as a function of wavelength. As indicated in Table 1, the primary absorbers in the mesosphere are ozone, molecular oxygen, and carbon dioxide. Typically, absorption of ultraviolet radiation by ozone and molecular oxygen has always been considered. However, absorption in the near and mid infrared by  $O_2$  (762 nm) and  $CO_2$  (2.0, 2.7, and 4.3  $\mu\text{m}$ ) cannot be neglected. In the middle mesosphere the  $CO_2$  and  $O_3$  heating are comparable, and the  $O_2$  near-infrared heating accounts for an additional 10% over the  $CO_2$  and  $O_3$  heating. In all three cases, full non-LTE calculations are required to account for substantial airglow loss. In the case of  $CO_2$  the radiative coupling between atmospheric layers must also be taken into account. The infrared solar heating by  $O_2$  and  $CO_2$  is reviewed in detail by *Mlynczak and Marshall* [1996] and by *Lopez-Puertas et al.* [1990], respectively. *Mlynczak et al.* [2000] also give a thorough evaluation of solar ultraviolet heating by ozone in the mesosphere and show it to be in good agreement with two-dimensional model calculations.

### 2.2.2. Chemical Heating Rates

[21] As shown in Table 2, large pools of chemical potential energy are created upon photolysis of  $O_2$  or  $O_3$ . In the case of the Schumann-Runge continuum, only 1% of the available photon energy is immediately made available for heat, while 72% shows up initially as chemical potential energy. Thus it should be no surprise that chemical reactions should play an important role in the energetics of the mesosphere. Long-range transport and subsequent recombination of atomic oxygen has long been known to occur in the upper mesosphere and lower thermosphere.

[22] The role of heating by exothermic chemical reactions involving odd-hydrogen species was apparently first mentioned by *Crutzen* [1971] and then again by *Brasseur and Offermann* [1986]. *Mlynczak and Solomon* [1993] carried out detailed studies of the role of mesospheric heating due to exothermic chemical reactions. They found that seven chemical reactions, listed in Table 3, are significant sources of heat. In particular, the reaction of atomic hydrogen and ozone may be the single largest source of heat between 83 and 95 km altitude. Furthermore, the heating due to exothermic chemical reactions is competitive with and, between about 70 and 95 km, exceeds the heating due directly to solar radiation.

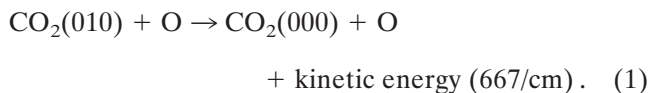
### 2.2.3. Radiative Cooling Rates

[23] Radiative cooling in the mesosphere is accomplished primarily through emission by carbon dioxide at 15  $\mu\text{m}$ . Between about 75 km and 110 km, emission by

**Table 3. Exothermic Reactions Important in the Mesospheric Energy Budget**

Reaction	Exothermicity, kcal/mole
$\text{H} + \text{O}_3 \rightarrow \text{OH} + \text{O}_2$	-76.90
$\text{H} + \text{O}_2 + \text{M} \rightarrow \text{HO}_2 + \text{M}$	-49.10
$\text{O} + \text{HO}_2 \rightarrow \text{OH} + \text{O}_2$	-53.27
$\text{O} + \text{OH} \rightarrow \text{H} + \text{O}_2$	-16.77
$\text{O} + \text{O} + \text{M} \rightarrow \text{O}_2 + \text{M}$	-119.40
$\text{O} + \text{O}_2 + \text{M} \rightarrow \text{O}_3 + \text{M}$	-25.47

$\text{CO}_2$  is the only significant cooling mechanism. In the lower mesosphere, cooling by ozone and by water vapor is important in addition to cooling by  $\text{CO}_2$ . P. J. Crutzen (see discussion of *Houghton* [1970]) suggested that atomic oxygen would be important in facilitating infrared radiative cooling. The key to understanding just how large this effect could be depends on the rate coefficient for vibrational relaxation by atomic oxygen,



This rate is very difficult to measure in the laboratory because of the difficulty of simultaneously producing vibrationally excited  $\text{CO}_2$  in the presence of atomic oxygen and then determining the decay rates, especially at low temperatures ( $\sim 160$  K) typical of the mesosphere. P. J. Crutzen, in his comment in *Houghton's* [1970] paper, showed that the calculated cooling rate at 100 km altitude could vary by a factor of 4 depending on the value of the O- $\text{CO}_2$  quenching rate. The upper limit for this rate suggested by P. J. Crutzen (see discussion by *Houghton* [1970]) is  $6 \times 10^{-8}$  atm s or  $6.2 \times 10^{-13}$  cm<sup>3</sup>/s, which is about a factor of 4 lower than the middle of the contemporary range of this rate. Recent laboratory measurement [*Khvorostovskaya et al.*, 2003] exhibits weak temperature dependence of this rate with a value close to  $1.5 \times 10^{-12}$  cm<sup>3</sup>/s within the 200–350 K range. However, measurements for as low as 140–160 K temperature range are still required. We wish to emphasize that while the rate of quenching of  $\text{CO}_2$  by O is often focused upon (because it is the quantity that is measurable in the laboratory), it is the collisional excitation of  $\text{CO}_2$  by O that provides the internal energy that is radiated, thereby cooling the atmosphere. The collisional excitation rate is determined from the collisional quenching rate by applying the principle of detailed balance.

[24] In order to compute the rate of  $\text{CO}_2$  cooling in the mesosphere the  $\text{CO}_2$  abundance must be known.  $\text{CO}_2$  has a long lifetime against photolysis in the mesosphere, and on the basis of photochemical considerations the standard expectation is that the  $\text{CO}_2$  concentration should be nearly well mixed below the turbopause ( $\sim 105$  km). Above the turbopause, diffusive separation occurs based on the molecular mass of each

species, and the mixing ratio is anticipated to deviate from the well-mixed value. This standard picture has been called into question by the analyses reported by *Lopez-Puertas and Taylor* [1989] based on observations of non-LTE  $\text{CO}_2$  emission at 4.3  $\mu\text{m}$  made by the Stratospheric and Mesospheric Sounder instrument on the Nimbus VII satellite and by the Improved Stratospheric and Mesospheric Sounder instrument on the UARS satellite. These analyses show that the mesospheric  $\text{CO}_2$  mixing ratio begins to deviate from well mixed as low as 80 km in altitude. At present, there is nothing to suggest that the effect is an artifact due to some misunderstood process or mechanism in the non-LTE model of  $\text{CO}_2$  vibrations. Thus the reasons for the observed, steep falloff in the volume mixing ratio of  $\text{CO}_2$  are not well understood. The status of our understanding of mesospheric  $\text{CO}_2$  is given by *Lopez-Puertas et al.* [2000].

### 2.3. Other Sources of Energy and Dynamical Influences

[25] Measurements and theoretical modeling efforts have also suggested that dynamical processes can lead to the heating or cooling of the mesosphere [e.g., *Lübken*, 1997; *Gardner and Yang*, 1998; *Liu et al.*, 2000]. For example, the existence of turbulence in the mesosphere is likely evidence of dissipation of some wave feature and likely leads to local heating. In addition, the observed thermal inversion layers in the middle and upper mesosphere appear to develop on timescales that require heating rates much larger than can be attributed solely to radiative or chemical effects as we currently understand them. *Liu et al.* [2000] showed that heating rates as large as 10 K/h (compare with the daily average solar and chemical heating rates shown in sections 2.2.1 and 2.2.2) could occur because of breaking gravity waves.

[26] To define the magnitude of dynamical processes as sources or sinks of energy in the mesosphere on a global basis is a very difficult task. Unlike the more conventional solar, chemical, and infrared sources and sinks of energy, dynamical processes have no measurable radiative signal associated with them and hence are impossible to measure with conventional remote sensing techniques. It is true that the effects of dynamics may be manifest, for example, in the structure of the observed airglow. However, airglow variations are simply reflecting the changes in composition due to the dynamics and not heating or cooling associated with a dynamical phenomenon.

[27] In the context of a space-based remote sensing mission such as TIMED, the only way to assess dynamical sources and sinks is to accurately determine the radiative and chemical sources and sinks that can be measured directly simultaneous with the temperature profile. Combined with wind measurements, the net effect of dynamical processes can be inferred as a residual. This approach, which is effectively what will be used to analyze the TIMED data, will not yield any information on a specific dynamical process but should be sufficient to de-

termine the extent to which dynamical phenomena are significant sources of energy and thereby influence the large-scale thermal structure of the mesosphere.

### 3. MEASUREMENTS

#### 3.1. Techniques and Associated Uncertainties

[28] The observational data records available for mesospheric temperature trend estimations are limited. In general, there are broadly four ways by which MLT temperature could be measured, three of which are direct methods, namely, ground-based, in situ (rocket-sonde), and satellite probing. Trends can also be estimated using indirect methods on the basis of ionospheric parameters, occurrence frequency of noctilucent clouds, and the descending height trend of the sodium emission layer. All these techniques are discussed briefly here, and reported trend results are discussed in section 5. Some kinds of instruments employed over long periods of time (like rocketsondes, etc.) were modified from time to time as technology improved. This is likely to introduce considerable uncertainties in longer time series analysis when data from different instrument versions are combined. In addition to this each technique has its own merits and disadvantages with respect to uncertainty. The magnitude of uncertainty varies with altitude in some techniques. For example, the impact of aerodynamic flow and modifications in instrumentation for M-100 rocket temperature sensor data is more prominent in the mesosphere than for lower heights. While satellites provide global coverage, ground-based data have the advantage that the information gathered at a fixed location is available (nearly) continuously. However, an interpretation of temporal variations in terms of varying spatial structures is not possible in the latter case. Ground-based measurements so far have the longest and most continuous sets of records, which is very useful for trend analysis. Quality control is also important for the more recent data sets obtained by fully automatic data collection. While transcription errors like wrong signs or missing digits [Weatherhead et al., 2002] may not be an issue in this case, bad-quality data due to glitches can readily enter the record and may require editing. At the same time many results reported recently have been derived from a single data set acquired by the different authors (or their group), where documentation problems related to instrument modifications do not arise. Of course, these newer data sets are still often rather short. The main experimental methods used so far for monitoring the mesospheric temperature structure are the following: (1) hydroxyl airglow rotational temperature, (2) O<sub>2</sub> airglow rotational temperature, (3) Doppler temperature derived from the atomic oxygen line, (4) rocketsonde temperature sensors, (5) Rayleigh lidar, (6) sodium lidar, (7) rocket grenade and falling sphere, (8) satellite probing (i.e., Wind Imaging Interferometer (WINDII) aboard the Upper Atmo-

sphere Research Satellite (UARS), Halogen Occultation Experiment (HALOE) aboard UARS, Stratospheric Aerosol and Gas Experiment (SAGE II), and Solar Mesosphere Explorer (SME) satellite), and (9) indirect techniques (i.e., frequency of appearance of noctilucent clouds (NLC), ionospheric data, low-frequency phase heights, reflection and A3 radio wave absorption, sodium layer/emission, etc.). The majority of the techniques listed may involve some inherent uncertainty and some biases. In sections 3.1.1–3.1.8 we will briefly describe some of the major uncertainties/errors associated with most of these techniques.

##### 3.1.1. Hydroxyl Airglow Emission

[29] The most widely used technique for mesopause region temperature determinations is based on line intensity measurements in hydroxyl airglow bands. Because most of the results presented for the mesopause region are based on this technique, we will discuss it in detail. Rocket measurements [Baker and Stair, 1988], the comparison of hydroxyl airglow temperatures with sodium lidar temperature profiles [She and Lowe, 1998], and triangulations with airglow imagers [e.g., Kubota et al., 1999; Ejiri et al., 2002] have confirmed the notion of a mean emission height of 87 km and a mean thickness of 8 km for the hydroxyl layer but also the presence of height variations in the range  $87 \pm 4$  km. These ground-based measurements have been confirmed and extended by direct satellite measurements of the height made from limb-looking instruments on the UARS satellite [e.g., Lowe et al., 1996; Melo et al., 2000]. Temperatures derived in this manner include the possible influence of emission layer height and profile variations that may complicate the interpretation of observed trends. Many measurements of OH rotational temperature have been made with the tilting filter technique. Instruments of this type are very sensitive to changes in filter characteristics, and the interference filters used are notorious for their lack of long-term stability. Some of the OH rotational temperature measurements, however, have been made with grating spectrometers, which have much better long-term stability and which are therefore far more suitable for trend determination.

[30] The hydroxyl airglow has been used to study the temperature of its emission region throughout the 50 years since its discovery by Meinel [1950]. The temperature measured is the hydroxyl rotational temperature, obtained by measuring the relative intensities of two or more lines in one of the vibration-rotation bands of the ground state of OH. There are >40 such bands occurring from the blue to the near-infrared region of the spectrum, although owing to various observational constraints, only a fraction of that number have actually been used extensively. The technique is based on the assumption that the population distribution in the rotational states ( $\leq 5$  [Perminov and Semenov, 1992]) of the upper hydroxyl state is a Boltzmann distribution in equilibrium with the translational temperature of the sur-

rounding medium. The validity of this assumption is among those assumptions discussed below.

[31] Two main issues need to be clarified to fully understand the utility and the reliability of hydroxyl rotational temperatures. Broadly described, these are issues related to the details of the measurement itself and those related to the interpretation of how to relate the hydroxyl rotational temperature to the temperature structure of the atmosphere itself. These issues will be dealt with in sequence in the remainder of this section.

[32] The open structure of the hydroxyl bands makes the spectral resolution necessary to isolate the lines used for temperature measurement and to provide good background subtraction relatively easy to achieve. In the absence of adequate resolution, correction for background emissions resulting from other airglow features such as the NO<sub>2</sub> continuum and from scattering of contaminant ambient light from clouds becomes difficult. Temperatures obtained with instruments lacking good procedures for the elimination of background effects are suspect; *Greet et al.* [1998] provides an excellent discussion of the importance of background subtraction.

[33] Instruments that have been used for the measurement of the hydroxyl rotational temperature include grating spectrographs [e.g., *Meinel*, 1950; *Krassovsky et al.*, 1962] and spectrometers [e.g., *Myrabo and Harang*, 1988], Fabry-Perot spectrometers [e.g., *Hernandez and Killeen*, 1988; *Greet et al.*, 1994], tilting-filter photometers [e.g., *Meriwether*, 1975; *Scheer*, 1987; *Takahashi et al.*, 1998], and near-infrared Fourier transform spectrometers [e.g., *Turnbull and Lowe*, 1983; *Mulligan et al.*, 1995]. In recent years the Fourier transform spectrometer operating in the region 1200–1650 nm has established itself as the instrument of choice for many groups for a variety of reasons. It provides a high signal-to-noise ratio because of superior optical throughput combined with the greater intensity of the hydroxyl bands in this spectral region. The scattered light level in this region is much lower than in the visible because of much reduced Rayleigh scattering. Finally, the Fourier transform instrument provides simultaneous observation of all spectral features, an important consideration since rapid changes in the intensity of the lines due to short-period gravity waves occur.

[34] The determination of rotational temperature requires knowledge of the rotational transition probabilities or line strength factors for the transitions observed. Unlike most molecules, the line strength factors for OH vary significantly from band to band mainly as a result of strong vibration-rotation coupling. Despite several attempts [*Mies*, 1974; *Langhoff et al.*, 1986; *Turnbull and Lowe*, 1988; *Nelson et al.*, 1990], no fully reliable set of these molecular parameters exists.

[35] *Turnbull and Lowe* [1989] have discussed the magnitude of the differences in temperature that can result from using the different available sets. For some bands the difference can be as great as 10 K or higher. *Greet et al.* [1998] have reported a 12-K difference in 6-2 band temperatures depending on which transition prob-

ability was used. *French et al.* [2000] have attempted to determine experimentally which set of transition probabilities is the most reliable for the 6-2 band. Until a fully validated set of transition probabilities becomes available, the absolute accuracy of any hydroxyl rotational temperature must be assumed to have a systematic error up to 5 K, although the uncertainty of the bands of the lower vibrational sequences appears to be less. Since the magnitude of this systematic uncertainty can vary from band to band even in bands arising from the same upper vibrational state, the effect of this uncertainty must be borne in mind when studying long-term changes in the temperature. Combining results measured at different times from different bands with uncertain transition probabilities can lead to false trends.

[36] The final measurement issue is whether there is any preference as to which lines should be chosen for the measurement of temperature. In principle, if the population were fully thermalized, any line would be an appropriate choice. However, it has been established in laboratory studies [*Polyani and Sloan*, 1975] that the nascent distribution of newly formed OH molecules has a significant fraction of the molecules in highly excited rotational states. A comparison of the radiative lifetime of the upper vibrational states with the collision frequency at 87 km suggests that there is time for fewer than 10 thermalizing collisions prior to emission. However, because energy transfer from translation to rotation is fast, this may be adequate. Observationally, *Pendleton et al.* [1993] have shown that although the lowest-lying states appear to be thermalized at the ambient temperature, there is a remnant population that shows a high degree of rotational excitation. To avoid this problem, only lines arising from the lowest-lying rotational states should be used in the temperature determination.

[37] The second broad class of issues relates to the interpretation of the relationship between hydroxyl rotational temperature and the atmospheric temperature. These issues arise because of the lack of vertical resolution in a ground-based measurement, so that the measured rotational temperature is some form of average over the entire emitting layer. Many authors assume that the emitting layer peaks at 87 km and has a half-width of ~8 km. They further assume that the observed rotational temperature is the intensity-weighted mean temperature of the emitting layer. To a good approximation these are appropriate assumptions. However, for time series extending up to several years in duration, their effects need to be evaluated with care.

[38] The height profile of the hydroxyl emission can readily be shown [e.g., *Melo et al.*, 2000] to be determined by the shape of the bottomside of the atomic oxygen emission. This analysis shows that the emission peak lies at the altitude at which the magnitude of the atomic oxygen scale height is just 0.5 of that of the neutral atmosphere. At night the altitude at which this occurs is controlled mainly by the rate of downward diffusion. Gravity waves, thermal tides, and planetary-

scale disturbances also cause vertical motion of the peak. Thus the hydroxyl rotational temperature corresponds, in general, neither to the temperature at a particular altitude nor to a particular pressure surface. Despite this limitation, *She and Lowe* [1998] were able to show that at midlatitude the hydroxyl rotational temperature could be used as a proxy for the  $87 \pm 4$  km temperature.

[39] A further complication results from the fact that the rate of collisional quenching of the hydroxyl vibrational levels is comparable to the rate of radiative deexcitation. Consequently, the OH height profile is different for each vibrational level. *Lopez-Moreno et al.* [1987] have modeled this effect for  $v = 2$  to 7 and found that there can be as much as a 2-km difference in altitude between the height profiles for high and low  $v$  values. *Krassovsky et al.* [1977] and *Lowe et al.* [1991] have confirmed this result by presenting gravity wave data in which the phase of a wave passing through the OH layer is different for different vibrational levels. The effect of this difference on temperature studies is minimized if temperatures from different vibrational levels are not combined.

[40] In summary, despite several difficulties, the hydroxyl rotational temperature remains a useful tool to infer atmospheric temperature structure provided that the limitations raised above are respected.

### 3.1.2. Molecular Oxygen Airglow

[41] Although less widely used in the past than the OH rotational temperature technique, the  $O_2$  atmospheric airglow band is also suitable for monitoring temperature in the mesopause region. It corresponds to a nominal height of 95 km, with a profile similar to OH, but also subject to some minor variations. The isolation of individual lines in this band would require higher resolution than for OH. However, even if the individual rotational components of the  $O_2$  band are not spectrally resolved, it is possible to extract temperatures with statistical errors not much worse than for OH [e.g., *Reisin and Scheer*, 2002]. This band is frequently included with the new generation of airglow imagers, so more  $O_2$  temperatures will become available for trend analysis in the future.

### 3.1.3. Rocketsonde Sensors and Instrumental Correction

[42] Rocketsonde temperature sensors are used to measure the temperature for the altitude range from roughly 20 km to  $\sim 75$  km. During the 1970s, sensor, payload, and correction methods associated with rockets were changed on a number of occasions, often without sufficient documentation. These early changes mainly affect the upper mesospheric part of the profile where measurements suffer more strongly from aerodynamic heating, sensor time lag, and radiative heating. Unavoidable modifications of measuring equipment and different techniques of data measurement and processing are responsible for inhomogeneities in the data sets. Important modifications of equipment, which result in a

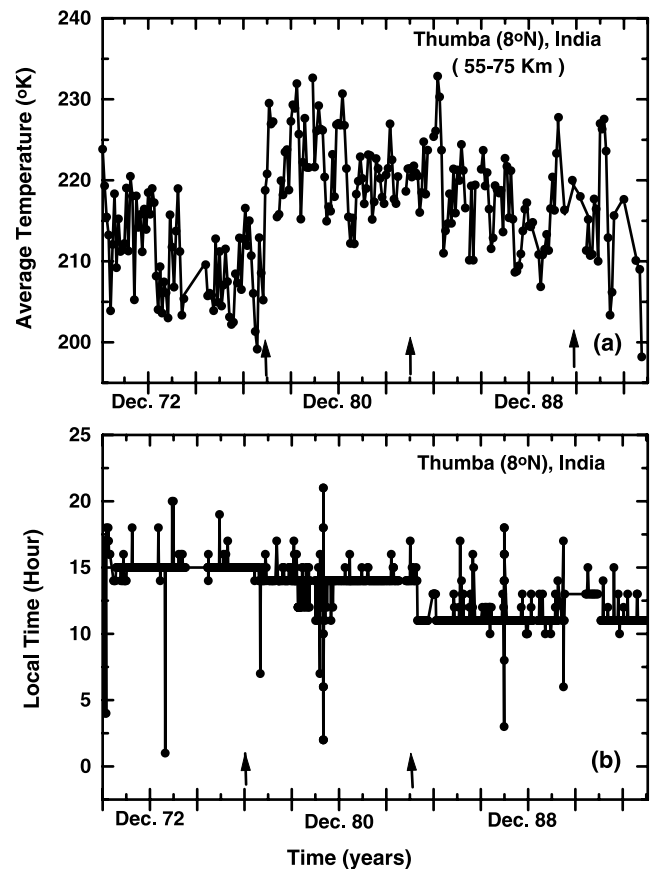


**Figure 2.** Illustration of breaks in the rocketsonde data due to instrumental modifications and tidal interferences. (a) Time series of temperature averaged over the altitude range 55–75 km. (b) Time series of local time of measurements for the rocketsonde data [Beig and Fadnavis, 2001].

marked offset in the temperature time series, are specific for each data series. For some series these changes are obvious. Some corrections can be applied, however, and continuity of the series can be better insured by using data prior to and after the modification or in processing the associated temperature drift using step functions within the regression analyses. Sometimes there are periods when different types of instruments are mixed. This procedure confuses the effect of the instrumentation change, and the more efficient way to take this into account is to remove data from some launches entirely to conserve the homogeneity within separate sequences of the data series. The influence of the beginning and end data on trend is important and may explain some of the dispersion of the trend results reported so far. Figure 2 shows how data can be biased by sensor modification. The time series of the average temperature for the altitude range from 55 to 75 km (Figure 2a) indicates that the rocketsonde sensor onboard the M-100 rocket was modified in November 1976, and a clear shift is noticed, which is marked by an arrow. Another minor modification in the sensor was made in December 1990. For further details on Figure 2a the reader is referred to *Beig and Fadnavis* [2001]. Such breaks in the time series

are not negligible and need appropriate corrections. Figure 2b shows a plot between the launch date and the actual time of measurement where breaks (indicated by arrows) coincide with the breaks in the temperature series (Figure 2a). This is reported to be due to tidal interferences and is discussed in detail in section 4.2.

### 3.1.4. Rocket Grenade and Falling Sphere

[43] Other techniques for measuring temperature have also been developed using rockets. Temperature profiles from the troposphere up to the mesosphere are obtained by the rocket grenade technique by measuring the speed of sound [Stroud *et al.*, 1960]. Typical uncertainties are less than  $\pm 3$  K below 75 km. The altitude resolution is 5–7 km. Another rocket-based technique is that of falling spheres. Densities and temperatures are derived from the deceleration of a sphere that is placed in the lower thermosphere by a small rocket and then falls through the atmosphere [Schmidlin, 1991; Lübken *et al.*, 1994]. Typical temperature uncertainties are 7, 3, and 1.5 K at 90, 80, and 70 km, respectively. The altitude resolution varies with height. Typically, the smallest scales detectable are of the order of 8, 3, and 1 km at 85, 60, and 40 km altitude, respectively.

### 3.1.5. Rayleigh Lidar

[44] Lidar is a technique that also provides temperature profiles for almost the same altitude range as that of rocketsondes. The method is based on the emission of a short-duration laser pulse in the zenith direction. The analysis of the backscattered light makes it possible to derive a temperature profile with good vertical resolution. However, for climate issues the resolution can be degraded to reduce statistical noise, and the integration time can be increased to several hours. As compared to rocket techniques, the use of a single instrument to record decadal series with reduced human and financial resources is one of the main advantages of this method for long-term atmospheric monitoring. One of the oldest techniques for temperature determinations on a routine basis uses Rayleigh scattering [Hauchecorne and Chanin, 1980]. The main sources of error in lidar-derived temperatures in the lower part of the profile (30–35 km) are due to the presence of aerosols, nonlinearity of the detector, and misalignment effects. In the upper part (75–80 km) the errors are mainly due to uncertainties in the reference pressure needed to initialize the analysis and photon noise [Keckhut *et al.*, 1995]. Some breaks in the temporal continuity of the lidar series may have been caused by changes of components. This is an expected outcome for any instruments operating over decades. However, the expected bias is located around the top and the bottom of the temperature profiles. Typically, measurements are obtained only in the first half of the night. Coverage obviously depends on weather conditions. For the Haute Provence lidar the integration time and the mean time of observation did not remain the same in the first 10 years of operation, and tidal effects may exist [Keckhut *et al.*, 1999]. Measurements are integrated over

several hours (from 2 to 12 hours). The main changes in the lidar system of the French group occurred in September 1994, as a result of replacement of the photon counting system.

### 3.1.6. Sodium Lidar

[45] The two-frequency, narrowband Na temperature lidar system relies on laser-induced resonance fluorescence from naturally occurring sodium atoms in the mesopause region. Since the sodium resonance fluorescence is around 14 orders of magnitude stronger than Rayleigh scattering, even a lidar with a modest power aperture product is capable of obtaining profiles with good signal to noise in the region of sodium abundance. The operating principle of this lidar has been described in detail [She *et al.*, 1992]. Depending on the photon noise, typical accuracies for the nightly mean temperature are 0.6 K near the peak (92 km) and 4–8 K at the edges (80 and 108 km) of the Na layer. The Colorado State University has run such an instrument on a routine basis at 40.6°N since 1992. The Colorado State Na lidar has a power aperture product of 0.06 W m<sup>2</sup>. Temperature measurement precision at night with 3.7-km and 1-hour resolution is 0.5 K at the Na layer peak ( $\sim 92$  km) and  $\sim 5$  K near the edge of the Na layer (at  $\sim 81$  and  $\sim 107$  km).

### 3.1.7. Satellite Data

[46] Satellite-based measurements are advantageous for global studies, but they bear some shortcomings. It takes a satellite 1 full day to describe a planetary-scale pattern, and a given point on the Earth is observed only once every several days at a given time of day. This may introduce spurious tidal effects in long-term trend detection. Asynoptic satellite data sampling leads to concerns relating to data aliasing and spatial/temporal ambiguities. Satellite measurements are subject to drift due to aging and exposure to charged particle fluxes in space. However, considerable efforts are made to estimate the effects of these problems using internal proxies. Also, unless the orbit is Sun-synchronous, the local solar time of the measurement will periodically change for each location. Another limitation of these measurements is their relatively limited temporal extension, until now. One of the first attempts at obtaining an interannual climatology in the mesosphere using satellite data was made with the SME experiment. The SME data reported by Clancy and Rusch [1989] involve Rayleigh scattering measurements with very poor signal-to-noise ratio. The fact that the temperature profiles above 70 km diverge strongly according to more recent measurements by Rayleigh and Na lidar suggests that the SME measurements are not reliable at these heights. The technique used measured sunlight scattered from the Earth's limb, so winter observations were not possible at high latitudes, and high-latitude summer observations could have been contaminated by polar mesospheric clouds.

[47] The longest mesospheric temperature series using a single instrument aboard a satellite was obtained

with the UARS mission. A long-term increase of the CO<sub>2</sub> mixing ratio consistent with its rate of increase in the troposphere has been allowed for in the HALOE retrieval algorithm. If that rate is not appropriate throughout the middle atmosphere, this assumption could affect a derived trend. No other long-term biases have been observed in the HALOE measurements. They have been checked for any remaining periodic or correlated structure in the time series model residuals. Sampling biases with time are not a problem. An adjustment has been made for the average effects of tides, prior to the analysis of HALOE time series. The WINDII experiment aboard UARS also provides good daytime temperature profiles in the altitude range 65–90 km, determined from measurements of Rayleigh scattered solar continuum at 553-nm wavelength. The technique is similar to that used by *Clancy and Rusch* [1989], where the measured integral line-of-sight Rayleigh scattering radiances are inverted to volume Rayleigh scattering rates, which are related to density, scale height, and temperature, employing the ideal gas law and hydrostatic equilibrium assumptions.

### 3.1.8. Ionospheric Techniques

[48] There are a number of records available from measurements of ionospheric parameters. One advantage of deducing the temperature trend from ionospheric data sets is that the records are several decades long, and hence the statistical significance is high. However, temperature trends derived from these sets are indirect estimates and suffer from some coarse approximations. For the upper ionosphere, data from many ionosonde stations have been analyzed by a number of authors. For the mesosphere, however, ionospheric data series are less abundant. Ionospheric absorption data are mainly available in the low-frequency (LF), middle-frequency, and high-frequency ranges as well as phase height data in the LF range. From absorption and phase height data in the LF range, attempts have been made to deduce information on temperature trends in the mesosphere. The mesosphere can easily be monitored by indirect phase height measurements in the LF range. Here the interference field between the ionospherically reflected sky wave and the ground wave of a commercial radio transmitter in the LF range (preferred frequency in the range between 50 and 180 kHz) is recorded at a distance of ~500–1500 km from the transmitter. In such a case the sky and ground waves have nearly the same amplitude and cause a typical interference pattern with maxima and minima of the recorded total field strength during the course of the day. Whereas the phase of the ground wave is relatively stable, the phase of the sky wave is determined by the systematically changing ionospheric reflection height, with higher values near sunset and sunrise and smaller values near noon. This diurnal variation of the reflection height during undisturbed conditions is mainly caused by the changing ionization due to the incident solar radiation in the EUV (espe-

cially Lyman  $\alpha$ ) as a function of the solar zenith angle. From the interference pattern of the recorded field strength it is easy to derive relative changes in the ionospheric reflection height. If observations at two or more similar measuring paths are available, then the ambiguity of the phase height measurements can be solved, and absolute reflection heights can be derived.

### 3.2. Data Details, Analysis Method, and Factors of Error

[49] Details of all the data sets obtained during the past few decades and available for evaluation of temperature trend in the MLT region are shown in Tables 4 and 5, which summarize the measurement procedures, length of data series, latitude, and altitudes. Table 5 also contains the deduced temperature trends along with error bars and related references, details of which will be discussed in section 5. The well-known natural periodicities in any temperature series include the annual oscillation, semiannual oscillation, seasonal variations, QBO, and solar cycle variations. In the past it was believed that the El Niño–Southern Oscillation was not very important in the mesosphere. However, recently, *Scheer and Reisin* [2000] have detected a significant effect in the mesopause region, which they attributed to the very strong 1997 ENSO event. Warming due to major volcanic eruptions is not expected in the mesosphere. However, observational evidence of volcanic influence on temperature was reported by *Keckhut et al.* [1995] and *She et al.* [1998] for this region. Recent trend analyses have usually removed several months of data after those events when computing trends or included an additional term in the analysis. In general, most of these variations will not affect the trend if the length of data is sufficiently large, as these phenomena are periodic or of relatively short duration, but since the data sets are only a few decades long, these factors may greatly influence the linear trend. While periodic signals are relatively well understood and most of the statistical models can remove them, the effects of episodic and sporadic events are difficult to model and remove. These phenomena may have forcing and long-term trends within their own cycles that confound the trend analysis. A proper trend analysis would lower the effective variability (or noise level) of the data series and thereby improve confidence in the trend calculation. It would also necessarily separate the different atmospheric responses, facilitating identification of any residual trend signal. Initially, analysis of rocketsonde data while deriving the linear trend did not take into account certain components of atmospheric variability. More recent studies [*Beig and Fadnavis*, 2001; *Keckhut et al.*, 1999; *Keckhut and Kodera*, 1999; *Dunkerton et al.*, 1998] have used multiregression models including seasonal, solar, and QBO proxies, etc., in addition to a linear trend term. Some data, such as those from satellite experiments, suffer from the short length of the data series and cannot be analyzed using a sophisticated regression model without the risk of de-

**Table 4. Temperature Trend in the Mesosphere (50–79 km) Region**

Reference	Technique <sup>a</sup>	Years of Analysis	Location	Height, km	Temperature Trend, K/decade
Angell [1991]	U.S. rocketsonde	1973–1985	8°S–55°N	50–55	–2.5
Dunkerton et al. [1998]	U.S. rocketsonde	1962–1991	8.6°S–37.5°N	50–60	–2.5 to –4.5
Keckhut et al. [1999]	U.S. rocketsonde	1969–1995	(8°S to 34°N) and (14°W to 167°W)	60 65–75	–3.3 (±0.9) –2.2 (±2)
Beig and Fadnavis [2001]	Indian rocketsonde	1971–1993	8.5°N, 77°E	50 60 70	–1.5 (±0.8) –3 (±1.3) –5.6 (±1.7)
Golitsyn et al. [1996]	Russian rocketsonde	1965/1969–1995	midlatitudes: (49°N, 44°E) and (47°N, 75°E)	50–60 70	–3.5 to –8.8 (±1.15) –5.2 (±1.30)
Golitsyn et al. [1996]	Russian rocketsonde	1964/1969–1995	high latitudes: (81°N, 58°E) and (68°S, 46°E)	50–60 70	–2 to –3.5 (±1.10) –10 (±2.05)
Komuro [1989] and Keckhut and Kodera [1999]	Japanese rocketsonde	1970–1989 1970–1995	39°N, 141.5°E	20–55	–2.5 (±1.1)
Lübken [2000, 2001]	rocket grenade and falling sphere	1987–2000	69°N, 10°E	50–85	–0.24 (±0.14) (summer)
Aikin et al. [1991]	satellite SSU channel and French lidar data	1980–1990	44°N, 6°E	55	–1.5 to –2
Keckhut et al. [1999]	Rayleigh Lidar	1979–2001	44°N, 6°E	65 75	–3 (± 2.2) –2 (± 2.5)
Remsberg et al. [2002]	UARS, HALOE-SR, and SS (satellite)	1991–2001	tropics and 20°N	50–62	–1.0 to –1.6

<sup>a</sup>SSU is stratospheric sounding unit; SR is sunrise; and SS is sunset.

ducing unrealistic components. Also, visual noctilucent cloud observations are limited to certain latitude bands, and solar angles and have a strong link with tides. This can bias long-term observations.

[50] In the case of a linear trend derived from the data by multiregression analysis, the confidence of the trend estimates is given by the following formula [Frederick, 1984]:

$$\sigma_t^2 = \frac{\sigma_r^2}{\sum_{i=1}^n [(t_i - \bar{t})^2]} (1 + \varphi). \quad (2)$$

The confidence is related to the short-term residual variance  $\sigma_r$ , and to the length of the data set  $t_i$ . The  $\bar{t}$  refers to average temperature. This scattering of the observations around the fitting function is a result of the different processes driving the variability on different timescales and can be considered as quasi-random noise. It can also be due to the instrument noise itself. So it appears that those instruments are more appropriate that provide noise levels smaller than the atmospheric variability. Atmospheric variability is not uniform and varies with location, altitude, and season. In the mesosphere the variability on a monthly basis is around 5–15 K [Leblanc et al., 1998]. The number of measurements,  $n$ , is also a key parameter. In practice, in the atmosphere nonrandom geophysical processes, such as waves, correlate with two successive measurements. The formula for trend uncertainty needs to be corrected by a factor that

takes into account the autocorrelation function [Frederick, 1984] that balances an oversampling. The autocorrelation  $\varphi$  of the mesospheric temperature starts to decrease significantly after several days. That does not mean that sampling intervals larger than 1 week are required. In the case of oversampling it is more appropriate to average data to reduce the residual geophysical variability (as discussed above). The optimum interval depends upon several factors such as the length of the data set, the measurement rate, and the residual geophysical variability. Sensitivity tests using mesospheric temperature data show that the optimum interval is between a week and a month [Hauchecorne et al., 1991]. The time required for the significant detection of an expected trend (Figure 3) can be extrapolated by choosing the temporal averaging, knowing the random monthly interannual variability. From the statistical point of view it appears that trends smaller than 2 K/decade can be detected significantly with at least 1 decade of continuous measurements.

[51] However, such measures are not always valid because the atmosphere is not only driven by short-term variability and climatic trends but also by many other processes on different timescales, including periods comparable to the length of the data set. For this reason, data analysis may require more sophisticated fitting of the data, including a linear combination of several functions. Seasonal effects provide the largest amplitudes;

Table 5. Temperature Trends in the Mesopause Region (80–100 km)

Reference	Technique	Years of Analysis	Location	Height, km	Temperature Trend, K/decade	Remarks
<i>Semenov and Shefov</i> [1999]	hydroxyl rotational temperature bands: several	1957–2000	42°–56°N and (37°–43°E)	mean OH emission layer height (87 ± 8 km)	–6.8 (±1)	
<i>Burns et al.</i> [2002] and <i>French</i> [2002]	hydroxyl rotational temperature, band: 6-2	1990, 1995–2001	69°S, 78°E	mean OH emission layer height (87 ± 8 km)	no discernible trend	
<i>Offermann et al.</i> [2003]	hydroxyl rotational temperature, band: 3-1	1980–1998	51.3°N, 7°E	mean OH emission layer height (87 ± 8 km)	+0.2 (±0.9)	
<i>Lowe</i> [1999, 2002]	hydroxyl rotational temperature, band: 3-1	1989–2001	43°N, 81°W	mean OH emission layer height (87 ± 8 km)	+0.6 (±2.3)	
<i>Espy and Segman</i> [2002]	hydroxyl rotational temperature, band: 3-1	1991–2001	59.5°N, 18°E	mean OH emission layer height (87 ± 8 km)	5 (±2.0) (winter) no trend (summer)	
<i>Reisin and Scheer</i> [2002]	hydroxyl rotational temperature, band: 6-2	1986, 1987, 1992, 1997–2001	31.8°S, 69.2°W	mean OH emission layer height (87 ± 8 km)	–10.5 (±0.8)	
<i>Sigemes et al.</i> [2003]	hydroxyl rotational temperature, band: 6-2	1983–2001	78°N, 15°E	mean OH emission layer height (87 ± 8 km)	+0.3 (±1.0) (winter)	
<i>Semenov et al.</i> [2002]	combined (major: hydroxyl rotational temperature bands: several)	1957–1976, 1984–1986, 1990–2000	41.8°N, 43°E and 55.7°N, 37°E	mean OH emission layer height (87 ± 8 km)	+0.3 (±0.8) (summer) –9 (±1.2) (winter)	analysis under process
H. Takahashi (unpublished data, 2002)	hydroxyl rotational temperature, band: 6-2	1994–2002	23°S, 45°W	mean OH emission layer height (87 ± 8 km)	not available	
<i>Reinsberg et al.</i> [2002]	UARS –HALOE –SR and SS (satellite)	1991–2001	45° to 45°N	80	no significant trend	
<i>Lübken</i> [2000, 2001]	rocket grenade and falling sphere	1987–2000	69°N, 10°E	50–85	–0.24 (±0.14) (summer)	
<i>Reisin and Scheer</i> [2002]	O <sub>2</sub> rotational temperature	1986–2000	31.8°S, 69.2°W	95	–0.3 (±1.5)	
<i>She and Krueger</i> [2003]	Na lidar	1990–1999	41°N, 105°W	92	0.0 (±2.5)	error limits represent 1σ error
<i>Semenov</i> [1997] and <i>Semenov et al.</i> [2002]	atomic oxygen line in 557.7 nm data	1965–1974	40°N, 106°W	97	–1 (±1)	
<i>Clemesha et al.</i> [1992, 1997]	centroid height of sodium emission	1972–1987	23°S, 45°W	20–92	–1.5	
<i>Fishkova et al.</i> [2001]; <i>Semenov et al.</i> [2002]	intensity of the sodium emission	1957–1992	41.8°N, 43°E	92	no trend (winter)	
<i>Bremer</i> [1997] and <i>Bremer and Berger</i> [2002]	ionospheric reflection height	1964–1995	51°N, 7°E	48–82	–1.4 to –2.1	
<i>Taubenheim et al.</i> [1997]	low-frequency radio signal reflection height data	1961–1997	51°N, 7°E	50–80	–6 (summer)	
<i>Nestorov et al.</i> [1991]	A-3 radio wave absorption	1959–1986	45°N, 13°E	mesosphere	–1.93	
<i>Gadsden</i> [1990] and <i>Gadsden</i> [1997, 1998]	occurrence frequency of noctilucent clouds	1964–1982 and 1964–1995	(54°–58°N) and (20°E–11°W)	82	–2.5	

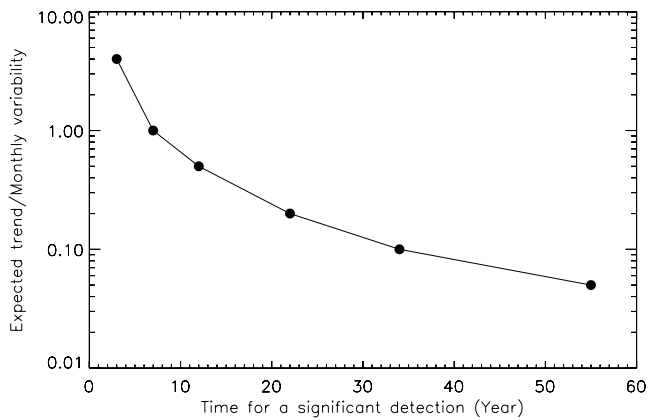


**Figure 3.** Simulations of the time required for a significant (95%) trend detection as a function of the ratio of expected trend over residual variability.

however, other fluctuations, such as the QBO, major volcanic eruptions, or the solar cycle, are known to induce significant changes in the mesosphere. One can take into account as far as possible the natural variability at longer periods that generates changes not associated with anthropogenic causes. The regression models include some simple functions. These functions are designed according to our knowledge of the possible physical links with proxies. The temporal shape of these functions may lead to misinterpretation if they provide a certain degree of correlation, which is the case for solar maxima and volcanic eruptions. Temperature responses to important natural and episodic factors are discussed separately in section 4.

[52] However, the fundamental factor limiting detection and quantification of a trend is the instrumental bias inducing changes in the mean measurements. A data set is considered homogeneous if anomalies are strictly due to climatic fluctuations. Trend estimates can be biased significantly if data series include artificial fluctuations of nonatmospheric origin. These discontinuities can be slow drifts as observed sometimes for space-borne instruments or sudden changes as experienced for ground-based instruments. Sudden spurious steps in the data series can be due to several causes that can be grouped into four categories: (1) improvement of the instrument, (2) algorithm modifications including filtering, (3) modifications of protocols and measurement conditions, and (4) accuracy and sensitivity improvements or sampling modifications.

[53] In a practical way, for instruments dedicated for a long-term commitment over several decades, it is virtually impossible to maintain the instrument unchanged, and possibilities for introducing discontinuities are numerous. This aspect has already been discussed in section 3.1 for individual techniques.

### 3.3. Objective Evaluation of Mesopause Region Data Sets

[54] Measurement of the hydroxyl rotational temperature to a precision of a few degrees is a relatively simple

task. Measuring it with the accuracy necessary to confirm model predictions for the long-term trend resulting from global change is a major observational challenge. Understanding the details of how to meet this challenge has evolved over the years with many of the requirements being very recent. What appears below is an attempt at an objective evaluation of how well existing data sets meet this challenge and is in no sense a criticism of the work that predates the need for the adoption of observational procedures necessary for the evaluation of long-term trends.

[55] Any attempt to measure long-term trends in the hydroxyl rotational temperature must address the question of the long-term stability of the instrument calibration. A major advantage of the hydroxyl method is that determining the absolute temperature requires only a relative calibration of the instrument response at two or more wavelengths. However, there are serious technical difficulties in ensuring the stability of the relative spectral response with a precision appropriate to the measurement of a trend that may be as small as 1 K/decade or even smaller. A 1% uncertainty in the relative spectral responsivity can imply as much as a 1–2% error in the temperature, depending on the lines being used. The fact that the lines used for temperature measurement are close in wavelength reduces the probability of a long-term drift in spectral response but does not eliminate the necessity of regular verification of the spectral response function. This is especially true for Fourier transform spectrometers whose spectral response depends on the alignment of the instrument as well as on the optical properties of its components.

[56] The hydroxyl rotational temperature is affected by a variety of phenomena on timescales ranging from a few minutes for short-period gravity waves to 11 years for the solar cycle. The trend analysis method must be chosen with these in mind. The most commonly used approach is to observe throughout the night provided meteorological conditions permit and then to combine the data obtained to form the nightly mean temperature. These nightly means are then used to form a data set for the study of phenomena such as long-term trends with characteristic times greater than 1 day. Each of the instruments in the studies listed below is capable of producing a nightly mean temperature with an instrumental uncertainty below 1 K. As a result, instrument noise makes a negligible contribution to the uncertainty in the nightly means. Much more important is the “geophysical noise” in the nightly means due to the imperfect averaging of the effects of gravity waves and the thermal tides. Both of these phenomena can have components with periods that exceed the length of the available observing time during a night. This is particularly true in the summer. The magnitude of this geophysical noise is arguably one of the major limiting factors in the determination of long-term trends.

[57] Of primary importance is the length of the data set required to determine a temperature trend. There is

no simple answer to this question. *Weatherhead et al.* [2002] have examined this question in general and point out the importance of unexplained variability of the data and the autocorrelation of the noise. They developed explicit formulae for the determination of the number of years needed to detect a trend of given magnitude, but these have not yet been applied to the specific problem of hydroxyl rotational temperature in which the available data sets frequently are unevenly sampled and sometimes have extensive gaps. In the evaluation below, it is assumed that at the minimum the data set should be long enough and sampled often enough to ensure that the effects of seasonal variations, solar cycle variations, and episodic temperature fluctuations do not compromise the determination of any underlying trend.

[58] Many groups have studied the hydroxyl rotational temperature in the last 50 years. With the exception of the unpublished trend results of the data set of *Takahashi et al.* [1995] these results have been briefly reviewed by *Beig* [2002]. Two of the data sets, those from the groups of N. N. Shefov and F. Sigernes, as published (*Golitsyn et al.* [1996] and *Nielsen et al.* [2002], respectively) do not meet the requirement for homogeneity (single hydroxyl band and single location) essential to prevent the introduction of potential systematic error, nor do the authors describe a regular calibration process. Both groups attempt to overcome this difficulty, but as described above, it is unlikely that this can be done without introducing systematic error. Homogeneous subsets of both time series might yield reliable trends.

[59] The remaining OH emission data sets, as discussed below, satisfy the homogeneity requirement. Of the remaining those from the groups of G. B. Burns [*Burns et al.*, 2002] and J. Scheer [*Reisin and Scheer*, 2002] are similar in that they combine a few recent years of well-calibrated frequently sampled data with earlier results that are either sparsely sampled or with questionable calibration. In neither case are the recent data of sufficient duration to establish a long-term trend reliably, though they have the potential to do so if they are extended for an appropriate interval. However, in the case of *Reisin and Scheer* [2002] the time series is long enough, although with gaps, and if we assume that midpoints are not that crucial if accurate beginning and end points are present, then, in principle, trends can be determined with a certain reliability. Apart from the as yet unanalyzed data of H. Takahashi (unpublished, 2002), the 3-1 band has been used by three different groups [i.e., *Espy and Stegman*, 2002; *Bittner et al.*, 2002; *Lowe*, 2002]. The measurements of *Espy and Stegman* [2002] are unique in that they attempt to minimize the effect of thermal tides on partial nights of observation by a fitting procedure. However, the length of their data set is marginal for the determination of a long-term trend, and they are unable to measure a solar cycle effect, possibly because their data do not include years of high solar activity. The longest data set is that of the D. Offermann group, described by *Bittner et al.* [2002] and

*Offermann et al.* [2003]. Extending over 21 years, it is both homogeneous and calibrated on an annual basis. The largest error found in the annual calibrations would produce a temperature error of at most 2 K. The data show large episodic temperature variations that make it difficult to establish a long-term trend. The data of R. P. Lowe are homogeneous and apparently well calibrated, but there is the possibility of a systematic error due to the use of three different instruments over the 11-year period of the measurements.

#### 4. NATURAL FACTORS OF VARIABILITY IN TREND CALCULATIONS

##### 4.1. Solar Cycle Variation

[60] Incoming solar radiation provides the external forcing for the Earth-atmosphere system. While the solar Lyman  $\alpha$  flux varies by a factor of  $\sim 2$  over a solar cycle, changes in the UV are smaller. Studies on the changes in solar UV spectral irradiance on timescales of the 27-day and 11-year solar cycles have been attempted by many workers in the past [e.g., *Donnelly*, 1991; *Woods and Rottman*, 1997]. Modeling of the mesospheric solar cycle response has evolved with time, as improvements have been made in the measurement techniques of the 11-year solar UV spectral changes. Most of the earlier predictions overestimated the mesospheric response, because they were based on incorrect solar UV radiation derived from data of insufficient quality and/or length. Since the SME and UARS missions the data are now becoming available to quantify the variations since 1981. The modeling work of *Chen et al.* [1997] reported a solar cycle response of several kelvins in the mesopause region. The interpretation of 11-year changes in temperature related to variations of solar UV has been a long-standing problem. The observed temperature variability at 70 km is not explicable in terms of corresponding 11-year changes in observed ozone [*Keating et al.*, 1987]. Searches for a strong dynamical feedback and attempts to invoke a strong odd-hydrogen photochemical heating effect have so far not been successful. Until recently, different data sets showed solar cycle responses different even in polarity.

[61] It was thought earlier that it would be hard to identify a trend in the MLT region if solar response is very large in magnitude, and we need longer data sets encompassing several solar cycles. Recent investigations revealed the presence of a solar component in MLT temperature in several data sets, but probably they are not as strong as thought earlier. A number of trend studies in which the 11-year periodicities have been removed have been reported for this region. However, the solar response in temperature, if not properly filtered out, is still one of the major sources of variation which may interfere with the detection of temperature trends for the MLT region. Data series available for the MLT region are short compared to what is available for

the stratosphere. In the late 1970s a few authors reported solar cycle-associated variability in mesosphere temperatures. *Shefov* [1969] reported a solar cycle variation in OH rotational temperature of the order of 20–25 K for midlatitudes. *Labitzke and Chanin* [1988] using rocketsonde data at 81°N reported solar cycle temperature variations of the order of 25 K at 80 km. An analysis of falling sphere and rocket grenade data of summer by *Lübken* [2000, 2001] revealed no statistically significant solar component for the altitude range 50–85 km. In recent times the long-term series of lidar data obtained at Haute Provence (44°N) has revealed a positive (in phase) solar response of 2 K/100 solar flux units (sfu) ( $1 \text{ sfu} = 10^{-22} \text{ W m}^{-2} \text{ Hz}^{-1}$ ) in the mesosphere up to 70 km. The response was found to fall off with height above 65 km, with a tendency toward a negative response above 80 km [*Keckhut et al.*, 1995]. *Keckhut et al.* [1995] also found the positive solar response to be stronger in winter than in summer.

[62] The time series of Russian rocketsonde measurements at four different sites (covering low to high latitudes) revealed a substantial positive solar response in the mesosphere [*Mohanakumar*, 1985, 1995]. The magnitude of the response varied with season and with latitude, maximizing at the Antarctic site Molodezhnaya (at 69°S). During winter the 11-year response was 12 K in the Arctic and  $\sim 17$  K in the Antarctic. The summer time response varied in the same way with latitude but was about half the wintertime values. The consequences of these effects were examined by *Groves* [1986] who found that pressure changes in this height range would vary by 18–35% depending on latitude. The reanalysis of the Thumba (8°N) data extending to more than two solar cycles revealed a value of trend coefficient that is substantially lower in magnitude [*Beig and Fadnavis*, 2001] compared with earlier analysis of the same data [*Kokin et al.*, 1990]. These differences are attributed to several factors including corrections, different statistical method, and, most importantly, the correct filtering of the solar signals from the trend signals. G. Beig and S. Fadnavis (Implication of solar signal in the correct detection of temperature trend over the equatorial middle atmosphere, manuscript in preparation, 2003) (hereinafter referred to as Beig and Fadnavis, manuscript in preparation, 2003) have recently also found a positive solar response of temperature in the mesosphere but of much lower magnitude than reported earlier. Beig and Fadnavis (manuscript in preparation, 2003) have stressed the fact that the high value of solar signal above 70 km at Thumba, where an unusually high negative trend (almost double that for other sites) as well as a high solar cycle coefficient was reported, might have biased the trend estimate made by earlier workers. The reanalysis also improved the agreement with other more recent results. The Thumba results indicate a stronger positive solar component in winter as compared to summer for the mesosphere, which is in agreement with midlatitude lidar results [*Keckhut et al.*, 1995].

[63] In OH emission data a clear positive solar cycle response was found by *Weill and Christophe* [1977]. Solar cycle dependence of the OH layer was recently confirmed by *Lowe* [1999] from satellite measurements. *Lowe* [1999] has found that the height and shape of the OH layer underwent systematic change with the solar cycle. It is now believed that there is a positive 11-year solar response of both the OH and green line emission rates [*Givishvili et al.*, 1996; *Batista et al.*, 1994].

[64] Some of the most recent results derived for solar response are discussed below for the mesopause region. Note that throughout this paper the quantity in parentheses with plus and minus sign represents the 2- $\sigma$  (two standard deviations) error except where otherwise specified. In the high-latitude northern hemisphere, two reliable data sets of sufficiently long duration have been used to derive the solar response of temperature in the mesopause region. *Lübken and von Zahn* [1991] have reported no solar response at 69°N at the upper range of their falling sphere measurement (85 km) for summer. *Sigernes et al.* [2003] reported that no solar signal is present in the time series of 20 years of OH airglow data from the auroral station Svalbard (78°N, 15°E). However, in the midlatitude Northern Hemisphere, where the greatest number of OH airglow temperature measurements are available, all studies signal a positive response to solar activity. *Espy and Stegman* [2002] have reported a positive solar coefficient of  $1.6 (\pm 0.8)$  K/100 sfu at the height of the OH layer over Stockholm (59°N, 18°E). *Lowe* [2002] has made OH layer measurements for one full solar cycle at Delaware Observatory (43°N, 81°W) and found a positive solar response of  $1.5 (\pm 1.1)$  K/100 sfu. *Semenov* [2000] has combined the OH data collected over several Russian stations covering the latitude band of 42°–56°N and reported a positive solar response of  $5.1 (\pm 1.5)$  K/100 sfu.

[65] *Bittner et al.* [2000] analyzed hydroxyl temperature data for Wuppertal (51°N, 7°E) for the period 1981–1995. They reported positive a solar correlation response for periods greater than  $\sim 30$  days and negative correlation for periods less than  $\sim 10$  days. *Offermann et al.* [2003] have analyzed 21 years of OH airglow data for solar  $F_{10.7}$  influences and reported an estimate of  $3 (\pm 1.6)$  K/100 sfu. A modern data set obtained from sodium lidar indicates a strong solar cycle response [*She and Krueger*, 2003] based on data obtained between 1990 and 2001. The solar response increases from zero at  $\sim 82$  km to 0.05 K/sfu at  $\sim 90$  km, and it remains positive until 101 km with a peak of 0.06 K/sfu at 99 km. Above 101 km it decreases quickly to zero at 104 km and becomes negative at 105 km. The solar response amplitude changes with altitude suggest that dynamics plays an important part even in perturbations with a long period of 5–10 years. If we study the Northern Hemisphere midlatitude results obtained by incoherent scatter radar, Rayleigh lidar [*Chanin et al.*, 1989], and sodium lidar [*She and Krueger*, 2003], an alternating negative and positive temperature response to solar activity as a func-

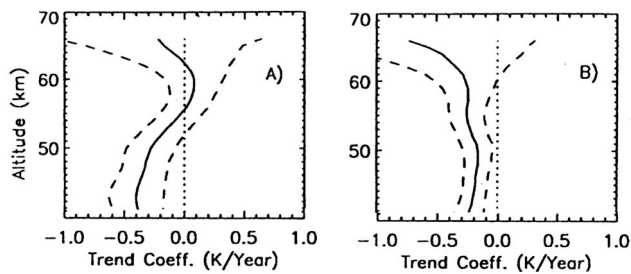


**Figure 4.** Trend profiles observed at Ascension Island (a) without and (b) with time of day selection.

tion of altitude between 30 and 140 km is found. This is strong evidence for the existence of dynamical coupling from the troposphere to the thermosphere, affecting solar activity–induced signatures. In the Southern Hemisphere, eight years of Davis (69°S, 78°E) winter averages yield a solar cycle response of 5.0 K/100 sfu with an error limit of  $\pm 1$  K owing to spectral response calibration [French, 2002]. Reisin and Scheer [2002] have collected data at the Southern Hemisphere lower midlatitude site El Leoncito (32°S, 69°W) and found no solar cycle effect in OH data, but they estimated an upper limit of 2–6 K/100 sfu, from the O<sub>2</sub> emission, at 95 km. However, some of the above data lengths are too short to distinguish a variation of this magnitude from the combination of a stronger solar cycle variation with possible significant cooling. Whether solar cycle activity is directly linked to nightly temperatures of the upper mesosphere or only via long interval averages has significant implications on the process by which a possible linkage might occur. We will have to wait for a few more years before we can make confident claims about the solar signature in MLT temperature structure.

#### 4.2. Tidal Influences

[66] Tides induce temperature changes of several kelvins in the mesosphere depending on the local solar time and altitude [Keckhut et al., 1995, 2001; Hagan et al., 1995]. The tidal effect is most significant in the equatorial mesosphere and must be considered when analyzing temperature series for trend detection. However, tidal amplitudes (diurnal and semidiurnal) in the high-latitude mesosphere are believed to be small [Forbes, 1982] and should not significantly influence trend analysis. Tidal temperature variations are noticed with phase structures, variable in height and season. Hence, if the time of the day of measurements changes, it can induce a spurious trend of several kelvins per decade. This kind of bias is not negligible compared to the expected trends and needs to be considered for trend studies. Normally, rockets are launched at a fixed time, but sometimes, launch times must be changed for various reasons. Even small changes may induce some spurious temperature changes. Local time of the measurements is a critical factor for rockets (Figure 4) because in addition to the atmospheric tidal changes there is a diurnal bias on the

sensor responses due to solar heating. This issue has recently been addressed for some tropical rocket stations by Keckhut et al. [1999] and Beig and Fadnavis [2001]. Lidar measurements are also subject to local time effects. Keckhut et al. [2001] have shown that tides have introduced biases in time series estimated with a tidal model varying over a range of  $\pm 1$  K. The solar occultation technique is better adapted for sounding temperature from space because it does not exhibit strong tidal effects because the measurements are made only twice a day synchronized with sunset and sunrise for a given geographical location. So measurements are obtained at the same local time from year to year at a particular season. Measurements made at a single longitude may yield a trend different from those obtained from global experiments that employ zonal averages. The time series in Figure 2a is a good illustration of the sensor correction and possible tidal effects, where averages of 55–75 km temperature minimize the noise and average out the inhomogeneities [from Beig and Fadnavis, 2001]. Although tides are not perfectly known, the occurrence of the first discontinuity, due to the different time of measurements (December 1977), incidentally coincided with the sensor correction time (see Figure 2b, where local time of measurement is plotted against time). The second break due to tides occurred in December 1983 as is evident from Figure 2b. The correction factor due to these effects varies with altitude. In the regression model a step function that takes care of such corrections should be included. The influence of tides in the vertical distribution of temperature trend is illustrated in Figure 4 [from Keckhut et al., 1999]. It is clear from Figure 4 that because of the tidal influence a difference of  $\sim 3$  K/decade may arise around 60 km. More important is the fact that results can be misinterpreted as a result of the change in sign of the trend, as can be seen if we compare the two trend profiles around 60 km in Figure 4, where the trend goes positive in one profile and remains negative in another.

#### 4.3. Others Factors (Volcanic Influence, QBO, ENSO, etc.)

[67] The influence of volcanic aerosols on atmospheric temperature is most vividly demonstrated by the changes after the most documented Mount Pinatubo eruption in 1991 [McCormick and Veiga, 1992]. A few months after the Pinatubo eruption, lower stratosphere temperature increases as high as 3.5 K were observed over large areas, from the equator to 30°N [Labitzke and McCormick, 1992]. However, studies on temperature change in the mesosphere attributable to volcanic influence have been lacking, except for a report based on Rayleigh lidar measurements [Keckhut et al., 1995] in southern France (44°N). Keckhut et al. observed a significant warming of 6 K in the mesosphere between 60 and 70 km in the summers of 1992 and 1993. However, the interest in volcanic influences has always existed, and a comprehensive three-dimensional model study [Rind et

*al.*, 1992], prior to the Mount Pinatubo eruption, showed that the warming of the lower stratosphere gives rise to an increase in tropical static stability, which alters the dynamics of the middle atmosphere, leading to high-latitude warming in regions of the upper stratosphere and lower mesosphere. Since the model output is limited to altitudes below 90 km, the impact in much of the mesopause region was not evaluated. The first observation of volcanic influence in the mesopause region was identified from 7 years of Na lidar temperature measurements in the mesopause region over Colorado [She *et al.*, 1998]. In a later paper, Krueger and She [1999] reported a volcanic response between 84 and 102 km, showing that a maximum warming between 7 and 14 K occurred between 1.5 and 2 years after the eruption. The detailed analysis based on 9 years of data is given by She *et al.* [2002]. The other result of the Pinatubo influence on this altitude region was reported by Lastovicka *et al.* [1998] who mentioned an increase of gravity wave activity in 1993 inferred from nighttime radio wave absorption in the lower ionosphere. Recently, Thulasiraman and Nee [2002] also reported warming in the UARS/High Resolution Doppler Imager temperatures attributable to the Mount Pinatubo eruption, adding credibility from a global perspective of volcanic influence in the mesopause region.

[68] The QBO is a well-known periodicity in stratospheric winds at the equator and low latitudes, where it is the dominant prevailing wind oscillation, with periods varying between 20 and 36 months. However, farther from the equator the QBO becomes masked by the semiannual oscillation that is already dominant at mid-latitudes and in and above the upper stratosphere. There has been some evidence of a QBO effect on the mesopause region wind field [Sprenger *et al.*, 1975; Jacobi *et al.*, 1996] at middle latitudes. Less is known about temperature variations due to the QBO. Hagan *et al.* [1999] have studied the possible relation between the amplitude of the diurnal tide and QBO but without confirming a definite link. Nielsen *et al.* [2002] estimate a QBO effect on OH temperatures in Svalbard (78°N) of about +5 K during the positive phase of QBO (i.e., when the equatorial zonal wind in the stratosphere blows eastward). Even if QBO effects as large as this are confirmed, they need not pose a problem for trend analysis, when taken into account or when the data span is sufficiently long. On the other hand, no QBO signatures were evident in OH rotational temperature data at Northern Hemisphere (NH) midlatitudes (Wuppertal, 51°N [Bittner *et al.*, 2002]) and in temperatures and airglow intensities of OH and O<sub>2</sub> at Southern Hemisphere lower midlatitudes (El Leoncito, 32°S [Reisin and Scheer, 2002]). All this probably means that QBO effects are not strong enough to affect long-term mesopause region trend studies anywhere.

[69] Strong perturbations of tropospheric circulation are caused by episodic changes in sea surface temperatures in the Pacific Ocean called El Niño–Southern

Oscillation. However, besides a strong regional and maybe even global impact on weather and stratospheric ozone concentration, reports of an ENSO effect in the upper atmosphere have appeared only recently. The connection is thought to be mediated by variations in the excitation and vertical propagation of gravity waves [Gavrilov *et al.*, 1999, 2000, 2002]. An effect of the North Atlantic Oscillation (another tropospheric perturbation of great geographic extension) on the mesopause region wind field was reported by Jacobi and Beckmann [1999]. Jacobi and Kürschner [2002] have also reported a correlation between NH mesopause region wind measurements and the periodicity of ENSO events. Statistical results like these refer predominantly to ENSO events of average strength. ENSO strength can be quantified as a ground pressure difference between two remote sites (Southern Oscillation index) or the sea surface temperature anomaly (SSTA) in different areas of the eastern Pacific Ocean. Medium-strength events are frequent enough to be of little influence on trends derived from long-term observations. The strongest events (in terms of SSTA, there have been only two in the last 50 years, namely, in 1983 and 1997) that are likely to have the greatest global impact and are capable of interfering more seriously with trend determinations occur at the spacing of decades. Scheer and Reisin [2000] have noticed a pronounced deficit in airglow brightness in mid-1997 in comparison with “normal conditions” in the past and the following years. They attributed this to the exceptionally strong ENSO event at that time. The effect could be quantified more precisely in their recent trend analysis [Reisin and Scheer, 2002] that also included an appreciable effect on mesopause region temperatures. The corresponding episodic anomaly of about -3.5 K at 87 km and -6 K at 95 km would have modified derived temperature trends if it had occurred in a more critical part of the data set and had not been accounted for.

## 5. EXPERIMENTAL RESULTS ON TRENDS

### 5.1. Lower and Middle Mesosphere Trends

[70] Table 4 summarizes the available details on reported temperature trends, measurement procedures, length of data series, latitude, longitude, and altitudes, obtained during the past few decades in the mesospheric region (50–79 km). We will briefly mention in sections 5.1.1–5.1.5 some important results obtained by various techniques in this region.

#### 5.1.1. Rocketsonde

[71] A large amount of temperature data have been provided by rocketsondes operated in the past. Rocket-borne temperature sensors, launched within the framework of intensive Russian and U.S. programs, have been used to monitor the lower and middle mesosphere. These programs (mainly during the 1970s and 1980s) covered launch sites spread all over the globe. However,

only a limited number of sites provided temperature profiles throughout the mesosphere. Funding for these programs was drastically cut, and operations had almost ceased for most locations by the end of the 1980s. The longest data series are found mainly in tropical and subtropical zones, except for a few sites at midlatitude such as Wallops Island. The former USSR provided a smaller network. Nevertheless, longer Russian data series can be found at high, middle, and low latitudes. The tropical site in India at Thumba (8°N) was operated cooperatively by Russia and India. A good decade-long data set is also available from Ryori (39°N) in Japan. However, in the latter case the maximum altitude at which rockets could collect data was only 60 km.

[72] The first analysis of U.S. rocketsonde data [Angell, 1987, 1991] revealed a mean cooling of 2.5 K/decade in the lower mesosphere. However, a 2- to 3-K temperature drop, observed in the early 1970s [Johnson and Gelman, 1985], coincides with a change in the principal observing system from the Arcasonde to the Datasonde system. This trend, observed over North America, although never really proven to be due to instrumental change, is in disagreement with radiosonde data. Since the 1980s the same payload and sensor have been used. Later studies were based on a reduced time interval for the data sets [Angell, 1987] to avoid the potential effects of instrumental changes. In contrast, Dunkerton et al. [1998] collected all historical data to increase the length of the series. Their analysis shows a clear signature of solar activity changes and reveals the need for using multiparametric analyses instead of a simple linear regression. However, reported variations in cooling rates among different sites ranging from 2.5 to 4.5 K/decade may be artificial. Dunkerton et al. [1998] found a mean cooling trend around the stratopause of 1.7 K/decade modulated by a solar cycle influence with an amplitude of 1.1 K.

[73] Meteorological rocketsonde temperature measurements available at seven sites from the United States and the former USSR between the 1960s and the 1990s are examined for changes and trends by Schmidlin [1991] using a basic linear regression. He found a different trend at each site and not necessarily always in the same direction varying between -2.4 and 1 K/decade at 50 km. Even over tropical and subtropical sites the variation was large, from 0.2 K/decade at Thumba (9°N) to -1 K/decade at Cape Canaveral (28°N). Keckhut et al. [1999] found a smaller dispersion of the trend after taking into account instrumental changes and tidal effects. Annual trend results from six locations in tropical and subtropical regions have been averaged as their differences are smaller than individual statistical uncertainties. Keckhut et al. [1999] found a cooling trend of  $1.7 \pm 0.7$  K/decade at 40–50 km reaching a maximum cooling of  $3.3 \pm 0.9$  K/decade at 60 km. In the upper mesosphere, only three subtropical rocketsonde stations provide sufficiently long data sets to compute trends, as reported by Keckhut et al. [1999]. The cooling is around

2 K/decade at upper mesospheric heights but is found not to be statistically significant.

[74] Data on the temperature of the stratosphere and mesosphere were also obtained from weekly launches of the Soviet meteorological rocket M-100. The most important modification of the equipment, which resulted in a marked change of the temperature data, was made in 1977–1978. Russian rocketsonde results were reported by Kokin et al. [1990] and Kokin and Lysenko [1994]. Subsequently, Golitsyn et al. [1996] presented consolidated results of Russian rocketsonde temperature trends for various latitudes by using the full length of the data series available. They reported results from the following data sets: high latitude, Heiss Island (81°N, 58°E) during 1964–1995 and Molodezhnaya (68°N, 46°E) during 1969–1995; midlatitude, Volgograd (49°N, 44°E) during 1965–1995 and Balakhash (47°N, 75°E) during 1973–1995; and low latitude, Thumba (8.5°N, 77°E) during 1971–1990. Golitsyn et al. [1996] reported a cooling trend of  $1.8 \pm 0.9$  K/decade at 50 km, which increases to  $3.5 \pm 1.2$  K/decade at 60 km and  $10 \pm 2.05$  K/decade at 70 km for high latitude. However, for midlatitude, cooling trends were found to be  $3.5 \pm 1$  K/decade at 50 km,  $8 \pm 1.25$  K/decade at 60 km, and  $5.2 \pm 1.3$  K/decade at 70 km. The corrections applied to the rocket data were changed several times during the 25 years of operation and may explain some of the large trend values observed in the mesosphere.

[75] The series of rocketsonde and radiosonde data collected over the equatorial station Thumba (8°N, 76°E), India, extending for about two solar cycles (1971–1993), were revisited by Beig and Fadnavis [2001]. These data were analyzed using two independent and modern regression models, which are based on multiple function regression theory and also take account of successive instrument modifications and tidal effects. A good inter-comparison of balloon and rocket data in their analysis indicates the consistency and robustness of their analysis. A negative trend of 2–3 K/decade in the lower mesosphere and a rise in cooling to 5.6 K/decade at 70 km was obtained. The two standard deviations error is found to range from  $\pm 0.5$  K/decade in the lower stratosphere to  $\pm 1.3$  K/decade in the middle mesosphere. A decrease of the trend near the stratopause is noticed in an annual trend analysis. The cooling was found to be slightly stronger in winter than in summer.

[76] The Ryori site (39°N) in Japan also provides a long temperature data series with regular rocket soundings. A previous analysis was made with data extending up to 1989 [Komuro, 1989] using a simple linear regression analysis. The maximum rocket apogee was around 60 km, limiting measurements to the lower mesosphere, which is lower than the range of U.S. and Soviet vehicles. An updated study was done recently, with data extending to 1995 and using a multifunction regression analysis. A significant cooling of  $2.5 (\pm 1.1)$  K/decade was found for the lower mesosphere [Keckhut and Kodera, 1999].

### 5.1.2. Rocket Grenade and Falling Sphere

[77] *Lübken* [2000, 2001] used several subsets of data to estimate the summer temperature trend at high latitude. Early rocket grenade data were collected from two launch sites, Kronogard at 66°N (six profiles) and Point Barrow at 71°N (15 profiles). Temperature was also deduced from density profiles derived from 69 falling spheres [*Schmidlin*, 1991] launched in summer at the Andoya Rocket Range (69°N) since 1987. The mean summer trend as reported by *Lübken* [2000, 2001] is  $-0.24 (\pm 0.14)$  K/decade, which is close to zero. It should be remembered, however, that this study is based on the comparison of two data series collected with two different techniques.

### 5.1.3. Rayleigh Lidar

[78] A more recent method for probing the middle atmosphere from the ground is the Rayleigh lidar technique. Temperature profiles from 30 to 75–80 km have been obtained since 1979 at the Observatoire de Haute Provence in southern France (44°N). The latest annual trend estimate shows cooling of 2 K/decade in the lower mesosphere increasing with altitude to a significant trend of 3 K/decade at 65 km. A smaller value of 2 K/decade is observed in the upper mesosphere, with a possible warming around 80 km, but with large uncertainties in this altitude range. As in the case of midlatitude rocketsonde measurements, a seasonal difference of the trend is observed. However, this result is of poor confidence for the winter trend owing to atmospheric variability and the limited amount of data.

### 5.1.4. Satellites

[79] *Aikin et al.* [1991] investigated trends at 44°N in the lower mesosphere using 10 years of data (1980–1990) from the stratospheric sounder unit (SSU) instrument channel 47X [*Nash*, 1988] on board the TIROS meteorological satellite but reported results mainly for the stratosphere. Global observations of ultraviolet limb radiance from the SME have been analyzed by *Clancy and Rusch* [1989] to obtain atmospheric temperature profiles over the altitude range 58–90 km between 1982 and 1986. However, the 5-year interval of the SME observations is too small for a trend analysis and will not be considered here. The SAGE II is an orbiting, solar occultation, multichannel photometer. It has been in operation since October 1984 and offers a nearly global coverage from 75°S to 75°N [*Burton and Thomason*, 2002]. The attenuation of solar transmission is measured in seven wavelength channels as the apparent path to the Sun descends or ascends through the atmosphere. Rayleigh extinction is derived between 40 and 65 km, leading to density profiles having a vertical resolution of 5 km. From 1984 to 2000 the preliminary derived trend in density is around  $-1\%$  /decade in nearly all latitude bands for the altitude range from 50 to 60 km [*Burton and Thomason*, 2002]. A new version of the density data has been included in the newly released v6.10 SAGE II

data set. An improved trend analysis of the new data is currently underway, but no results are available yet.

[80] The HALOE experiment aboard UARS has provided atmospheric temperature profiles from about 35 to 86 km since October 1991 using the technique of solar occultation by the Earth's limb in the 2.8- $\mu\text{m}$  CO<sub>2</sub> band. A long-term increase of the CO<sub>2</sub> mixing ratio consistent with its rate of increase in the troposphere has been accounted for in the HALOE retrieval algorithm. The measured characteristics of the HALOE instrument indicate no degradation that would affect its long-term trends. Retrieved temperature profiles reported by *Remsberg et al.* [2002] contain extrapolations to altitudes below 35 km using the National Centers for Environmental Prediction data set and above 86 km using the Mass Spectrometer Incoherent Scatter model climatology. The entire data set is based on the new (version 19) algorithm. Zonally averaged temperature time series at 12 pressure levels from 5 mb to 0.01 mb were analyzed within 10° wide latitude zones from 40°N to 40°S using the multiple linear regression (MLR) technique. Results for low latitudes were derived from a 30° wide latitude zone centered at the equator. Only those terms that are 95% significant have been retained in the final MLR models. *Remsberg et al.* [2002] analyzed for seasonal (annual and semiannual), interannual, solar cycle, and linear terms. An in-phase, solar cycle (SC) term is present in the data for the upper stratosphere. In the upper mesosphere the SC temperature maximum occurs 1–3 years after the maximum in solar activity. The HALOE data also indicate a significant long-term cooling trend of 1.0–1.6 K/decade at 1 mb in the tropics and at 0.2 and 0.3 mb at 20°N. Weaker and less significant cooling trends were found in the upper stratosphere for some of the other latitudes. These data were not analyzed for a seasonal or monthly trend because the occultation sampling was not frequent enough at each latitude zone.

[81] The WINDII experiment is also able to provide good temperature profiles [*Shepherd et al.*, 2001] by the same technique used by *Clancy and Rusch* [1989]. The WINDII experiment aboard the UARS provides mesospheric temperatures in the altitude range of 65–90 km altitude [*Shepherd et al.*, 2001]. However, no trend estimates have been computed with these new data so far. Some results related to WINDII data are discussed in section 5.2.1.

### 5.1.5. Seasonal/Latitudinal Differences

[82] Very few authors have investigated the seasonal behavior of trends for this region because even for annual trends the confidence levels are often marginal. Consequently, only qualitative effects can be reported. From U.S. rocket launches, mainly located in the tropical and subtropical zone, *Keckhut et al.* [1999] found no significant seasonal effects, while middle- and high-latitude Russian rocket measurements and the Rayleigh lidar in southern France have revealed a warming tendency in the upper stratosphere during winter and a

cooling tendency during summer. In the mesosphere, spring and fall seem to show a smaller cooling than winter and summer [Kokin and Lysenko, 1994; Semenov et al., 2002] for all the latitudes. Some studies [Lübken, 2000, 2001] have been restricted to summer because the variability is so small (compared to winter at middle and high latitudes) that trends are easier to detect. Using rocket grenade and falling sphere data, Lübken [2000, 2001] has reported zero temperature trend in summer for the entire mesosphere.

[83] The different plots shown in Figure 5 are very instructive; they indicate that there is a certain agreement for tropical-subtropical regions. A trend from 1 to 2–6 K/decade is seen, increasing with altitude at mid-latitudes. The cooling peaks in the lower mesosphere with a large uncertainty of 2–8 K/decade. At high latitudes, only two measurements are available, one from Russian rockets at Heiss Island and the other from falling spheres and rocket grenade measurements [Lübken, 2000, 2001], which are mutually contradictory in the lower and middle mesosphere regions.

## 5.2. Mesopause Region

### 5.2.1. Zonal, Annual Mean Trends

#### 5.2.1.1. Northern Hemisphere Trends

[84] The mesopause region is characterized by a dominance of dynamical control of temperature, which is in contrast to the lower region where solar heating (through ozone absorption) is the main forcing. Measurement records of temperature at the mesopause level using direct and indirect estimates, reported in the literature, are probably more numerous than those from the lower or middle part of the mesosphere. Most of the temperature trend results pertaining to the mesopause region are listed in Table 5, details of which are given below.

[85] Most of the results obtained from satellite techniques for the upper mesosphere have been described in section 5.1.4. Clancy and Rusch [1989] and Clancy et al. [1994] reported a 5-year (1982–1986) morphology of mesosphere temperatures derived from altitude variations of the ultraviolet limb radiance measured by the Solar Mesosphere Explorer satellite. They present monthly averages at 10° latitude and ~4 km altitude resolution for the 1982–1986 interval. Clancy and Rusch [1989] determine an 11 K uncertainty for the monthly means at 90 km. Their analysis was based on only 5 years of data, which is far too short for any reliable trend estimate. However, more recently, the WINDII experiment aboard the UARS provides good daytime temperature profiles in the altitude range 65–90 km. The data cover the period from November 1991 to April 1997 [Shepherd et al., 2001]. Case studies have been presented and discussed in detail by Shepherd et al. [2002, 2002b]; however, no trend estimates have been computed so far. Figure 6 illustrates the annual variability of daily zonal

mean mesospheric temperatures at 87 km, observed by WINDII in the 35°N–45°N latitude band over the period 1991–1997 (solid circles) [Shepherd et al., 2002, 2002b], Na lidar nightly mean temperatures observed at 87 ± 2.4 km at Fort Collins (41°N, 255°E) from 1990 to 1999 (squares) (courtesy of C. Y. She), and hydroxyl rotational temperatures from the Bear Lake Observatory (42°N, 212°E) at 87 km from 1991 to 1996 (shaded circles) (courtesy P. J. Espy). No tidal perturbations have been removed from the satellite data for this latitude band, although calculations of the contribution of the semidiurnal tide to the variability seen around days 250–300 have shown that this variability cannot be assigned exclusively to tides. The WINDII, Na lidar, and OH rotational temperature comparison illustrates the potential of combined ground-based and satellite data analysis in assessing the geophysical variability as an aid to the study of temperature trends in the upper mesosphere and the mesopause region.

[86] Available useful results on annual mean long-term temperature trends (K/decade) as reported in the recent literature for the mesopause region during the past 2 decades for both Northern and Southern Hemispheres are plotted in Figure 7. Sigernes et al. [2003] measured the temperature from Adventdalen (78°N, 15°E) near Longyearbyen, Svalbard, Norway, using the OH airglow technique. The length of the data set is from the winter of 1980/1981 to 2001. Nighttime measurements at this high-latitude site are only possible from November to February. A 1-m focal length Ebert-Fastie spectrometer has been used for measuring the OH(6-2) (1983–2001) or the OH(8-3) (1980–1983) vibrational band. The average rotational temperature of the OH airglow layer has been calculated from these bands. In general, there are very large variations in the Svalbard OH temperatures on timescales from minutes to months. The time series is very irregular from year to year; therefore it is very difficult to detect trends in this time series, as is the case for winter polar mesospheric data sets in general. Nielsen et al. [2002] have reported a cooling trend of 6 K/decade using the above data but with much larger error bars and without considering several corrections as noted by Sigernes et al. [2003]. In this recent assessment, Sigernes et al. [2003] conclude that there has been no significant trend during the past 20 years.

[87] As stated in section 5.1.2, Lübken [2000, 2001] using the rocket grenade and falling sphere techniques has reported a negligible temperature trend of around -0.24 (±0.14) K/decade for the mesopause region (up to 85 km) during summer for high latitudes. Semenov et al. [2002] and Golitsyn et al. [2000] have reported a zero temperature trend in the mesopause region (OH emission height) for the summer season obtained for mid-latitudes. By combining these two results, the Russian group concluded that the region for which the temperature trend is zero near the mesopause during summer occupies a wide interval of latitude. However, the Rus-

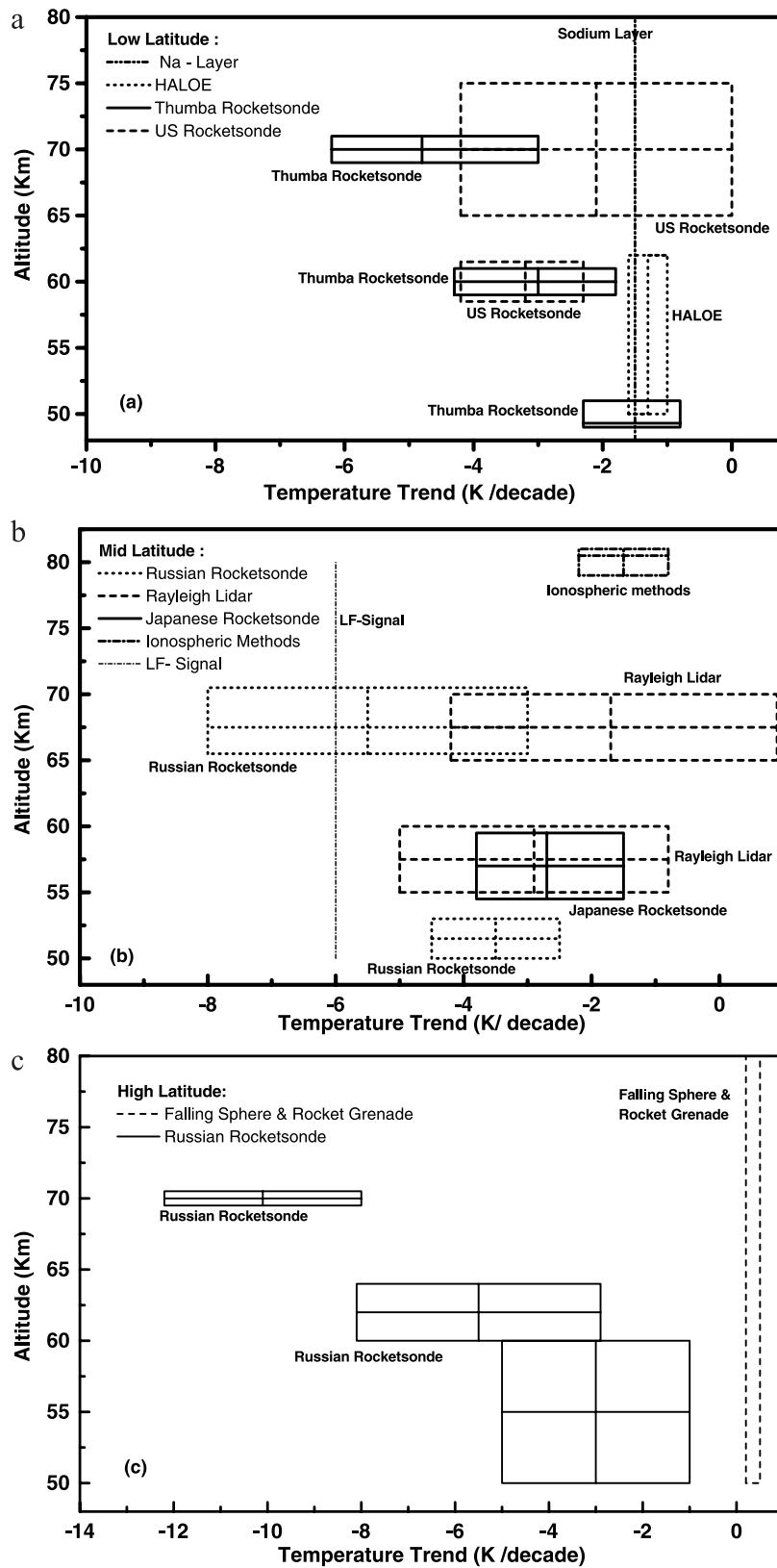


**Figure 5.** Temperature trend (K/decade) for the mesospheric region as reported in the literature by different authors using different techniques for three different latitude ranges as classified in this paper: (a) low latitudes, (b) midlatitudes, and (c) high latitudes. In Figures 5a–5c, trends at selected altitudes are shown with error limits.

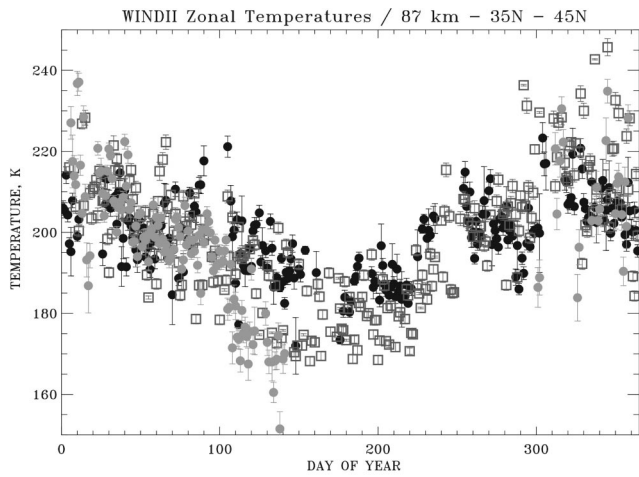


**Figure 6.** Comparison of WINDII temperature climatological means at 87 km, obtained at 35°N–45°N latitude from 1991 to 1997 (solid circles) with Na lidar temperatures at 87 ± 2.4 km at Fort Collins (41°N, 255°E) from 1990 to 1999 (squares) (courtesy C. Y. She), and OH rotational temperature climatology at 87 km at Bear Lake Observatory (42°N, 212°E) from 1991 to 1996 (shaded circles) (courtesy P. J. Espy).

sian rocket results [Golitsyn et al., 1996; Semenov et al., 2002] for the winter season are in contrast with the large negative trends reported at 81°N, which reach –12 K/decade at 75 km.

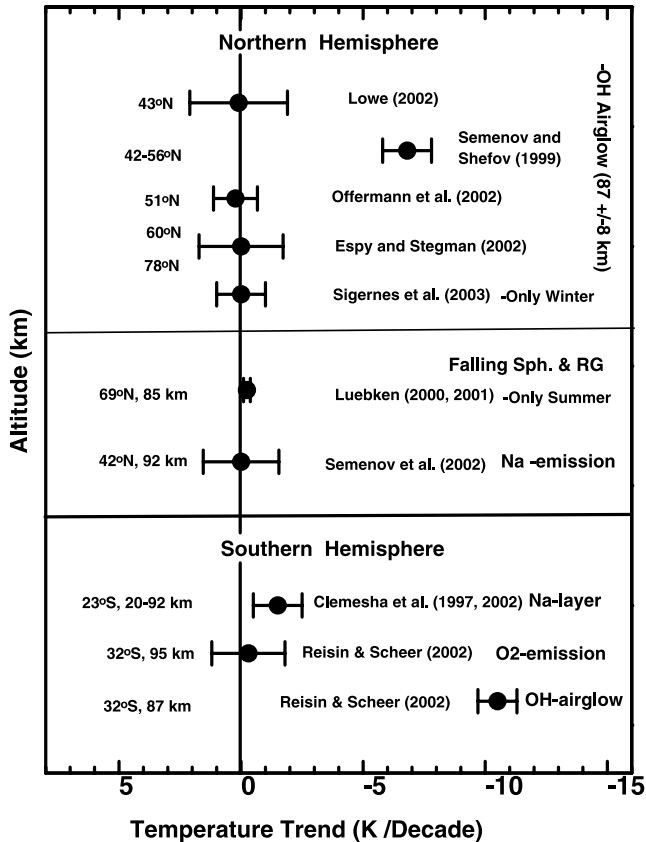


**Figure 7.** Annual mean long-term temperature trends (K/decade) as reported in the recent literature for the mesopause region during the past 2 decades.

[88] *Espy and Stegman* [2002] have been measuring the temperature above Stockholm (59.5°N, 18.2°E) since May 1991 using the hydroxyl rotational temperature from the (3,1) band. They found no significant trend during 7 months of the year but found a positive trend in January ( $5 \pm 2$  K/decade) and a negative one in September ( $2.1 \pm 1.8$  K/decade).

[89] A long data set is available from Wuppertal (51°N, 7°E) obtained during the period from 1980 to 2001 using the hydroxyl 3-1 band. Observations were made on an average of 200 nights per year. They exhibit about zero trends when analyzed on an annual basis. Instead, the data show considerable decadal variations that would complicate trend analysis for shorter subsets of data. However, when analyzed on a monthly basis, considerable trend values are obtained that appear to show systematic variations during the course of the year in the range  $\pm 1.5$  K/decade (maximum in June and minimum in September). Taking the annual mean of these, the values cancel almost completely and give a (nonsignificant) trend of  $0.2 (\pm 0.9)$  K/decade [Offermann et al., 2003].

[90] *Lowe* [2002] reported OH temperature data during the period from 1990 to 2000. These results are from Delaware observatory (42.5°N, 81.2°W) in Canada, using Fourier transform spectroscopy of the near-infrared hydroxyl airglow (3-1 and 4-2) bands. Observations were made on an average of 50 nights per year. Calibration was done by hourly comparison with an internal standard lamp and an annual comparison directly with an external standard lamp. Trend detection was performed by linear regression after removal of a seasonal trend. Data from Delaware observatory in Canada have so far not shown a trend significantly different from zero ( $0.1 \pm 2.4$  K/decade) [Lowe, 2002].

[91] Two pioneering studies of hydroxyl rotational temperature were carried out at the Abastumani Observatory in Georgia (41.8°N, 42.8°E) by *Fishkova* [1983] during the period from 1958 to 1970 and at the Zvenigorod Observatory (55.7°N, 36.8°E), as described by *Shefov* [1968, 1972]. Neither of these data sets as presented in these references is suitable for the determination of a long-term trend in rotational temperature; that of *Fishkova* [1983] is presented only as a smooth curve for the 9-3 and the 6-1 bands, without any explanation of the process by which the curves were derived. Similarly, *Shefov* [1968] presents a single smooth curve for the combined temperatures from the 4-1, 5-2, 6-2, and 7-3 bands. *Shefov* [1972] gives annual means for both his own data for 1958–1965 and that of L. M. *Fishkova* for 1958–1964 but does not explain how the large seasonal trend known to exist in the latitude range of these measurements was removed to obtain the annual mean. The more recent practice has been to base trend analyses on nightly mean temperatures from which the seasonal variation has been removed or to measure the trend in monthly mean temperature. *Semenov and Shefov* [1999] have discussed the basis of the empirical

model, including a long-term trend, which they give as  $-6.8 (\pm 1)$  K/decade based on the data of *Fishkova* [1983], *Shefov* [1969], and *Shefov and Piterskaya* [1984]. It represents exclusively the Shefov and the Fishkova data sets, but it also combines data from different latitudes and OH bands.

[92] There have been several attempts to combine these two data sets (including the extension of the Zvenigorod data set to include more recent years) to determine the long-term trend, sometimes in combination with additional data from other techniques and sources [*Golitsyn et al.*, 1996; *Semenov et al.*, 2002], focusing more on seasonal analysis of trends. As discussed in section 3.3, the determination of trends from inhomogeneous combinations of data from different bands, different latitudes, and different techniques must be treated with caution. These analyses indicate that near the mesopause the trend passes into a region of positive values. Between altitudes of 82 and 93 km, through all seasons, there is a transition zone where at some point the trend is practically equal to zero [*Semenov et al.*, 2002]. For summer this altitude of zero trend is around 85 km, whereas for winter it is around 92 km. However, the Zvenigorod data set by itself appears to constitute a homogeneous time series extending over more than three solar cycles. If the individual observations are still available, it would be highly desirable for them to be reanalyzed, using recent methodology, to provide realistic estimates of the uncertainties.

[93] With both volcanic and solar influences accounted for by the simplest model possible, a temperature trend based on the Na lidar data between 1990 and 2001 was deduced, with the trend overlapping zero within  $2\sigma$  uncertainty (or 95% confidence). However, the best estimate of the trend is a positive  $\sim 2$  K/decade between 83 and 90 km, going to zero ( $\pm 1.4$  K/decade) at 92 km and becoming negative from this height up to 102 km. A nearly constant trend of  $-2$  K/decade was found between 96 and 101 km. The trend turns positive above 103 km and steadily increases to 3.5 K/decade at 105 km. Though a positive trend between 83 and 90 km is in disagreement with the results from other instruments and at other latitudes [*Lübken*, 2000, 2001; *Semenov et al.*, 2002], it is consistent with *Keckhut et al.* [1995]. That the trend goes to zero and becomes positive again beyond 103 km is in agreement with *Semenov et al.* [2002] and a recent modeling result [*Akmaev*, 2002].

#### 5.2.1.2. Southern Hemisphere Trends

[94] The only mesopause region temperature measurements of trends presently available for the Southern Hemisphere are from the midlatitude station El Leoncito (32°S) [*Reisin and Scheer*, 2002] and the Antarctic station Davis [*Burns et al.*, 2002]. A long series of OH data from a station in Brazil at 23°S is also available since 1973. However, the more recent data from 1987 to 1994 using the OH(9,4) band and from 1994 to present using OH(6,2) should be more reliable [*Takahashi et al.*,

1995]. However, no trend analysis has been done from this later data set, which may be worthwhile to do in future. While the El Leoncito data have no seasonal coverage before 1998, the seasonal coverage at Davis is only limited by natural constraints (i.e., excluding 3 months around summer solstice). The same OH band (6-2) is observed at both sites, but at El Leoncito, temperature trends are also available for O<sub>2</sub> (at 95 km nominal) as well as intensity trends for both emissions. The El Leoncito trends are supposed to be free of a seasonal effect, because of the processing used, and of solar cycle effects for which there is no evidence in the OH data and only weak evidence for the O<sub>2</sub> emission. At El Leoncito, *Reisin and Scheer* [2002] derived a strongly negative trend for the OH rotational temperature ( $-10.5 \pm 0.8$  K/decade) from their data obtained in 1986/1987 and 1992 and from 1997 to 2001, but they derived a negligible trend of the order of  $-0.3$  K/decade for the O<sub>2</sub> emission. For the O<sub>2</sub> emission the uncertainties are asymmetric, because of a possible solar cycle effect (in contrast to the situation with OH), leading to trends between  $+1.1$  K/decade and  $-2.1$  K/decade. That is, the trend is consistent with zero. Model results that show trends changing sign near 100 km [*Akmaev*, 2002] suggest that the observed differences between the two emission layers may be real. The trends of *Reisin and Scheer* [2002] were determined by linear regression over the mean values, with due regard to episodic variability (the 1997 ENSO signatures, etc.). Only for O<sub>2</sub>, was there some evidence for a solar cycle effect that was estimated to adjust the uncertainty limits of the derived temperature and intensity trends, as mentioned above.

[95] *Burns et al.* [2002] discuss observations at the Antarctic station Davis (69°S, 1990 and 1995–2000). At Davis, mean temperatures representative of midwinter derived from the data for most of the year show variability attributable about as much to solar activity as to possible long-term trends, so that the separation of the two effects is presently not possible. The interannual variability they observe is consistent with a solar cycle variation of  $\sim 7$  K. The evidence for a trend is still too faint to be safely distinguished from a possibly strong solar cycle effect.

[96] The only other trend result available for the Southern Hemisphere is not a temperature trend but the observation of a descending trend of the atmospheric sodium layer (more precisely, the layer centroid height,  $-375$  m/decade [*Clemesha et al.*, 1992, 1997]). However, this result cannot be related simply to any mesopause region temperature trend. A discussion of these results is included in section 5.3. There may well be a relation between the observed positive airglow brightness trends (as reported by *Golitsyn et al.* [1996] and *Reisin and Scheer* [2002]) and decreasing layer heights as observed for the sodium layer, but this question has not yet been treated in the literature.

### 5.2.2. Regional Trends and Short-Term Differences

[97] Trend data presently available do not give a clear-cut picture of latitudinal effects that can easily be interpreted without some guidance by models. A possible systematic variation of trends with latitude is suggested by some modeling studies. For example, modeling results for realistic scenarios of CO<sub>2</sub> increase predict a latitudinal dependence in the mesopause region [Akmaev, 2002]. This may be consistent with the absence of observed trends at the Arctic summer mesopause. Note, however, that longitudinal structures that may affect observations are presently not included (or not reliably included) in the models.

[98] On the other hand, the considerable latitudinal dependence of the seasonal temperature variation may have an impact on the accuracy of trends derived from observational data. That is, for data obtained at higher latitudes (where the seasonal variation may be the dominant factor of variability) and that do not uniformly cover all the seasons (again, a problem particularly likely to affect optical observations at high latitudes), the correction for season is more delicate and, unless thoroughly resolved, may leave spurious contaminations in the derived trends.

[99] One must keep in mind, however, that geographical variations of wave activity (due to the spatial distribution of sources like convection, orography, variations in solar forcing depending on humidity, etc.) and the conditions of vertical propagation in the lower and middle atmosphere may give rise to local differences in observable upper atmosphere trends (e.g., see the recent discussion by Bittner *et al.* [2002]; also Nielsen *et al.* [2002] discuss a relation between mesopause region temperatures and stratospheric winds). This means that, strictly speaking, only differences in trend results obtained at close-by sites may be regarded as contradictory. Some results on the temperature trends on a seasonal basis are discussed in section 5.2.1 and are plotted in Figure 8. The salient feature in Figure 8 is an agreement in all the data sets for the summer season where no trend is noticed during the past few decades at the height of the OH emission layer. In the case of the winter season a zero trend is also noticed for two high-latitude stations, while the Russian results indicate a cooling at midlatitudes.

### 5.2.3. Long-Term Variations of Temperature Variability

[100] Middle atmosphere temperatures show strong day-to-day variations at a given altitude and location. This variability can, for instance, be described by the standard deviation from the monthly temperature mean ( $\sigma$ ). Doing so, two surprising facts are obtained: (1) The standard deviation  $\sigma$  (or respective variances  $\sigma^2$ ) can be fairly large and frequently are considerably larger than the estimated precision of the measurements. (2) The  $\sigma$  values are not always constant in time, as one would expect if they represent a measurement error. They rather can vary on various timescales. For example, the

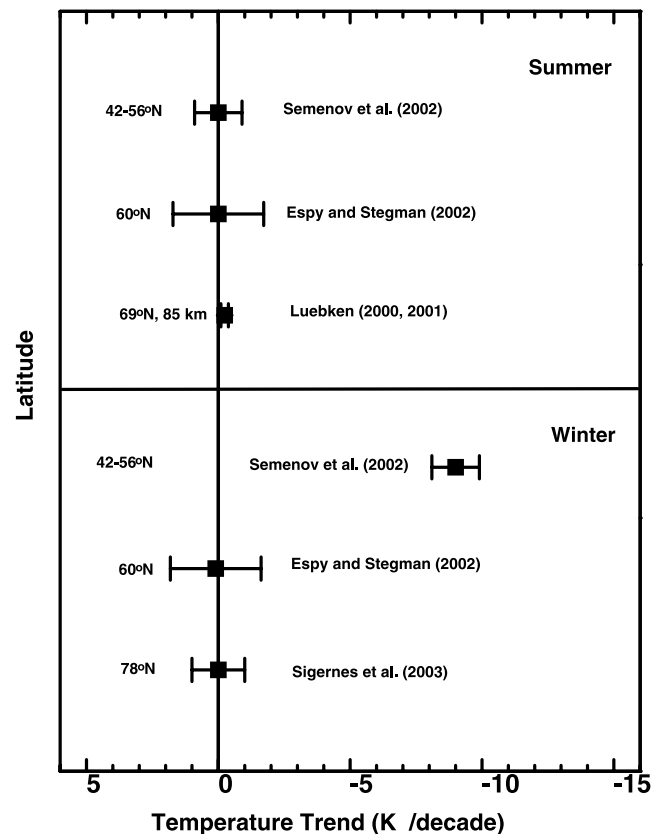


**Figure 8.** Long-term temperature trends (K/decade) for summer and winter seasons as reported in the recent literature for the mesopause region. Results are arranged in order of descending latitude.

temperatures derived at Wuppertal (51°N, 7°E) from the (3,1) emissions of hydroxyl in the upper mesosphere (87 km) show standard deviations of ~5–6 K. The precision of the single data point (nightly mean) is estimated to be 1–2 K, i.e., much smaller than the fluctuations seen (for details see Bittner *et al.* [2002]).

[101] There are no indications for a seasonal variation of the Wuppertal standard deviations, even though the temperature swing itself is large during the course of the year. This has been discussed by Bittner *et al.* [2002] and has been compared to lower altitudes. In contrast to 87 km, large seasonal variations of temperature variability (standard deviations) are found in the lower mesosphere and middle stratosphere, the values being much larger in winter than in summer. Similar results had earlier been obtained by Leblanc *et al.* [1998]. Changes of the variability of the OH data at Wuppertal are seen, however, if longer timescales are considered. This is illustrated by Figure 9a. Here the annual means of the Wuppertal fluctuations are given in terms of the annual mean standard deviation for the years 1981–1997. A substantial long-term variation of temperature variability is seen in Figure 9a, as is indicated by the dashed line (polynomial fit to the data points). A similar result is obtained at lower mesosphere/stratopause altitudes, as shown in Figure 9b from SSU data (for details see Bittner *et al.*

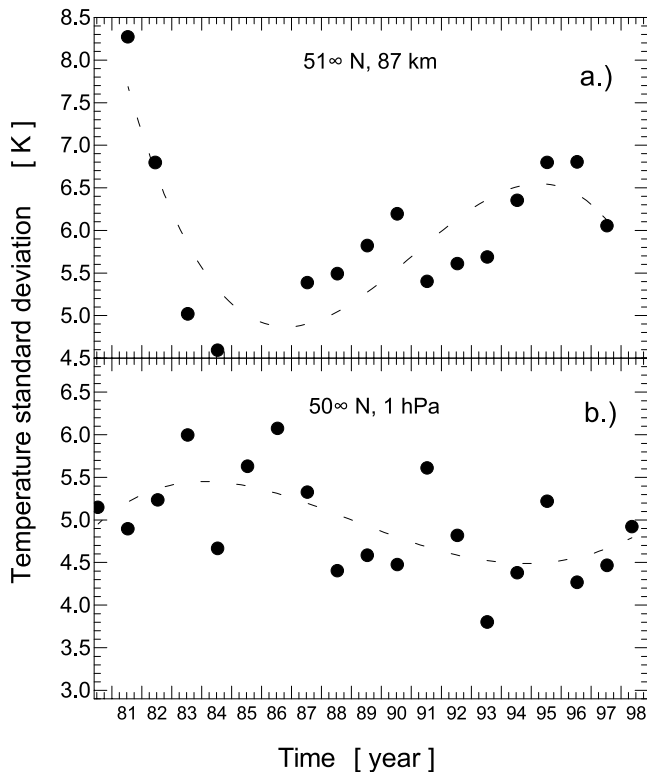


**Figure 9.** Long-term changes of temperature variability. Annual means of standard deviations are given at (a) 87 km, ( $51^{\circ}\text{N}$ ,  $7^{\circ}\text{E}$ ) and (b) 1 hPa ( $50^{\circ}\text{N}$ ,  $5^{\circ}\text{E}$ ) [from *Bittner et al.*, 2002]. Reprinted with permission from Elsevier.

[2002]). The dashed lines in Figure 9 indicate that the long-term variations contain a systematic pattern. They even suggest an anticorrelation of the temperatures at the two altitudes. Many more data of this type have been presented by *Bittner et al.* [2002].

[102] Considering the magnitudes of the standard deviations and their apparent systematic time variations, it appears unlikely that they are measurement errors. This is especially true as the standard deviation,  $\sigma$ , is a fairly robust parameter. It is insensitive to temperature biases that might originate from the measurement method or from instrumental errors. It would be affected by erroneous multiplicative factors though. If such a factor should, however, be  $>5\text{--}10\%$ , it would presumably be detected in the primary data, i.e., in the temperatures themselves. In this case a suspicious proportionality between excursions of the temperature and its standard deviation should occur. It is therefore suggested that the standard deviation of temperature as described here is an atmospheric parameter *sui generis* (at least for measurements with high precision) and that the fluctuations it represents are mostly in the atmosphere and not so much in the instruments.

[103] Following these lines, changes in temperature variance  $\sigma^2$  have tentatively been interpreted as being indicative of changes in atmospheric wave action by *Bittner et al.* [2002]. Changes of variances at a given altitude have therefore been compared to long-term

temperature changes at altitudes  $\sim 30$  km lower. Three altitude pairs in the mesosphere (and stratosphere) have been considered (at  $50^{\circ}\text{N}$  and  $70^{\circ}\text{N}$ ), and significant correlations have been found (significance level around 95% [*Bittner et al.*, 2002]). The sensitivity of temperature changes at the lower level to changes of wave activity ( $\sigma^2$ ) at the higher altitude has been determined. It has been compared to respective sensitivities derived from the SKYHI general circulation model. A very reasonable agreement is obtained [*Bittner et al.*, 2002]. These results are in line with the “downward control principle” [*Haynes et al.*, 1991].

[104] Summarizing these results, it appears worthwhile to study the variations of atmospheric variability on a broader basis. On the one hand, it would be desirable to find out whether the standard deviations of atmospheric dynamical parameters other than temperature are also suitable indicators of long-term changes. On the other hand, the temperature analysis needs improvements: (1) The database needs to be increased. Figure 9 contains 15–18 data points, which is just marginal for significant statistics. (2) The altitude resolution needs to be improved. The SSU temperatures and the OH temperatures are from fairly broad atmospheric layers (of the order of 10 km), which tend to suppress waves with small vertical wavelengths. (3) The analysis of *Bittner et al.* [2002] is restricted to the winter in western Europe ( $50^{\circ}\text{--}70^{\circ}\text{N}$ ). Other times of the year and other locations in the world might be worth studying, especially in the Southern Hemisphere.

### 5.3. Indirect Trend Estimates

[105] Ionospheric absorption measurements have been carried out at different measuring stations. However, only *Nestorov et al.* [1991] tried to derive mesospheric temperature changes using field strength observations of a far distant transmitter in the LF range (164 kHz and distance 1720 km). By a regression analysis they obtained a connection between ionospheric LF absorption during the summer months near noon and the mesospheric temperature, and they estimated a temperature decrease of about  $-5.2$  K at heights between 70 and 80 km for the time interval between 1959 and 1986. The observed increase of ionospheric absorption may be caused by a decrease of the gradient of the electron density between 70 and 80 km, which can be explained by an increasing formation of water cluster ions near 80 km due to the temperature decrease.

[106] Long-term observations of phase heights have been carried out regularly at Kühlungsborn since 1959 on a frequency of 162 kHz (path length 1023 km and midpoint coordinates of  $50.7^{\circ}\text{N}$ ,  $6.6^{\circ}\text{E}$ ). The reflection height of this measuring path corresponds to a height of constant electron density of  $\sim 450/\text{cm}^3$ . The reflection height at constant solar zenith angle ( $\sim 82$  km for  $\chi = 78.4^{\circ}$ ) shows a significant lowering during the last four solar cycles as can be seen in the top plot of Figure 10. Here all monthly trends are negative with a significance

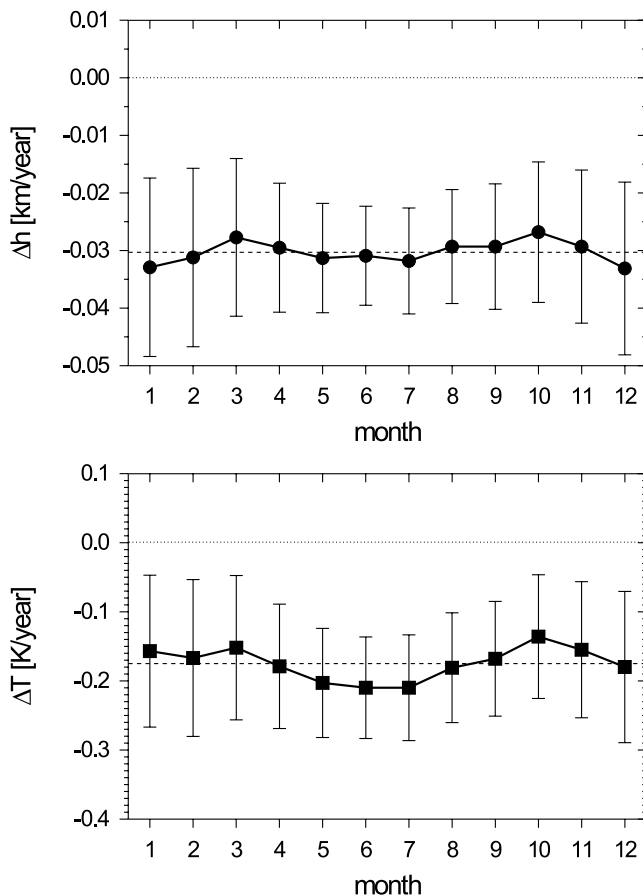


**Figure 10.** Seasonal variation of mean trends of (top) the low-frequency (LF) reflection height as well as of (bottom) the mean temperature trends for the height interval 48–82 km as derived from LF phase height observations (162 kHz, midpoint 50.7°N, 6.6°E, and constant solar zenith angle  $\chi = 78.4^\circ$ ) between 1959 and 2001. For the derivation of the temperature trends it was assumed that trends of the density of nitric oxide and of the effective recombination coefficient can be neglected at the reflection height. The included error bars mark the limits of the 95% significance level. The dashed lines mark the mean yearly trends.

level of >95% as shown by the error bars. These long-term trends can be explained by a temperature decrease below the reflection height. Using trend results derived by Taubenheim et al. [1994] for the height of the 1-hPa pressure level (48 km) from satellite observations, mean temperature trends can be derived from LF phase height measurements for the height interval between 48 and 82 km. The derived temperature trends are presented in the bottom plot of Figure 10. Here it has been assumed that no essential long-term changes of the nitric oxide density and of the effective recombination coefficient occur at the reflection height near 82 km. All monthly temperature trends are significant with >95% ranging from  $-1.4$  K/decade to  $-2.1$  K/decade with mean errors of 95% significance from 0.7 K/decade to 1.1 K/decade. The derived temperature trends are even stronger if trends of the nitric oxide density and of the effective recombina-

tion coefficient are assumed (estimated from model predictions of different greenhouse gas experiments). In this case the derived mean temperature trends are higher than the trend values presented in the bottom plot of Figure 10 (mean yearly trend of about  $-0.28$  K/year instead of  $-0.18$  K/year as marked by the dashed line in the bottom plot of Figure 10). Further details of the phase height analysis are given by Bremer and Berger [2002]. Bremer and Berger compare trend results (based on their LF phase height observations at 51°N) with model predictions that not only consider a realistic CO<sub>2</sub> increase but also an O<sub>3</sub> decrease and find reasonable agreement.

[107] A long-term change in the height of the atmospheric sodium layer has been interpreted as possibly indicating a cooling trend in the upper atmosphere. Clemesha et al. [1992, 1997] analyzed sodium profiles obtained at São José dos Campos, Brazil (23°S), and found a trend of  $-37 \pm 9$  m/yr for the centroid height of the sodium layer observed between 1972 and 1994. If this trend is indeed the result of atmospheric subsidence (and Clemesha et al. [1997] throw some doubt on this interpretation), then the magnitude of the trend is related to the long-term variation in the temperature structure of the entire atmosphere below the sodium layer, which is centered on a height of  $\sim 92$  km. Clemesha et al. [2002] calculated the effect on constant density levels of the temperature trend derived from the Thumba rocket measurements by Beig and Fadnavis [2001] and compared this to the temperature trend needed to produce the observed change in sodium layer centroid height. In both cases, zero trend below 20 km was assumed, and in the case of the Thumba data a constant trend of  $-5.5$  K/decade above 70 km was assumed, the maximum height for the rocket data. The results of this analysis showed that for a height of 92 km a constant temperature trend of  $-1.5$  K/decade from 20 km up would produce a height trend of about  $-375$  m/decade, close to the observed trend in the sodium layer centroid, and that the Thumba profile would result in a sinking of the constant density levels by  $\sim 730$  m/decade. Thus it can be concluded that if we interpret the centroid trend in terms of atmospheric subsidence, the observed height trend would correspond to  $\sim 50\%$  of that derived from the rocket measurements or to a height-independent trend (above 20 km) of close to  $-1.5$  K/decade.

[108] The analysis of the sodium measurements from Brazil has recently been updated to include data up to the end of 2001. It is found that the trend observed in the earlier data has not continued and that a rise in the height of the sodium layer has occurred over the past 10 years. Analyzing the complete data set, which now covers a period of 30 years, no significant net trend is found. This is an interesting example of the difficulties involved in the interpretation of long data series. In the case of the sodium data a clear downward height trend was observed between 1972 and 1987, and it was suggested

that this might be the result of global change caused by increased atmospheric CO<sub>2</sub>. It now appears that this cannot be the case because the sodium layer height has returned to its earlier value. It must be concluded that although statistically significant changes in the height of the atmospheric sodium layer occur over periods of tens of years, these changes are not indicative of a long-term global trend.

[109] The result of long-term measurements of the intensity of the sodium emission (1957–1992) is reported by *Semenov et al.* [2002] for Abastumani (41.8°N). They calculated the correlation between sodium emission intensity (in rayleighs) and temperature at the height of ~92 km. They reported no trend at 92 km for the winter season. However, it is airglow intensity not height that is being measured, and the contamination by OH(8,2) makes Na emission intensity measurements virtually worthless.

[110] *Gadsden* [1998] reports an increase in noctilucent cloud (~83 km) observations over northwest Europe. One hypothesis for this variation is a small gradual temperature decrease in mesopause summer temperatures amounting to 7 K from 1964 to 1996 [*Gadsden*, 1990]. Alternatively, an increase in water vapor concentrations stemming from anthropogenic increases in tropospheric methane [*Thomas et al.*, 1989] may be partly responsible. Earlier, *Gadsden* [1990, 1997] analyzed the occurrence frequency of noctilucent clouds as observed by a network of observers and discovered a systematic increase by a factor of ~2 from the middle of the 1960s to the present time. He found that the seasonal and altitudinal distribution of noctilucent cloud occurrence remains invariant and that this precludes explanation of the trend by changes of observing conditions. In 1992–1993 a significant decrease in the occurrence frequency of the noctilucent clouds occurred. Whether or not this was due to the 1991 Pinatubo eruption is problematic [*Thomas and Olivero*, 2001]. On the other hand, *Thomas and Olivero* [2001] pointed out that this decrease occurred at solar maximum when noctilucent cloud activity is normally low. It should be noted that recent reanalysis of the NLC data and further observations near Moscow do not show any significant evidence of noctilucent cloud occurrence frequency increase [*Romejko et al.*, 2003; *Kirkwood and Stebel*, 2003]. Furthermore, it should be noted that *Lübken et al.* [1996] have pointed to the stability of the noctilucent cloud occurrence height (~83 km), which does not appear to have varied since it was first estimated ~100 years ago. *Lübken et al.* [1996] believe that this fact manifests a stability of the cloud formation conditions and puts significant limits on possible thermal variations in the upper mesosphere because of anthropogenic factors. It must be remembered, of course, that early estimates of noctilucent cloud height were very approximate. Only in recent years have accurate measurements of NLC height become possible by lidar.

## 6. MODEL SIMULATIONS OF TRENDS

### 6.1. Models for Trend Simulations

[111] The measurements reported in section 5 suggest that rapid changes in most regions of the upper atmosphere are occurring much faster than model predictions. This indicates that there is an important need to understand the underlying physics, chemistry, and dynamics of the mesosphere-thermosphere-ionosphere region and its response to natural and anthropogenic variability. In this section, we include a brief discussion of model investigations carried out in the recent past, with the aim of estimating temperature trends in the mesosphere and lower thermosphere due to anthropogenic sources. Some recent results from global models used for evaluation of global change in the upper atmosphere are also included.

[112] Theoretical models based on a fundamental understanding of interactive radiation, dynamics, and chemical processes are an important tool for studying the effect of different mechanisms on trends in the MLT temperature. Observed features can then be interpreted in terms of specific processes. Unfortunately, there are relatively few modeling studies of global change in the MLT region compared to lower regions. To some extent this is due to the limited availability of numerical models with adequate parameterizations of radiative transfer applicable to arbitrary mixing ratios for optically active greenhouse gases. Some important information related to radiative transfer in the upper atmosphere has only recently become available. Modeling results are often inconclusive and sometimes even contradictory, as is found for observations of this region. Nevertheless, there have been a few studies to investigate how the atmosphere above the stratopause might respond to the global change expected to occur in the troposphere and stratosphere, and these are summarized below.

[113] *Roble and Dickinson* [1989] pioneered work in this area. They reported the impact of global change by using a one-dimensional radiative-photochemical model to study the sensitivity to doubling of CO<sub>2</sub> and CH<sub>4</sub> in the mesosphere and thermosphere (60–500 km), but they did not include the detailed chemistry and growth rates of some important greenhouse gases like N<sub>2</sub>O and CFCs. *Portmann et al.* [1995] and *Beig and Mitra* [1997] have used two-dimensional interactive models with detailed chemistry. *Rind et al.* [1990], *Berger and Dameris* [1993], and *Akmaev and Fomichev* [1998] have used three-dimensional (3-D) dynamical models extending into the thermosphere but with little chemistry. All these studies only considered possible future temperature changes using the standard double-CO<sub>2</sub> scenario formulated in the *WMO* [1995, 1999] or *Intergovernmental Panel on Climate Change* [1995] reports. There are presently only two detailed modeling studies published concerning simulations for the past few decades and comparing outcomes with observations. *Akmaev and Fomichev* [2000] have reported a benchmark estimate of

radiative forcing in the MLT due to the increase of CO<sub>2</sub> mixing ratio observed over the last 4 decades using a spectral MLT model but without detailed chemistry. Recently, *Beig* [2000a] used the observed trends of several major forcing parameters, namely, CO<sub>2</sub>, N<sub>2</sub>O, CH<sub>4</sub>, and CFCs, during the past several decades [*WMO*, 1995, 1999] as input to a two-dimensional interactive model to evaluate the response of temperature and composition. This model considered the detailed chemistry of the MLT region.

[114] In recent times, efforts have been made to develop more sophisticated global general circulation models for use in the evaluation of global change in the upper atmosphere. Some important results from two such models will be discussed in section 6.3. These models are (1) the National Center for Atmospheric Research (NCAR) thermosphere-ionosphere-mesosphere electrodynamics general circulation model (TIME-GCM), which is the latest in a series of three-dimensional time-dependent models that have been developed over the past 2 decades, and (2) the Canadian Middle Atmosphere Model, a three-dimensional GCM which has been used in a series of multiyear experiments to examine the thermal response and ozone feedback induced by CO<sub>2</sub> doubling.

## 6.2. Past Model Results and Discussion

[115] *Fels et al.* [1980] first employed a three-dimensional GCM in a study of the sensitivity of the upper atmosphere to perturbations in ozone and carbon dioxide. They investigated the radiative and dynamical response of the atmosphere to a uniform 50% reduction of ozone and a uniform doubling of CO<sub>2</sub>. Special attention was paid to incorporating the parameterized form of the feedback due to ozone photochemistry in the stratosphere. With doubled CO<sub>2</sub> they predicted a cooling of up to 8 K in the mesosphere. Although the GCM had an upper boundary at ~80 km, the simulations in the mesosphere should be considered with caution as the model did not account for small-scale gravity waves (GW) that are currently believed to play a crucial role in the dynamics and thermal structure of the mesosphere.

[116] *Roble and Dickinson* [1989] predicted a global average cooling by ~10–15 K in the mesosphere and up to 50 K in the thermosphere for the doubled-CO<sub>2</sub> scenario. Because of thermal compression in an atmosphere with hydrostatic balance this cooling resulted in a reduction of atmospheric density by >40% at a given height in the thermosphere. *Rishbeth and Roble* [1992] broadly confirmed the findings for the thermosphere using a crude three-dimensional GCM with chemistry. The lower boundary of this model was placed at ~95 km, so that the results were only applicable in the thermosphere above ~120 km. It should be noted that both studies used a relatively low value, compared to recent data [e.g., *Shved et al.*, 1991, 1998], of the quenching rate coefficient for collisions of atomic oxygen and carbon dioxide that are important for radiative transfer in the

15- $\mu$ m band of CO<sub>2</sub> in the region of breakdown (above ~70 km) of local thermodynamic equilibrium (LTE).

[117] A study of the double-CO<sub>2</sub> climate was conducted by *Rind et al.* [1990] using a GCM without chemical feedback. *Rind et al.* [1990] also reported an overall increase of the eddy energy in the middle atmosphere due to both planetary and gravity waves. This was attributed to a reduction in the gross atmospheric stability due to a relative warming in the troposphere and a cooling in the middle atmosphere. Vertical destabilization affects the propagation of planetary and gravity waves throughout the middle atmosphere. It also favors stronger planetary and gravity wave generation in the lower atmosphere at least within the parameterization of GW sources. It should be noted that the effect of destabilization could be overestimated because of possible overestimation of the thermal response at the surface (~4.2 K) in the experiments of *Rind et al.* [1990].

[118] *Berger and Dameris* [1993] studied the effects of CO<sub>2</sub> doubling with a 3-D mechanistic model extending from the surface to 150 km. The model incorporated a gravity wave parameterization based on the formulation by *Lindzen* [1981]. They predicted a maximum cooling of ~40 K at 105–110 km that reduced to ~1–2 K near the upper boundary. This does not quite agree with the results of *Roble and Dickinson* [1989] and *Rishbeth and Roble* [1992] according to which the cooling is of the order of 10 K in the upper mesosphere and should grow with height to ~40–50 K. The study by *Berger and Dameris* [1993] also used a low value for the quenching rate coefficient.

[119] *Portmann et al.* [1995] used a two-dimensional model with detailed chemistry extending up to 110 km. They demonstrated the importance of dynamical feedback by GW momentum deposition in the mesosphere. They found that as a result of this feedback the middle atmosphere would cool because of increased CO<sub>2</sub> even in regions with a positive radiative forcing. They predicted cooling above 100 km at about half the rate reported by *Berger and Dameris* [1993].

[120] *Beig and Mitra* [1997] used a two-dimensional interactive model of radiation, dynamics, and chemistry that extends from the surface to ~85 km. It incorporated detailed chemistry, but all the dynamical processes were not properly accounted for in their model study, for example, the new parameterization of the 15- $\mu$ m CO<sub>2</sub> band above the altitude of breakdown of local thermal equilibrium. *Beig* [2000a] has further extended the earlier version to 120 km and included several new mechanisms including the parameterization of the 15- $\mu$ m CO<sub>2</sub> band above 70 km [*Fomichev et al.*, 1998] in simulating the radiative response for the past several decades as well as for the doubled-CO<sub>2</sub> scenario. The prediction of future climate responses was examined as semicontinuous time lines of quantities, such as chlorine loading and other trace gas variations, well into the 21st century. It is assumed that the tropospheric volume mixing ratio of carbon dioxide by the end of 2050 would be twice that

of the present-day value (1995 reference level), and it is taken as 712 ppm. The methane mixing ratio is also considered to be doubled (3.4 ppm) relative to 1995. Nitrous oxide and CFCs are taken as per the business-as-usual scenario [Beig and Mitra, 1997] and yield an N<sub>2</sub>O volume mixing ratio of 365 ppb and total chlorine loading due to the CFCs of 11.7 ppb for 2050. Concentrations of all other species, including SO<sub>x</sub>, are kept at ambient levels, with the assumption that they may not play a significant role. Beig [2000a] has reported a cooling of the order of 14 K at the stratopause, which reduces to 11 K above 70 km and again increases dramatically in the lower thermosphere. The results of Beig [2000a] for the past few decades of simulations indicate a cooling trend of 4–4.8 K/decade for altitudes ranging from 80 to 120 km at 10°N, which are in reasonably good agreement with observed trends for the same latitude range. Although Beig [2000a] has accounted for the feedback of NO in his study, the model did not adequately account for detailed dynamical processes like small-scale gravity waves that are currently believed to play a crucial role.

[121] Akmaev and Fomichev [1998, 2000] used the three-dimensional middle atmospheric (15–120 km) model originally developed and described by Akmaev et al. [1992]. To prevent spurious reflections of strong tidal waves from the upper boundary, the model has been extended into the thermosphere [Akmaev et al., 1996, 1997]. The model has a lower boundary at 100 mb and the upper boundary at ~220 km. A variety of physical processes important in the middle and upper atmosphere are represented in this model. They have accounted for the new parameterization of the 15-μm CO<sub>2</sub> band [Fomichev et al., 1998]. Akmaev and Fomichev [2000] have slightly adjusted the parameterization of radiative cooling in the 15-μm CO<sub>2</sub> band from their earlier version at 70 km to better match the new reference cooling rates [Ogibalov et al., 2000]. Akmaev and Fomichev [1998] have found a cooling of 8 K in the upper mesosphere and 40–50 K in the thermosphere for the doubled-CO<sub>2</sub> scenario. Recently, Akmaev and Fomichev [2000] have reported benchmark estimates for the increase in CO<sub>2</sub> mixing ratio from 313 to 360 ppm observed over the last 4 decades. They found a cooling of ~3 K in the mesosphere, which practically vanishes at 100–120 km and increases to 10–15 K in the thermosphere. Although this model has been demonstrated to realistically reproduce present-day climatology in the MLT, one must realize the limitations of the model configuration, in particular, for simulations with perturbed abundances of radiatively active tracers. The model does not include an interactive composition and cannot account for chemical feedbacks that are particularly important in the middle and upper mesosphere because of temperature-dependent reaction rates. Although radiative loss of energy is accounted for via the solar EUV heating efficiency [Roble, 1995], the model may underestimate feedback in the lower thermosphere

due to the dependence of the NO cooling rate on temperature.

[122] These studies suggest that global change effects are significant throughout the mesosphere, thermosphere, and ionosphere. The atmosphere expands as it is heated and contracts as it cools. Therefore the troposphere should expand slightly as it is warmed by a few degrees, but the upper atmosphere should contract much more because of the greater cooling. As a result the density at a given height in the upper atmosphere should decrease considerably. In addition to the changes in the major constituents of the mesosphere and thermosphere, there are significant variations that occur in the concentrations of minor neutral gas constituents such as O<sub>3</sub>, H<sub>2</sub>O, OH, HO<sub>2</sub>, CO, NO, NO<sub>2</sub>, N(<sup>4</sup>), and others. The minor species change because many of the chemical rate constants for these species are highly temperature-sensitive, and turbulent diffusion and advective transport, which determine their vertical distributions, depend on the vertical temperature structure. A doubling of the current-day methane concentration should also increase the H<sub>2</sub>O, and colder mesopause temperatures should result in an increase in noctilucent clouds. However, a detailed discussion of the changes in other species is beyond the scope of this paper.

### 6.3. Recent Global Models for Evaluating Global Change and Some Results

[123] Section 5 summarized the observational trends occurring in the mesosphere, thermosphere, and ionosphere. To better understand these trends, global models of the atmosphere are needed not only in an attempt to simulate the observed trends but also to examine future global variability and change. There are many models, and some have been summarized in section 6.2. In this section some results from two recent GCMs are discussed in detail.

[124] One such recent up-to-date model is the NCAR TIME-GCM. It is the latest in a series of three-dimensional time-dependent models that have been developed over the past 2 decades to simulate the circulation, temperature, and compositional structure of the upper atmosphere and ionosphere. It combines all of the features of the thermospheric general circulation models described by Dickinson et al. [1981, 1984], the thermosphere ionosphere general circulation model described by Roble et al. [1988], and thermosphere ionosphere electrodynamic general circulation model described by Richmond et al. [1992], and the model has been extended downward to 30 km altitude including aeronomical processes appropriate for the mesosphere and upper stratosphere, as described by Roble and Ridley [1994], Roble et al. [1987], and Roble [1995]. The most recent aeronomical updates to these original papers are given by Roble [2000].

[125] The Roble [2000] model was recently used in an attempt to examine possible changes to upper atmosphere structure from present-day conditions to the end

**Table 6. Assumed Mixing Ratio of Long-Lived Species at the TIME-GCM Lower Boundary**

Species	Present Day	2100 A.D.
CO <sub>2</sub>	350E-6 <sup>a</sup>	700E-6
CH <sub>4</sub>	6.7E-7	13.4E-7
CO	1.1E-8	2.2E-8
NO <sub>x</sub> (NO <sub>2</sub> +NO)	6.9E-9	24E-9
H <sub>2</sub>	0.5E-6	1.0E-6
H <sub>2</sub> O	4.4E-6	8.8E-6
O <sub>x</sub> (O+O <sub>3</sub> )	8.3E-6	4.1E-6
Cl <sub>x</sub> (Cl+ClO)	G-S profile <sup>b</sup>	G-S profile <sup>b</sup> multiplied by 2
N <sub>2</sub> O	G-S profile <sup>b</sup>	G-S profile <sup>b</sup> multiplied by 1.5
T	225 K	215 K

<sup>a</sup>Read, for example, 350E-6 as  $350 \times 10^{-6}$ .

<sup>b</sup>G-S is the Garcia and Solomon [1985] profile for these species.

of the 21st century. With these boundary conditions and specified inputs for the parameterizations all other physical and chemical processes are calculated self-consistently. The TIME-GCM was run with the standard December solstice forcings necessary to obtain a reasonable agreement with the observations [McLandress et al., 1996]. This tuned simulation is considered the base case for present-day atmospheric conditions.

[126] A similar set of calculations were then made assuming a perturbed atmosphere using an assumed trace gas scenario given in Table 6 for present-day conditions and a hypothetical scenario for the end of the 21st century. The scenarios are similar to those used by Bruhl and Crutzen [1988] in their one-dimensional model that was used to study global change. The lower boundary tides, gravity waves, and climatological latitudinal distributions are assumed to remain the same for the present-day and year 2100 simulations.

[127] The calculated neutral gas temperature and the H<sub>2</sub>O mixing ratio for the year 2100 assumed scenario are calculated. The calculated difference fields for the same quantities for this case minus the present-day conditions are shown in Figure 11. Most calculations have assumed only a CO<sub>2</sub>-doubling scenario, but in this case we consider additional trace gas increases. The combined effect nearly doubles the temperature decrease for the case when only doubled CO<sub>2</sub> is considered with a much greater dynamic response and H<sub>2</sub>O increase. This clearly indicates that it is important to consider the combined effect of all trace gas variations when attempting to understand possible changes in the upper atmosphere during the 21st century.

[128] Another recent 3-D GCM is the Canadian Middle Atmosphere Model, which has been used in a series of multiyear experiments to examine the thermal response and ozone radiative feedback induced by doubling of CO<sub>2</sub> from the current state. The model extends from the surface up to ~100 km. It includes comprehensive tropospheric physics, realistic radiative schemes, and orographic and nonorographic gravity wave drag schemes. This model also has an interactive gas phase

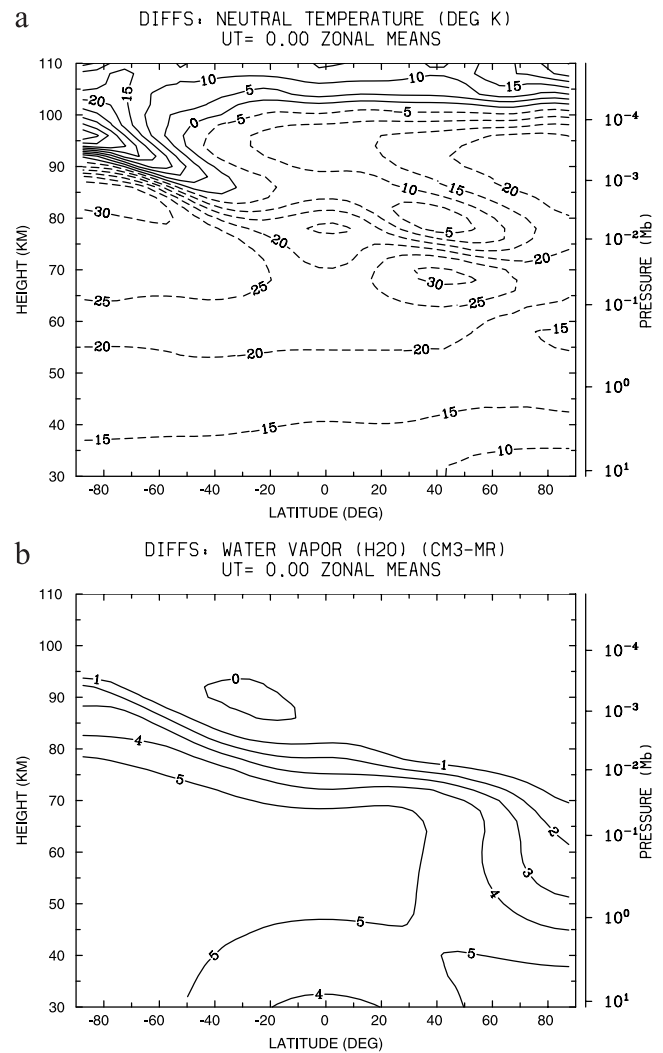


**Figure 11.** Calculated (a) neutral gas temperature and (b) H<sub>2</sub>O mixing ratio for the 2100 A.D. assumed scenario using the thermosphere-ionosphere-mesosphere electrodynamics general circulation model of the National Center for Atmospheric Research. The calculated difference fields for this case minus the present-day conditions are shown in Figure 11 for the above mentioned fields, respectively. Most calculations have assumed only a CO<sub>2</sub>-doubling scenario, but in this case, additional trace gas increases are considered, as shown in Table 6 (for detail see text).

chemistry module with inclusion of chemical heating in the upper mesosphere. Full description of the model is given by de Grandpré et al. [2000]. To estimate the significance of the ozone radiative feedback in climate change, numerical experiments have been run with and without inclusion of interactive chemistry. Without inclusion of interactive chemistry, global average temperature response maximizes in the lower mesosphere at ~14 K and reduces to 6 K near the mesopause. The latitude-altitude distribution of the response shows significant latitudinal structure with particularly weak (and statistically insignificant) temperature change near the polar summer mesopause. Inclusion of interactive chem-

istry results in an increase of  $O_3$  by  $\sim 15\%$  in the upper stratosphere and mesosphere and, consequently, leads to a reduction of the thermal response by 2–4 K because of increase of solar heating.

[129] In the mesopause region (80–100 km), doubling of  $CO_2$  results in 5–6 K cooling on a globally averaged basis. Taking into account that the  $CO_2$  amount has increased by  $\sim 15\%$  for the last 40 years and that the thermal response to  $CO_2$  increase appears to be approximately proportional to the relative change in  $CO_2$  [Akmaev and Fomichev, 2000], it suggests an average cooling of  $\sim 0.2$  K per decade. Even doubling this number to account for the combined effect of all trace gas variation as suggested by the TIME-GCM results gives us a trend of  $\sim 0.4$  K per decade that is apparently below the natural atmospheric variability. This appears to be consistent with most measurements presented in section 5.2, which could not detect temperature trend in the mesopause region during the last few decades.

[130] Being an atmospheric GCM with comprehensive tropospheric physics, the CMAM provides a very important tool for investigating the coupling between the troposphere and the middle atmosphere. A specific experiment has been carried out with the use of the CMAM in order to examine the importance of changes in surface conditions for climate simulation. The sea surface temperatures (SST) and sea ice coverage for this experiment have been prescribed from doubled- $CO_2$  conditions in a separate transient simulation using a coupled atmosphere-ocean GCM with a climatological ozone layer [Boer et al., 2000]. Figure 12 presents the difference in model thermal response to doubling of  $CO_2$  with and without taking into account changes in the surface conditions. As can be seen, inclusion of the SST changes produces a major heating of up to 4 K in the troposphere that is known as a greenhouse effect. In the middle atmosphere the effect is smaller but not negligible. Inclusion of the SST changes forces a warm anomaly of up to 5–6 K in the polar stratosphere and mesosphere regions and provides a thermal response with a high statistical confidence level (above 99%) throughout the stratosphere even on a globally averaged basis. To understand the physical processes responsible for the behavior, further analysis is required. However, it is most likely related to planetary wave activity. Changing surface conditions affect the upward propagating planetary waves, which, in turn, may affect the polar vortex.

## 7. SUMMARY

### 7.1. Summary of Observational Results

[131] During the past decade several attempts have been made to analyze different series of long-term observations and to deduce mesospheric temperature trends. The comparison of the results obtained by different observations separated by several decades is complicated, as discussed in this paper. The difficulties are

Thermal response to SST changes with  $O_3$  radiative feedback (K) [ $2\times CO_2$  & SST -  $2\times CO_2$ , interactive  $O_3$ , 20 year mean]

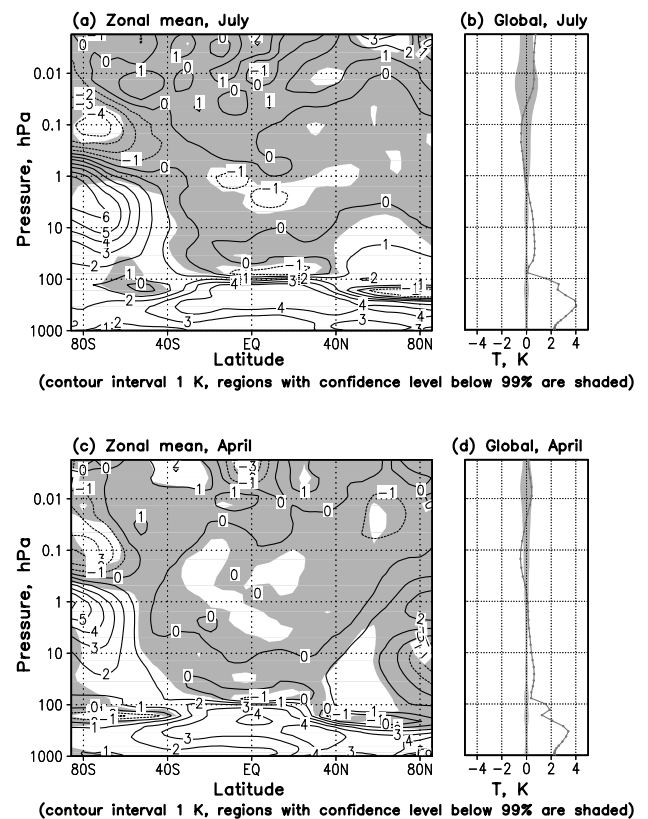


**Figure 12.** Thermal response to sea surface temperature (SST) changes with ozone radiative feedback using the Canadian Middle Atmosphere Model simulations. Figure 12 indicates the temperature difference (K) in model thermal response to doubling of  $CO_2$  with and without taking into account changes in the surface conditions for two different months: (a and b) July and (c and d) April.

related to maintenance of the same equipment sensitivity, noise level (of an anthropogenic nature in particular), and the method of data processing. All these factors should be considered very carefully. Nevertheless, there are a number of occasions where a majority of the temperature trend results indicate consistency, and some of the differences are even understandable.

[132] Seasonal analyses are not numerous below the mesopause, mainly because dividing the data reduces the statistical confidence of the derived trends. While Keckhut et al. [1999] found marginally significant changes with season for the tropical and subtropical U.S. rocket stations in the lower mesosphere, middle- and high-latitude rocket series seem to yield some more significant trends when split into seasons [Kokin and Lysenko, 1994; Keckhut et al., 1995; Keckhut and Kadera, 1999]. The seasonal variation around or at the mesopause appears to be significant in long-term analysis and may explain some of the diverse results reported so far.

[133] The present status of mesospheric temperature trends based on the available measurements can be broadly described as follows:

1. Negative trends are recognized in the lower and middle mesosphere with amplitudes of a few degrees per decade. This is similar to the trends obtained with numerical simulations of the doubled-CO<sub>2</sub> scenario.

2. Apparent large cooling trends up to 8 K/decade or more in the upper mesosphere exist, mainly from rocketsondes where rocket sensors may involve significant uncertainties if not properly corrected.

3. A few results indicate no trend in temperature. However, as discussed in this article, such results are associated with local/regional effects or seasonal sampling at high latitude only, as also suggested by numerical model simulations.

#### 7.1.1. Lower and Middle Mesosphere (50–79 km)

[134] In tropical latitudes the recent study of *Keckhut et al.* [1999] gives a good view of observed trends in this region. Similar results are reported by *Beig and Fadvanis* [2001] for the equatorial region, using a multiple regression analysis. They are representative of most other trend studies of this atmospheric region. At midlatitudes the lower mesosphere shows a cooling trend of around 2 K per decade in several studies, but in the middle mesosphere, Russian rockets reveal a larger cooling (~7 K/decade) than the Haute Provence lidar. In the middle mesosphere of the polar regions, two studies reveal opposite results. Russian data show large cooling, which increases with altitude, while *Lübken* [2000, 2001] found essentially a zero trend in summer.

#### 7.1.2. Mesopause Region (80–100 km)

[135] For the mesopause region, there are a growing number of results centered on or consistent with zero temperature trends. However, a few sites report negative trends, as large as –7 to –10 K/decade, at least in some limited height range, but neither these nor the zero trends are qualitatively inconsistent with a “thermal shrinking” of the upper atmosphere as a consequence of the greenhouse effect. On the other hand, significant positive trends that would contradict such a possibility have not been reported from sufficiently long data series. The results of only one study (which is from an indirect technique), that of the centroid height of the atmospheric sodium layer, appear to be contrary to the possibility of such thermal shrinking. The most reliable data sets show no significant trend, with an uncertainty of at least 2 K/decade. Still, the number and size of available data sets is sufficient neither to permit generalizing the observed trends for the entire globe with full confidence nor to safely discriminate against decadal variations of other origin. Many new data sets will become available and grow in size so that these limitations will probably be overcome in the future.

#### 7.2. Summary of Model Results

[136] Development of sophisticated models suitable for investigation and interpretation of the long-term trends in the MLT region is currently at its initial stage.

An ideal model for the MLT region should be a three-dimensional one with a vertical domain from the surface up to, at least, the turbopause level (~120 km) and should have a realistic radiative scheme and interactive chemistry module. To understand observed trends and examine future global variability, such a model has to be run in a transient mode with inclusion of both solar variability and increase of the major greenhouse gases, such as CO<sub>2</sub>, CH<sub>4</sub>, CFCs, and N<sub>2</sub>O. Unfortunately, none of the existing models satisfy all of these conditions, and no such simulations have been done to date. However, a useful step in this direction has been made during the last 10–15 years. Simulations with the TIME-GCM showed that the combined effect of the increase in the major greenhouse gases nearly doubles the thermal response in comparison to the case when only the CO<sub>2</sub> effect is considered. Results from the CMAM illustrate the importance of including the change in surface conditions in climate simulation for the polar mesospheric regions. *Akmaev and Fomichev* [1998] found that the presence of tides can noticeably modify the atmospheric response in the vicinity of the mesopause.

[137] Although most of the existing studies of MLT region trends have considered only the doubled-CO<sub>2</sub> scenario and did not have a troposphere component, they have shown reasonably good qualitative and, for some height regions, quantitative agreement with observations. Qualitatively, this includes both vertical and latitudinal structures of the thermal response in the MLT. In the vertical the response maximizes near the stratopause, gradually decreases in the upper mesosphere, and increases again in the thermosphere. The latitudinal structure of the response shows an increase of cooling toward both poles in the middle mesosphere and a decrease toward the summer pole in the upper mesosphere. Quantitatively, the simulated cooling trend in the middle mesosphere produced only by CO<sub>2</sub> increase is usually below the observed level. However, including other greenhouse gases and taking into account a “thermal shrinking” of the upper atmosphere results in a cooling of a few degrees per decade, a number which is close to the lower limit of the observed trend. In the mesopause region (80–100 km) the model simulations have produced trends usually below 1 K/decade, apparently below the natural atmospheric variability and consistent with most observations in this region.

## 8. OUTLOOK

### 8.1. General Recommendations

[138] As mentioned in section 1, the present effort is aimed at fulfilling the first objective of the MTTA, to make available a consolidated review of mesospheric temperature trends and to outline the current status by synthesizing the major published results on both observations and modeling. This has been achieved in this paper. However, the next step should be devoted to

rigorous data analysis with a common statistical model for detailed temperature trend assessment for the MLT region. This should be the immediate priority. As is evident in this report, development of sophisticated models suitable for investigation and interpretation of the long-term trends in the MLT region is currently at its initial stage. An ideal model for the MLT region should be a three-dimensional one with a vertical domain from the surface up to  $\sim 120$  km, with a realistic radiative scheme and an interactive chemistry module. To understand observed trends and examine future global variability, such a model has to be run in a transient mode with the inclusion of both solar variability and an increase of the major greenhouse gases. This should be attempted in the future. Some other important points are outlined below:

1. In a practical way, for instruments dedicated for long-term operation over several decades it is virtually impossible to maintain the instrument unchanged, and data discontinuities can be induced in many ways. We can qualify a series as “quasi-homogeneous” when induced changes are negligible compared to the expected climatic changes. Limited instrumental changes are required, and it is most important that instrument modifications be thoroughly documented. This information, known as metadata, is crucial for long-term monitoring. If instrumental changes that are expected to impact on the absolute value of a measurement have been reported and well identified in time, there is a good possibility for taking into account their effects in trend estimates.

2. The use of a common statistical model to uniformly remove episodic and periodic signals from all data sets would greatly enhance comparability. However, the various forcings are neither all clearly identified nor well known. This is relatively more difficult in polar regions where, in addition to the well-known UV solar flux effects, particle fluxes from the Sun and space may have some effect. Forcing may also come from below through the vertical propagation of waves.

3. We need to emphasize the need for multiple observation techniques at a given location. This is the only way in which systematic errors can really be assessed. In addition, overlap between measurement techniques when technology changes is essential. Overlap is essential to understanding differences between measurement systems and algorithms.

4. It is found that systematic observations of the temperature of the mesosphere-thermosphere region are relatively less robust and shorter in length than for the stratosphere. The effort in terms of needed observations, while general, should emphasize tropical sites for the mesopause-thermosphere and high latitudes for the mesosphere. However, probing the mesosphere and thermosphere requires a high rate of measurement because of the large natural daily variability.

5. Considering the different nature of instrumental changes and taking advantage of the nonsimultaneous instrumental changes of ground-based instruments, it will be

valuable, for global trend estimates in the mesosphere, to compare ground-based and satellite measurements at several sites. This will make it possible to investigate drift in satellite measurements and the continuity between successive satellites. However, temporal coincidences and/or possible tidal adjustments need to be addressed to be able to separate the effects of instrument changes. With such continuous global data sets, different methods for deriving trends may be tested and applied. Unfortunately, at least for the mesopause region, very few satellites suitable for this task have been launched to date.

6. The observations at the altitude of the OH emission in general do not cover long time spans (a considerable number of data sets commence only in the 1990s), but they do cover a larger number of sites compared with other observations of this region. They provide a unique opportunity for separating a number of effects, necessary for the correct detection of trends. On the other hand, sodium lidar observation, which can provide exact altitude information between 80 and 105 km, can be used to determine the altitude dependence of trends. Unfortunately, at this point, only one station has temperature measurements exceeding 11 years.

7. *Shepherd et al.* [1997] have pointed out the usefulness of airglow brightness observations for trend detection, and this needs to be followed up. However, as things stand, only the very long term Russian results for the OH bands reported by *Semenov et al.* [2002] and the recent results for OH and O<sub>2</sub> reported by *Reisin and Scheer* [2002] are available for this purpose. Both agree in signaling positive intensity trends.

8. Solar cycle variations and the process(es) by which they occur need to be better understood. Some researchers report a significant solar cycle variation, and others do not. It is important to search for solar cycle variations in a consistent manner. The observation of *Bittner et al.* [2000] that OH temperatures at Wuppertal are negatively correlated with solar activity indices for periods of  $< 10$  days and are positively correlated for periods of  $> 30$  days may provide some insight into possible processes. Given the short interval over which detailed OH temperatures have been measured at some sites, separating out any possible solar cycle influence is vital before realistic long-term trends can be determined.

9. Long-term seasonal behavior needs to be addressed to better understand the feedback to the general radiative cooling.

10. Wave activity is expected to change because of global mesospheric cooling. Numerical simulation studies are required to characterize and quantify those changes that can be observed with instruments that monitor temperature fluctuations.

## 8.2. Future Studies

[139] The recently launched Thermosphere-Ionosphere-Mesosphere Energetics and Dynamics (TIMED) mission offers a new opportunity in measurements for trend detection. In particular, the Sounding of the At-

mosphere using Broadband Emission Radiometry (SABER) experiment [e.g., *Mlynczak*, 1997] measures the fundamental infrared emissions by which the mesosphere and thermosphere cool, namely, the 15- $\mu\text{m}$  band of carbon dioxide and the 5.3- $\mu\text{m}$  band of nitric oxide. In particular, radiation in the 5.3- $\mu\text{m}$  nitric oxide band is the primary radiative cooling mechanism for the atmosphere above 120 km. Owing to the weak line nature of this transition the rate of energy loss is readily determined by a simple geometric inversion of the measured limb radiance [e.g., *Mlynczak*, 2002]. This measurement of energy loss and cooling, because it is directly indicative of the thermodynamic processes involved, may show trends more readily and sooner than other parameters.

[140] The model studies described above have been motivated by the realization that global change is not confined to the lower atmosphere but that the consequences of human activities may be more global and extend into the upper atmosphere and even affect plasma processes that couple the solar wind to the Earth's upper atmosphere. Indeed, the application of current, well-tested models of the upper atmosphere suggests that significant changes to the present-day structure of the atmosphere above  $\sim 50$  km will occur by the middle of the 21st century. A change in species and temperature structure should also have an effect on the ion composition of the ionospheric regions. Even though the atmospheric models that predict these global mean changes are quite sophisticated, there are still many uncertainties concerning the chemistry, reaction rates, and various atmospheric processes, such as turbulence and energy transport by gravity and planetary waves, suggesting caution in evaluating the magnitude of the predicted changes in chemical structure in response to atmospheric cooling. In addition to the changes in thermal and compositional structure on a global mean basis, there are also variations in the latitudinal distribution of heat and momentum sources that alter the mean meridional and global circulation patterns from present-day conditions. More attention needs to be given to the necessity of an accurate representation of the troposphere in the model simulations. There are many changes that could occur in the troposphere that could influence the mesosphere via changes in gravity wave propagation, tides, etc. For example, if under global warming conditions cloudiness were to change, we could see a change in the radiative heating of the troposphere and hence wave propagation and tides. The studies conducted so far are only suggestive of possible changes, and there is an important need for further investigations. This also means we must continue model development using coupled models of the Earth's atmosphere, ionosphere, and magnetosphere to evaluate the entire atmospheric readjustment to global change induced by human activity. Studies of the possible effects of global change on the upper atmosphere are in their infancy, and a number of important questions emerge:

1. How will gravity, tidal, and planetary wave propagation characteristics change in response to an altered atmospheric structure?
2. How will energy, mass, and momentum exchange rates between atmospheric regions change in response to increased  $\text{CO}_2$  cooling and a contracted upper atmosphere?
3. Will present-day solar-terrestrial couplings be altered by changed upper atmosphere and ionosphere structures?
4. Will new upper atmosphere chemical and physical processes become important as a result of an altered atmospheric structure (e.g., heterogeneous chemistry was found to be important for understanding changes in the Antarctic ozone hole)?
5. Will an altered upper atmosphere structure have an important feedback on the troposphere and weather systems?
6. How will current-day technological systems be affected because of a changed upper atmosphere environment?
7. How has the actual mesosphere temperature structure changed in the past, and how is it expected to change in the future?
8. Can present models completely explain these temperature changes?

[141] These questions, which are only a few of the many that emerge from the realization that the present-day atmospheric structure may be changing, suggest opportunities for future research into global change in the upper atmosphere.

[142] **ACKNOWLEDGMENTS.** This work initially started by the MTTA (Mesospheric Temperature Trend Assessment) panel of IAGA working group II.F, as the first goal in their overall objectives and many of the inferences are drawn here from the first MTTA executive summary. We thank J. Lastovicka for facilitating and being supportive of this work as chair of WG-II.F. We are thankful to three anonymous reviewers and Kendal McGuffie, editor responsible for this paper, for their useful suggestions and constructive criticisms, which have improved the quality of this paper.

[143] Kendall McGuffie, the Editor responsible for this paper, thanks two technical reviewers and one cross-disciplinary reviewer.

## REFERENCES

- Aikin, A. C., M. L. Chanin, J. Nash, and D. J. Kendig, Temperature trends in the lower mesosphere, *Geophys. Res. Lett.*, **18**, 416–419, 1991.
- Akmaev, R. A., Modeling the cooling due to  $\text{CO}_2$  increases in the mesosphere and lower thermosphere, *Phys. Chem. Earth*, **27**, 521–528, 2002.
- Akmaev, R. A., and V. I. Fomichev, Cooling of the mesosphere and lower thermosphere due to doubling of  $\text{CO}_2$ , *Ann. Geophys.*, **16**, 1501–1512, 1998.
- Akmaev, R. A., and V. I. Fomichev, A model estimate of cooling in the mesosphere and lower thermosphere due to  $\text{CO}_2$  increase over the last 3–4 decades, *Geophys. Res. Lett.*,

- 27, 2113–2116, 2000.
- Akmaev, R. A., V. I. Fomichev, N. M. Gavrilov, and G. M. Shved, Simulation of the zonal mean climatology of the middle atmosphere with a three-dimensional spectral model for solstice and equinox conditions, *J. Atmos. Terr. Phys.*, *54*, 119–128, 1992.
- Akmaev, R. A., J. M. Forbes, and M. E. Hagan, Simulation of tides with a spectral mesosphere/lower thermosphere model, *Geophys. Res. Lett.*, *23*, 2173–2176, 1996.
- Akmaev, R. A., V. A. Yudin, and D. A. Ortland, SMLTM simulations of the diurnal tide: Comparison with UARS observations, *Ann. Geophys.*, *15*, 1187–1197, 1997.
- Angell, J. K., Rocketsonde evidence for a stratospheric temperature decrease in the western hemisphere during 1973–85, *Mon. Weather Rev.*, *115*, 2569–2577, 1987.
- Angell, J. K., Stratospheric temperature change as a function of height and sunspot number density during 1972–89 based on rocketsonde and radiosonde data, *J. Clim.*, *4*, 1170–1180, 1991.
- Baker, D. J., A. T. Stair, Rocket measurements of the altitude distribution of the hydroxyl airglow, *Phys. Scr.*, *37*, 611–622, 1988.
- Batista, P. P., H. Takahashi, and B. R. Clemesha, Solar cycle and the QBO effect on the mesospheric temperature and nightglow emissions at a low latitude station, *Adv. Space Res.*, *14*(9), 221–224, 1994.
- Beig, G., The relative importance of solar activity and anthropogenic influences on the ion composition, temperature, and associated neutrals of the middle atmosphere, *J. Geophys. Res.*, *105*, 19,841–19,856, 2000a.
- Beig, G., Long-term forcing of greenhouse gases and natural events on atmospheric chemical composition and thermal structure, in *Long Term Changes and Trends in the Atmosphere*, vol. I, edited by G. Beig, New Age Int., pp. 88–114, New Delhi, 2000b.
- Beig, G., Overview of the mesospheric temperature trend and factors of uncertainty, *Phys. Chem. Earth*, *27*, 509–519, 2002.
- Beig, G., and S. Fadnavis, In search of greenhouse signals in the equatorial middle atmosphere, *Geophys. Res. Lett.*, *28*, 4603–4606, 2001.
- Beig, G., and A. P. Mitra, Atmospheric and ionospheric response to trace gas perturbations through the ice age to the next century in the middle atmosphere, part I—Chemical composition and thermal structure, *J. Atmos. Sol. Terr. Phys.*, *59*, 1245–1259, 1997.
- Berger, U., and M. Dameris, Cooling of the upper atmosphere due to CO<sub>2</sub> increases: “A model study,” *Ann. Geophys.*, *11*, 809–819, 1993.
- Bittner, M., D. Offermann, and H.-H. Graef, Mesopause temperature variability above a midlatitude station in Europe, *J. Geophys. Res.*, *105*, 2045–2058, 2000.
- Bittner, M., D. Offermann, H.-H. Graef, M. Donner, and K. Hamilton, An 18-year time series of OH rotational temperatures and middle atmosphere decadal variations, *J. Atmos. Sol. Terr. Phys.*, *64*, 1147–1166, 2002.
- Boer, G. J., G. Flato, M. C. Reader, and D. Ramsden, A transient climate change simulation with greenhouse gas and aerosol forcing: Experimental design and comparison with the instrumental record for the twentieth century, *Clim. Dyn.*, *16*, 405–425, 2000.
- Brasseur, G., The response of the middle atmosphere to long-term and short-term solar variability: A two-dimensional model, *J. Geophys. Res.*, *98*, 23,079–23,090, 1993.
- Brasseur, G., and D. Offermann, Recombination of atomic oxygen near the mesopause: Interpretation of rocket data, *J. Geophys. Res.*, *91*, 10,818–10,824, 1986.
- Brasseur, G., and S. Solomon, *Aeronomy of the Middle Atmosphere*, 2nd ed., D. Reidel, Norwell Mass., 1986.
- Bremer, J., Long-term trends in the meso- and thermosphere, *Adv. Space Res.*, *20*(11), 2075–2083, 1997.
- Bremer, J., Trends in the ionospheric E and F-regions over Europe, *Ann. Geophys.*, *16*, 986–996, 1998.
- Bremer, J., and U. Berger, Mesospheric temperature trends derived from ground-based LF phase-height observations at mid-latitudes: Comparison with model simulations, *J. Atmos. Sol. Terr. Phys.*, *64*, 805–816, 2002.
- Bruhl, C., and P. J. Crutzen, Scenarios of possible changes in atmospheric temperatures and ozone concentrations due to man’s activities, estimated with a one-dimensional coupled photochemical climate model, *Clim. Dyn.*, *2*, 173–203, 1988.
- Burns, G. B., W. J. R. French, P. A. Greet, F. A. Phillips, P. F. B. Williams, K. Finlayson, and G. Klich, Seasonal variations and inter-year trends in seven years of hydroxyl airglow rotational temperature at Davis station (69°S, 78°E), Antarctica, *J. Atmos. Sol. Terr. Phys.*, *64*, 1167–1174, 2002.
- Burton, S. P., and L. W. Thomason, SAGE II contribution to mesospheric temperature trend assessment 1. Present status and issues, *Tech. Rep. II-F*, Joint Working Group LT-TIME “Long-Term Trends in the Ionosphere, Thermosphere and Mesosphere” of IAGA and ICMA, Pune, India, 2002.
- Chanin, M.-L., Long-term trend in the middle atmosphere temperature, in *Role of the Stratosphere in Global Change*, edited by M.-L. Chanin, *NATO ASI Ser., Ser. I*, vol. 8, pp. 301–317, Springer-Verlag, New York, 1993.
- Chanin, M.-L., P. Keckhut, A. Hauchecorne, and K. Labitzke, The solar activity—Q.B.O. effect in the lower thermosphere, *Ann. Geophys.*, *7*, 463–470, 1989.
- Chen, L., J. London, and G. Brasseur, Middle atmospheric ozone and temperature responses to solar irradiance variations over 27-day periods, *J. Geophys. Res.*, *102*, 29,957–29,979, 1997.
- Clancy, R. T., and D. W. Rusch, Climatology and trends of mesospheric temperatures (58–90 km) based on 1982–1986 SME limb scattering profiles, *J. Geophys. Res.*, *94*, 3377–3393, 1989.
- Clancy, R. T., W. R. David, and M. T. Callan, Temperature minima in the average thermal structure of the middle mesosphere (70–80 km) from analysis of 40- to 92-km SME global temperature profiles, *J. Geophys. Res.*, *99*, 19,001–19,020, 1994.
- Clemesha, B. R., D. M. Simonich, and P. P. Batista, A long-term trend in the height of the atmospheric sodium layer: Possible evidence for global change, *Geophys. Res. Lett.*, *19*, 457–460, 1992.
- Clemesha, B. R., P. P. Batista, and D. M. Simonich, Long-term and solar cycle changes in the atmospheric sodium layer, *J. Atmos. Sol. Terr. Phys.*, *13*, 1673–1678, 1997.
- Clemesha, B. R., P. P. Batista, and D. M. Simonich, Comment on “In search of greenhouse signals in the equatorial middle atmosphere” by Gufran Beig and S. Fadnavis, *Geophys. Res. Lett.*, *29*(16), 1810, doi:10.1029/2002GL015097, 2002.
- Crutzen, P. J., Energy conversions and mean vertical motions in the high latitude summer mesosphere and lower thermosphere, in *Mesospheric Models and Related Experiments*, edited by G. Fiocco, pp. 78–88, D. Reidel, Norwell, Mass., 1971.
- Danilov, A. D., Long-term changes of the mesosphere and lower thermosphere temperature and composition, *Adv. Space Res.*, *20*, 2137–2147, 1997.
- de Grandpré, J., S. R. Beagley, V. I. Fomichev, E. Griffioen, J. C. McConnell, A. S. Medvedev, and T. G. Shepherd, Ozone climatology using interactive chemistry: Results from the Canadian middle atmosphere model, *J. Geophys. Res.*, *105*, 26,475–26,491, 2000.
- Dickinson, R. E., E. C. Ridley, and R. G. Roble, A three-

- dimensional general circulation model of the thermosphere, *J. Geophys. Res.*, *86*, 1499–1512, 1981.
- Dickinson, R. E., E. C. Ridley, and R. G. Roble, Thermospheric general circulation with coupled dynamics and composition, *J. Atmos. Sci.*, *41*, 205–219, 1984.
- Donnelly, R. F., Solar UV spectral irradiance variations, *J. Geomagn. Geoelectr.*, *43*, 835–842, 1991.
- Dunkerton, T. J., D. P. Delisi, and M. P. Baldwin, Middle atmosphere cooling trend in historical rocketsonde data, *Geophys. Res. Lett.*, *25*, 3371–3374, 1998.
- Ebel, A., Contributions of gravity waves to the momentum, heat and turbulent energy budget of the upper mesosphere and lower thermosphere, *J. Atmos. Terr. Phys.*, *46*, 727–737, 1984.
- Ejiri, M. K., K. Shiokawa, T. Ogawa, M. Kubota, T. Nakamura, and T. Tsuda, Dual-site imaging observations of small-scale wave structures through OH and OI nightglow emissions, *Geophys. Res. Lett.*, *29*(10), 1445, doi:10.1029/2001GL014257, 2002.
- Espy, P. J., and J. Stegman, Trends and variability of mesospheric temperature at high-latitudes, *Phys. Chem. Earth*, *27*, 543–553, 2002.
- Fels, S. B., J. D. Mahilman, M. D. Schwarzkopf, and R. W. Sinclair, Stratospheric sensitivity to perturbations in ozone and carbon dioxide: Radiative and dynamical response, *J. Atmos. Sci.*, *37*, 2265–2297, 1980.
- Fishkova, L. M., *The Night Airglow of the Earth Mid-Latitude Upper Atmosphere*, p. 59, Metsniereba, Tbilisi, 1983.
- Fishkova, L. M., N. M. Martsvaladze, and N. N. Shefov, Long-term variations of the sodium emission of the nocturnal upper atmosphere (in Russian), *Geomagn. Aeron.*, *41*, 528–531, 2001.
- Fomichev, V. I., J.-P. Blanchet, and D. S. Turner, Matrix parameterization of the 15  $\mu\text{m}$  CO<sub>2</sub> band cooling in the middle and upper atmosphere for variable CO<sub>2</sub> concentration, *J. Geophys. Res.*, *103*, 11,505–11,528, 1998.
- Fomichev, V. I., W. E. Ward, S. R. Beagley, C. McLandress, J. C. McConnell, N. A. McFarlane, and T. G. Shepherd, Extended Canadian middle atmosphere model: Zonal-mean climatology and physical parameterizations, *J. Geophys. Res.*, *107*(D10), 4087, doi:10.1029/2001JD000479, 2002.
- Forbes, J. M., Atmospheric tides: 2. The solar and lunar semi-diurnal components, *J. Geophys. Res.*, *87*, 5241–5252, 1982.
- Frederick, J. E., Measurement requirements for the detection of ozone trends, in *Ozone Correlative Measurements Workshop, NASA Conf. Publ.*, 2362, B1–B19, 1984.
- French, W. J. R., Hydroxyl airglow temperatures above Davis Station, Antarctica, Ph.D. thesis, Univ. of Tasmania, Hobart, 2002.
- French, W. J. R., G. B. Burns, K. Finlayson, P. A. Greet, R. P. Lowe, and P. F. B. Williams, Hydroxyl (6-2) airglow emission intensity ratios for rotational temperature determination, *Ann. Geophys.*, *18*, 1293–1303, 2000.
- Gadsden, M., A secular change in noctilucent cloud occurrence, *J. Atmos. Terr. Phys.*, *52*, 247–251, 1990.
- Gadsden, M., The secular changes in noctilucent cloud occurrence: Study of a 31-year sequence to clarify the causes, *Adv. Space Res.*, *20*(11), 2097–2100, 1997.
- Gadsden, M., The north-west Europe data on noctilucent clouds: A survey, *J. Atmos. Sol. Terr. Phys.*, *60*, 1163–1174, 1998.
- Garcia, R. R., and S. Solomon, The effect of breaking gravity waves on the dynamics and chemical composition of the mesosphere and lower thermosphere, *J. Geophys. Res.*, *90*, 3850–3868, 1985.
- Gardner, C. S., and W. Yang, Measurements of the dynamical cooling rate associated with the vertical transport of heat by dissipating gravity waves in the mesopause region at the Starfire Optical Range, New Mexico, *J. Geophys. Res.*, *103*, 16,909–16,927, 1998.
- Gavrilov, N. M., S. Fukao, and T. Nakamura, Peculiarities of interannual changes in the mean wind and gravity wave characteristics in the mesosphere over Shigaraki, Japan, *Geophys. Res. Lett.*, *26*, 2457–2460, 1999.
- Gavrilov, N. M., S. Fukao, and T. Nakamura, Gravity wave intensity and momentum fluxes in the mesosphere over Shigaraki, Japan (35°N, 136°E) during 1986–1997, *Ann. Geophys.*, *18*, 834–843, 2000.
- Gavrilov, N. M., S. Fukao, T. Nakamura, C. Jacobi, D. Kürschner, A. H. Manson, and C. E. Meek, Comparative study of interannual changes of the mean winds and gravity wave activity in the middle atmosphere over Japan, central Europe and Canada, *J. Atmos. Sol. Terr. Phys.*, *64*, 1003–1010, 2002.
- Givishvili, G. V., L. N. Leshchenko, E. V. Lysenko, S. P. Perov, A. I. Semenov, N. P. Sergeenko, L. M. Fishkova, and N. N. Shefov, Long-term trends of some characteristics of the Earth's atmosphere: I. Experimental results, *Izv. Russ. Acad. Sci. Atmos. Oceanic Phys.*, Engl. Transl., *32*, 303–312, 1996.
- Golitsyn, G. S., A. I. Semenov, N. N. Shefov, L. M. Fishkova, E. V. Lysenko, and S. P. Perov, Long-term temperature trends in the middle and upper atmosphere, *Geophys. Res. Lett.*, *23*, 1741–1744, 1996.
- Golitsyn, G. S., A. I. Semenov, and N. N. Shefov, Seasonal variations of the long-term temperature trend in the mesopause region, *Geomagn. Aeron.*, *40*(2), 198–200, 2000.
- Greet, P. A., J. Innis, and P. L. Dyson, High-resolution Fabry-Perot observations of mesospheric OH (6-2) emissions, *Geophys. Res. Lett.*, *21*, 1153–1156, 1994.
- Greet, P. A., W. J. R. French, G. B. Burns, P. F. B. Williams, R. P. Lowe, and K. Finlayson, OH(6-2) spectra and rotational temperature measurements at Davis, Antarctica, *Ann. Geophys.*, *16*, 77–89, 1998.
- Groves, G. V., An empirical model for solar cycle changes in mesospheric structure at longitudes 44–77°E, *Planet. Space Sci.*, *34*, 1037–1041, 1986.
- Hagan, M. E., J. M. Forbes, and F. Vial, On modeling migrating solar tides, *Geophys. Res. Lett.*, *22*, 893–896, 1995.
- Hagan, M. E., M. D. Burrage, J. M. Forbes, J. Hackney, W. J. Randel, and X. Zhang, QBO effects on the diurnal tide in the upper atmosphere, *Earth Planets Space*, *51*, 571–578, 1999.
- Hauchecorne, A., and M.-L. Chanin, Density and temperature profiles obtained by lidar between 35 and 70 km, *Geophys. Res. Lett.*, *7*, 565–568, 1980.
- Hauchecorne, A., M.-L. Chanin, and P. Keckhut, Climatology and trends of the middle atmospheric temperature (33–87 km) as seen by Rayleigh lidar over the south of France, *J. Geophys. Res.*, *96*, 15,297–15,309, 1991.
- Haynes, P. M., C. J. Marks, M. E. McIntyre, T. G. Shepherd, and K. P. Shine, On the “downward control” by eddy-induced mean zonal forces, *J. Atmos. Sol. Terr. Phys.*, *48*, 651–678, 1991.
- Hernandez, G., and T. L. Killeen, Optical measurements of wind and kinetic temperatures in the upper atmosphere, *Adv. Space Res.*, *8*(N5–6), 149–312, 1988.
- Hines, C. O., Dynamical heating of the upper atmosphere, *J. Geophys. Res.*, *70*, 177–183, 1965.
- Hood, L. L., The solar cycle variation of total ozone: Dynamical forcing in the lower stratosphere, *J. Geophys. Res.*, *102*, 1355–1370, 1997.
- Hood, L. L., Z. Hauang, and S. W. Bougher, Mesospheric effects of solar ultraviolet variations: Further analysis of SME IR ozone and Nimbus 7 SAMS temperature data, *J. Geophys. Res.*, *96*, 12,989–13,002, 1991.

- Houghton, J. T., Absorption and emission by carbon-dioxide in the mesosphere, *Q. J. R. Meteorol. Soc.*, *96*, 767–770, 1970.
- Intergovernmental Panel on Climate Change, *Radiative Forcing of Climate and an Evaluation of the IPCC IS92 Emission Scenarios*, edited by J. T. Houghton et al., Cambridge Univ. Press, New York, 1995.
- Jacobi, C., and B.-R. Beckmann, On the connection between upper atmospheric dynamics and tropospheric parameters: Correlations between mesopause region winds and the North Atlantic Oscillation, *Clim. Change*, *43*(3), 629–643, 1999.
- Jacobi, C., and D. Kürschner, A possible connection of mid-latitude mesosphere/lower thermosphere zonal winds and the southern oscillation, *Phys. Chem. Earth*, *27*, 571–577, 2002.
- Jacobi, C., R. Schminder, and D. Kürschner, On the influence of the stratospheric quasi-biennial oscillation on the mesopause zonal wind over central Europe, *Meteorol. Z. N.F.*, *5*, 218–223, 1996.
- Johnson, J. K., and M. E. Gelman, Trends in the upper stratospheric temperature as observed by rocketsondes (1965–83), *Handb. MAP*, *18*, 24–27, 1985.
- Keating, G. M., M. C. Pitts, G. Brasseur, and A. de Rudder, Response of middle atmosphere to short-term solar ultraviolet variations: 1. Observations, *J. Geophys. Res.*, *92*, 889–902, 1987.
- Keckhut, P., and K. Kodera, Long-term changes of the upper stratosphere as seen by rocketsondes at Ryori (39°N, 141°E), *Ann. Geophys.*, *17*, 1210–1217, 1999.
- Keckhut, P., A. Hauchecorne, and M. L. Chanin, Midlatitude long-term variability of the atmosphere: Trends and cyclic and episodic changes, *J. Geophys. Res.*, *100*, 18,887–18,897, 1995.
- Keckhut, P. A., F. J. Schmidlin, A. Hauchecorne, and M. L. Chanin, Stratospheric and mesospheric cooling trend estimates from U.S. rocketsondes at low latitude stations (8°S – 34°N), taking into account instrumental changes and natural variability, *J. Atmos. Sol. Terr. Phys.*, *61*, 447–459, 1999.
- Keckhut, P., J. D. Wild, M. Gelman, A. J. Miller, and A. Hauchecorne, Investigations on long-term temperature changes in the upper stratosphere using lidar data and NCEP analyses, *J. Geophys. Res.*, *106*, 7937–7944, 2001.
- Kellog, W. W., Chemical heating above the mesopause in winter, *J. Meteorol.*, *18*, 373–381, 1961.
- Khvorostovskaya, L. E., I. Y. Potekhin, G. M. Shved, V. P. Ogibalov, and T. V. Usyukova, Measurement of rate constant for quenching CO<sub>2</sub> (010) by atomic oxygen at low temperatures: Re-assessment of cooling rate by the CO<sub>2</sub>, 15- $\mu$ m emission in the lower thermosphere, *Atmos. Oceanic Phys.*, in press, 2003.
- Kirkwood, S., and K. Stebel, Influence of planetary waves on noctilucent cloud occurrence over NW Europe, *J. Geophys. Res.*, *108*(D8), 8440, doi:10.1029/2002JD002356, 2003.
- Kokin, G. A., and E. V. Lysenko, On temperature trends of the atmosphere from rocket and radiosonde data, *J. Atmos. Terr. Phys.*, *56*, 1035–1040, 1994.
- Kokin, G. A., E. V. Lysenko, and S. K. Rosenfeld, Temperature change in the stratosphere and mesosphere during 1964–1988 based on rocket sounding data (in Russian), *Izv. Akad. Nauk. Phys. Atmos. Okeana*, *26*, 702–710, 1990.
- Komuro, H., Long-term cooling in the stratosphere observed by aerological rockets at Ryori, Japan, *J. Meteorol. Soc. Jpn.*, *68*, 1081–1082, 1989.
- Krassovsky, V. I., N. N. Shefov, and V. I. Yarin, Atlas of the airglow spectrum  $\lambda$  3000–12400 Å, *Planet. Space Sci.*, *9*, 883–915, 1962.
- Krassovsky, V. I., B. P. Potapov, A. I. Semenov, M. V. Shagaev, N. N. Shefov, V. G. Sobolev, and T. I. Toroshelidze, Inter-nal gravity waves near the mesopause and the hydroxyl emission, *Ann. Geophys.*, *13*, 347–356, 1977.
- Krueger, D. A., and C. Y. She, Observed “long-term” temperature change in a midlatitude mesopause region in response to external perturbation, *Earth Planets Space*, *51*, 809–814, 1999.
- Kubota, M., M. Ishii, K. Shiokawa, M. K. Ejiri, and T. Ogawa, Height measurements of nightglow structures observed by all-sky imagers, *Adv. Space Res.*, *24*, 593–596, 1999.
- Labitzke, K., and M. L. Chanin, Changes in the middle atmosphere in winter related to the 11 year solar cycle, *Ann. Geophys.*, *6*, 643–644, 1988.
- Labitzke, K., and M. P. McCormick, Stratospheric temperature increases due to Pinatubo aerosols, *Geophys. Res. Lett.*, *19*, 207–210, 1992.
- Langhoff, S. R., H.-J. Werner, and P. Rosmus, Theoretical transition probabilities for the OH Meinel system, *J. Mol. Spectrosc.*, *118*, 507–529, 1986.
- Lastovicka, J., Trends in planetary wave activity, *Stud. Geophys. Geod.*, *38*, 206–212, 1994.
- Lastovicka, J., D. Buresova, and J. Boska, Does the QBO and the Mt. Pinatubo volcanic eruption affect the gravity wave activity in the lower ionosphere?, *Stud. Geophys. Geod.*, *42*, 170–182, 1998.
- Leblanc, T., I. S. McDermid, P. Keckhut, A. Hauchecorne, C. Y. She, and D. A. Krueger, Temperature climatology of the middle atmosphere from long-term lidar measurements at middle and low latitudes, *J. Geophys. Res.*, *103*, 17,191–17,204, 1998.
- Lindzen, R. S., Turbulence and stress owing to gravity wave and tidal breakdown, *J. Geophys. Res.*, *86*, 9707–9714, 1981.
- Liu, H., M. E. Hagan, and R. G. Roble, Local mean state changes due to gravity wave breaking modulated by the diurnal tide, *J. Geophys. Res.*, *105*, 12,381–12,396, 2000.
- Lopez-Moreno, J. J., R. Rodrigo, F. Moreno, M. Lopez-Puertas, and A. Molina, Altitude distribution of vibrationally-excited states of atmospheric hydroxyl at levels v-2 to v-7, *Planet. Space Sci.*, *35*, 1029–1038, 1987.
- Lopez-Puertas, M., and F. W. Taylor, Carbon dioxide 4.3  $\mu$ m emission in the Earth’s atmosphere: A comparison between NIMBUS 7 SAMS measurements and non-LTE radiative transfer calculations, *J. Geophys. Res.*, *94*, 13,045–13,068, 1989.
- Lopez-Puertas, M., M. A. Lopez-Valverde, and F. W. Taylor, Studies of solar heating by CO<sub>2</sub> in the upper atmosphere using a non-LTE model and satellite data, *J. Atmos. Sci.*, *47*, 809–822, 1990.
- Lopez-Puertas, M., M. A. Lopez-Valverde, R. R. Garcia, and R. G. Roble, A review of CO<sub>2</sub> and CO abundances in the mesosphere, in *Atmospheric Science Across the Stratopause*, *Geophys. Monogr. Ser.*, vol. 123, edited by D. E. Siskind, S. D. Eckermann, and M. E. Summers, pp. 83–100, AGU, Washington, D. C., 2000.
- Lowe, R., Trend in the temperature of the mid latitude mesopause region, paper presented at First International Workshop on Long-Term Changes and Trends in the Atmosphere, Indian Inst. of Trop. Meteorol., Pune, India, 1999.
- Lowe, R. P., Long-term trends in the temperature of the mesopause region at mid-latitude as measured by the hydroxyl airglow, paper presented at the 276 WE-Heraeus-Seminar on Trends in the Upper Atmosphere, Wilhelm und Else Heraeus-Stift., Khlungsborn, Germany, 2002.
- Lowe, R. P., K. L. Gilbert, and D. N. Turnbull, High latitude summer observations of the hydroxyl airglow, *Planet. Space Sci.*, *39*, 1263–1270, 1991.
- Lowe, R. P., L. M. Leblanc, and K. L. Gilbert, WINDII/UARS observation of twilight behaviours of the hydroxyl airglow at mid-latitude equinox, *J. Atmos. Terr. Phys.*, *58*, 1863–1869, 1996.

- Lübken, F. J., Seasonal variation of turbulent energy dissipation rates at high latitudes as determined by in situ measurements of neutral density fluctuations, *J. Geophys. Res.*, *102*, 13,441–13,456, 1997.
- Lübken, F. J., Nearly zero temperature trend in the polar summer mesosphere, *Geophys. Res. Lett.*, *27*, 3603–3606, 2000.
- Lübken, F. J., No long term change of the thermal structure in the mesosphere at high latitudes during summer, *Adv. Space Res.*, *28*(7), 947–953, 2001.
- Lübken, F.-J., and U. von Zahn, Thermal structure of the mesopause region at polar latitudes, *J. Geophys. Res.*, *96*, 20,841–20,857, 1991.
- Lübken, F.-J., W. Hillert, G. Lehmacher, U. von Zahn, M. Bittner, D. Offermann, F. Schmidlin, A. Hauchecorne, M. Mourier, and P. Czechowsky, Intercomparison of density and temperature profiles obtained by lidar, ionization gauges, falling spheres, datasondes, and radiosondes during the DYANA campaign, *J. Atmos. Terr. Phys.*, *56*, 1969–1984, 1994.
- Lübken, F. J., K. H. Fricke, and M. Langer, Noctilucent clouds and the thermal structure near the Arctic mesopause in summer, *J. Geophys. Res.*, *101*, 9489–9508, 1996.
- McCormick, M. P., and R. E. Veiga, SAGE-II measurements of early Pinatubo aerosols, *Geophys. Res. Lett.*, *19*, 155–158, 1992.
- McLandress, C., G. G. Shepherd, B. H. Solheim, M. D. Burrage, P. B. Hays, and W. R. Skinner, Combined mesosphere/thermosphere winds using WINDII and HRDI data from the Upper Atmosphere Research Satellite, *J. Geophys. Res.*, *101*, 10,441–10,453, 1996.
- Meinel, A. B., OH emission band in the spectrum of the night sky, I, *Astrophys. J.*, *III*, 555–564, 1950.
- Melo, Stella, M. J., R. P. Lowe, and J. P. Russell, Double-peaked hydroxyl airglow profiles observed from WINDII/UARS, *J. Geophys. Res.*, *105*, 12,397–12,403, 2000.
- Meriwether, J. W., High latitude airglow observations of correlated short-term fluctuations in the hydroxyl Meinel 8-3 band intensity and rotational temperature, *Planet. Space Sci.*, *23*, 1211–1221, 1975.
- Mies, F. H., Calculated vibrational transition probabilities of OH ( $X^2A$ ), *J. Mol. Spectrosc.*, *53*, 150–180, 1974.
- Mlynczak, M. G., Energetics of the mesosphere and lower thermosphere and the SABER experiment, *Adv. Space Res.*, *20*, 1177–1183, 1997.
- Mlynczak, M. G., A contemporary assessment of the mesospheric energy budget, in *Atmospheric Science Across the Stratopause*, *Geophys. Monogr. Ser.*, vol. 123, edited by D. E. Siskind, S. D. Eckermann, and M. E. Summers, pp. 37–52, AGU, Washington, D. C., 2000.
- Mlynczak, M., A comparison of space-based energy budgets of the mesosphere and troposphere, *J. Atmos. Sol. Terr. Phys.*, *64*, 877–887, 2002.
- Mlynczak, M. G., and B. T. Marshall, A reexamination of the role of solar heating in the O<sub>2</sub> atmospheric and infrared atmospheric bands, *Geophys. Res. Lett.*, *23*, 657–660, 1996.
- Mlynczak, M. G., and S. Solomon, A detailed evaluation of the heating efficiency in the middle atmosphere, *J. Geophys. Res.*, *98*, 10,517–10,541, 1993.
- Mlynczak, M. G., C. J. Mertens, R. R. Garcia, and R. W. Portmann, A detailed evaluation of the stratospheric heat budget: 2. Global radiation balance and diabatic circulations, *J. Geophys. Res.*, *104*, 6039–6066, 1999.
- Mlynczak, M. G., R. Roble, R. Garcia, and M. Hagan, Solar energy deposition rates in the mesosphere derived from airglow observations: Implications for the ozone deficit problem, *J. Geophys. Res.*, *105*, 17,527–17,538, 2000.
- Mohanakumar, K., An investigation on the influence of solar cycle on mesospheric temperature, *Planet. Space Sci.*, *33*, 795–805, 1985.
- Mohanakumar, K., Solar activity forcing of the middle atmosphere, *Ann. Geophys.*, *13*, 879–885, 1995.
- Mulligan, F. J., D. F. Horgan, J. G. Galligan, and E. M. Griffin, Mesopause temperatures and integrated band brightness calculated from airglow OH emissions recorded at Maynooth (53.2°N, 6.4°W) during 1993, *J. Atmos. Terr. Phys.*, *57*, 1623–1637, 1995.
- Murgatroyd, R. J., and R. M. Goody, Sources and sinks of radiative energy from 30 to 90 km, *Q. J. R. Meteorol. Soc.*, *87*, 225–234, 1958.
- Myrabo, H. K., and O. E. Harang, Temperatures and tides in the high-latitude mesopause region as observed in the OH night airglow emissions, *J. Atmos. Terr. Phys.*, *50*, 739–748, 1988.
- Nash, J., Extension of explicit radiance observations by the stratospheric sounding unit into the lower stratosphere and lower mesosphere, *Q. J. R. Meteorol. Soc.*, *114*, 1153–1171, 1988.
- Nelson, D. D., Jr., A. Schiffman, D. J. Nesbitt, J. J. Orlando, and J. B. Burkholder, H + O<sub>3</sub> Fourier-transform infrared emission and laser absorption studies of OH( $X^2A$ ) radical: An experimental dipole moment function and state-to-state Einstein  $A$  coefficients, *J. Chem. Phys.*, *93*, 7003–7019, 1990.
- Nestorov, G., D. Pancheva, and A. D. Danilov, Climatic changes of the ionospheric radio wave absorption in the SW-region, *Geomagn. Aeron.*, *31*, 1070–1079, 1991.
- Nielsen, K. P., F. Sigernes, E. Raustein, and C. S. Deehr, The 20-year change of the Svalbard OH-temperatures, *Phys. Chem. Earth*, *27*, 555–561, 2002.
- Offermann, D., M. Donner, P. Knieling, K. Hamilton, A. Menzel, B. Naujokat, and P. Winkler, Indications of long-term changes in middle atmosphere transports, *Adv. Space Res.*, in press, 2003.
- Ogibalov, V. P., V. I. Fomichev, and A. A. Kutepov, Radiative heating effected by infrared CO<sub>2</sub> bands in the middle and upper atmosphere, *Atmos. Oceanic Phys.*, *36*, 454–464, 2000.
- Pendleton, W. R., P. J. Espy, and M. R. Hammond, Evidence for non-local-thermodynamic-equilibrium rotation in the OH nightglow, *J. Geophys. Res.*, *98*, 11,567–11,579, 1993.
- Perminov, V. I., and A. I. Semenov, Non-equilibrium rotational temperatures of the OH bands with high vibrational excitation, *Geomagn. Aeron.*, *32*, 175–178, 1992.
- Polyani, J., and J. J. Sloan, Detailed rate coefficients for the reactions  $H + O_3 \rightarrow OH(v',J') + O_2$  and  $H + NO_2 \rightarrow OH(v',J') + NO$ , *Int. J. Chem. Kinet.*, *1*, 51–60, 1975.
- Portmann, R. W., G. E. Thomas, S. Solomon, and R. R. Garcia, The importance of dynamical feedbacks on doubled CO<sub>2</sub>-induced changes in the thermal structure of the mesosphere, *Geophys. Res. Lett.*, *22*, 1733–1736, 1995.
- Ramaswamy, V., et al., Stratospheric temperature trends: Observations and model simulations, *Rev. Geophys.*, *39*, 71–122, 2001.
- Reisin, E. R., and J. Scheer, Searching for trends in mesopause region airglow intensities and temperatures at El Leoncito, *Phys. Chem. Earth*, *27*, 563–569, 2002.
- Remsberg, E. E., P. P. Bhatt, and L. E. Deaver, Seasonal and longer-term variations in middle atmosphere temperature from HALOE and UARS, *J. Geophys. Res.*, *107*(D19), 4411, doi: 10.1029/2001JD001366, 2002.
- Richmond, A. D., E. C. Ridley, and R. G. Roble, A thermosphere/ionosphere general circulation model with coupled electrodynamics, *Geophys. Res. Lett.*, *19*, 601–604, 1992.
- Rind, D., R. Suozzo, N. K. Balachandran, and P. Prather, Climate change and the middle atmosphere, 1. The doubled CO<sub>2</sub> climate, *J. Atmos. Sci.*, *47*, 475–494, 1990.
- Rind, D., N. K. Balachandran, and R. Suozzo, Climate change and the middle atmosphere. part II: The impact of volcanic

- aerosols, *J. Clim.*, 5, 189–208, 1992.
- Rishbeth, H., and R. G. Roble, Cooling of the upper atmosphere by enhanced greenhouse gases: Modelling the thermospheric and ionospheric effects, *Planet. Space Sci.*, 40, 1011–1026, 1992.
- Roble, R. G., Energetics of the mesosphere and thermosphere, in *The Upper Mesosphere and Lower Thermosphere: A Review of Experiment and Theory*, *Geophys. Monogr. Ser.*, vol. 87, edited by R. M. Johnson and T. L. Killeen, pp. 1–21, AGU, Washington, D. C., 1995.
- Roble, R. G., On the feasibility of developing a global atmospheric model extending from the ground to the exosphere, in *Atmospheric Science Across the Stratopause*, *Geophys. Monogr. Ser.*, vol. 123, edited by D. E. Siskind, S. D. Eckermann, and M. E. Summers, pp. 53–68, AGU, Washington, D. C., 2000.
- Roble, R. G., and R. E. Dickinson, How will changes in carbon dioxide and methane modify the mean structure of the mesosphere and thermosphere?, *Geophys. Res. Lett.*, 16, 1441–1444, 1989.
- Roble, R. G., and E. C. Ridley, A thermosphere-ionosphere-mesosphere-electrodynamics general circulation model (TIME-GCM): Equinox solar cycle minimum simulations (30–500 km), *Geophys. Res. Lett.*, 21, 417–420, 1994.
- Roble, R. G., E. C. Ridley, and R. E. Dickinson, On the global mean structure of the thermosphere, *J. Geophys. Res.*, 92, 8745–8758, 1987.
- Roble, R. G., E. C. Ridley, A. D. Richmond, and R. E. Dickinson, A coupled thermosphere/ionosphere general circulation model, *Geophys. Res. Lett.*, 15, 1325–1328, 1988.
- Rodgers, C. D., F. W. Taylor, A. H. Muggeridge, M. Lopez-Puertas, and M. A. Lopez-Valverde, Local thermodynamic equilibrium of carbon dioxide in the upper atmosphere, *Geophys. Res. Lett.*, 19, 589–592, 1992.
- Romejko, V. A., P. A. Dalin, and N. C. Pertsev, Forty years of noctilucent cloud observations near Moscow: Database and simple statistics, *J. Geophys. Res.*, 108(D8), 8443 doi: 10.1029/2002JD002364, 2003.
- Scheer, J., Programmable tilting filter spectrometer for studying gravity waves in the upper atmosphere, *Appl. Opt.*, 26, 3077–3082, 1987.
- Scheer, J., and E. R. Reisin, Unusually low airglow intensities in the Southern Hemisphere midlatitude mesopause region, *Earth Planets Space*, 52, 261–266, 2000.
- Schmidlin, F. J., The inflatable sphere: A technique for the accurate measurement of middle atmosphere temperatures, *J. Geophys. Res.*, 96, 22,673–22,682, 1991.
- Semenov, A. I., Long-term changes in the height profiles of ozone and atomic oxygen in the lower thermosphere (in Russian), *Geomag. Aeron.*, 37, 354–360, 1997.
- Semenov, A. I., Long-term temperature trends for different seasons by hydroxyl emission, *Phys. Chem. Earth, Part B, Hydrol. Oceans Atmos.*, 25, 525–529, 2000.
- Semenov, A. I., and N. N. Shefov, Empirical model of hydroxyl emission variations, *Int. J. Geomagn. Aeron.* 1, 229–242, 1999.
- Semenov, A. I., N. N. Shefov, E. V. Lysenko, G. V. Givishvili, and A. V. Tikhonov, The seasonal peculiarities of behavior of the long-term temperature trends in the middle atmosphere at the mid-latitudes, *Phys. Chem. Earth*, 27, 529–534, 2002.
- Serafimov, K., and M. Serafimova, Possible radioindications of anthropogenic influences on the mesosphere and lower thermosphere, *J. Atmos. Terr. Phys.*, 54, 847–850, 1992.
- She, C. Y., and D. A. Krueger, Impact of natural variability in the 11-year mesopause region temperature observation over Fort Collins, CO (41°N, 105°W), *Adv. Space Res.*, in press, 2003.
- She, C. Y., and R. P. Lowe, Seasonal temperature variation in the mesopause region at mid-latitude: Comparison of lidar and hydroxyl rotational temperatures based on WINDII/UARS OH height profiles, *J. Atmos. Sol. Terr. Phys.*, 60, 1573–1583, 1998.
- She, C. Y., J. R. Yu, H. Latifi, and R. E. Bills, High-spectral-resolution lidar for mesospheric sodium temperature measurements, *Appl. Opt.*, 31, 2095–2106, 1992.
- She, C. Y., S. W. Thiel, and D. A. Krueger, Observed episodic warming at 86 and 100 km between 1990 and 1997: Effects of Mount Pinatubo eruption, *Geophys. Res. Lett.*, 25, 497–500, 1998.
- She, C. Y., J. Sherman, J. D. Vance, T. Yuan, Z. Hu, B. P. Williams, K. Arnold, P. Acott, and D. A. Krueger, Evidence of solar cycle effect in the mesopause region: Observed temperatures in 1999 and 2000 at 98.5 km over Fort Collins, CO (41°N, 105°W), *J. Atmos. Sol. Terr. Phys.*, 64, 1651–1657, 2002.
- Shefov, N. N., Intensity and rotational temperature variations of hydroxyl emission in the night-glow, *Nature*, 218, 1238–1239, 1968.
- Shefov, N. N., Hydroxyl emission of the upper atmosphere-I. The behavior during a solar cycle, seasons and geomagnetic disturbances, *Planet. Space Sci.*, 17, 797–813, 1969.
- Shefov, N. N., Hydroxyl emission, *Ann. Geophys.*, 28, 137–173, 1972.
- Shefov, N. N., and N. A. Piterskaya, Spectral spatial and temporal characteristics of the background airglow, *Polyarn. Siyaniya Svechenie Nochnogo Neba*, 31, 23–27, 1984.
- Shepherd, G. G., N. J. Siddiqi, R. H. Wiens, and S. P. Zhang, Airglow measurements of possible changes in the ionosphere and middle atmosphere, *Adv. Space Res.*, 20, 2127–2135, 1997.
- Shepherd, M. G., B. Reid, S. P. Zhang, B. H. Solheim, G. G. Shepherd, V. B. Wickwar, and J. P. Herron, Retrieval and validation of mesospheric temperatures from the Wind Imaging Interferometer observations, *J. Geophys. Res.*, 106, 24,813–24,829, 2001.
- Shepherd, M. G., P. J. Espy, C. Y. She, W. Hocking, P. Keckhut, G. Gavriljeva, G. G. Shepherd, and B. Naujokat, Springtime transition in upper mesospheric temperature in the northern hemisphere, *J. Atmos. Sol. Terr. Phys.*, 64, 1183–1199, 2002a.
- Shepherd, M. G., Y. J. Rochon, and G. G. Shepherd, Longitudinal variability of mesospheric temperatures at middle and high latitudes—The WINDII perspective, paper presented at the WE-Heraeus-Seminar on Trends in the Upper Atmosphere, Wilhelm und Else Heraeus-Stift., Kühlungsborn, Germany, 2002b.
- Shved, G. M., Role of airglow in the cooling of the atmosphere near the mesopause, *Geomagn. Aeron.*, 3, 500–501, 1972.
- Shved, G. M., L. E. Khvorodtsovskaya, I. Yu. Potekhin, A. I. Demianikov, A. A. Kutepov, and V. I. Fomichev, Measurement of the quenching rate constant for collisions CO<sub>2</sub> (01<sup>0</sup>)-O: The importance of the rate constant for the thermal regime and radiation in the lower thermosphere, *Atmos. Ocean. Phys.*, 27, 431–437, 1991.
- Shved, G. M., A. A. Kutepov, and V. P. Oglibalov, Non-local thermodynamic equilibrium in CO<sub>2</sub> in the middle atmosphere. I. Input data and populations of the v<sub>3</sub> mode manifold states, *J. Atmos. Sol. Terr. Phys.*, 60, 289–314, 1998.
- Sigernes, F., N. Shumilov, C. S. Deehr, K. P. Nielsen, T. Svenøe, and O. Havnes, Hydroxyl rotational temperature record from the auroral station in Adventdalen, Svalbard (78°N, 15°E), *J. Geophys. Res.*, 108(A9), 1342, doi:10.1029/2001JA009023, 2003.
- Sprenger, K., K. M. Greisiger, and R. Schindler, Evidence of quasi-biennial wind oscillation in the mid-latitude lower thermosphere, obtained from ionospheric drift measure-

- ments in the LF range, *J. Atmos. Terr. Phys.*, *37*, 1391–1393, 1975.
- Stroud, W. G., W. Nordberg, W. R. Bandeen, F. L. Bartman, and P. Titus, Rocket-grenade measurements of temperatures and winds in the mesosphere over Churchill, Canada, *J. Geophys. Res.*, *65*, 2307–2323, 1960.
- Takahashi, H., B. R. Clemesha, and P. P. Batista, Predominant semi-annual oscillation of upper mesospheric airglow intensities and temperatures in the equatorial region, *J. Atmos. Terr. Phys.*, *57*, 407–414, 1995.
- Takahashi, H., P. P. Batista, R. A. Buriti, D. Gobbi, T. Nakamura, T. Tsuda, and S. Fukao, Simultaneous measurements of airglow OH emission and meteor wind by a scanning photometer and the MU radar, *J. Atmos. Sol. Terr. Phys.*, *60*, 1649–1668, 1998.
- Taubenheim, J., G. V. Cossart, and G. Entzian, Evidence of CO<sub>2</sub>-induced progressive cooling of the middle atmosphere derived from radio observations, *Adv. Space Res.*, *10*(10), 171–174, 1990.
- Taubenheim, J., K. Berendorf, W. Krüger, and G. Entzian, Height dependence of long-term trends in the middle atmosphere, paper presented at the EGS XIX General Assembly, Eur. Geophys. Soc., Grenoble, 1994.
- Taubenheim, J., G. Entzian, and K. Berendorf, Long-term decrease of mesospheric temperature, 1963 through 1995, inferred from radio wave reflection heights, *Adv. Space Res.*, *20*, 2059–2063, 1997.
- Thomas, G. E., Global change in the mesosphere-lower thermosphere region: Has it already arrived?, *J. Atmos. Terr. Phys.*, *58*, 1629–1656, 1996.
- Thomas, G. E., J. J. Olivero, E. J. Jensen, W. Schröder, and O. B. Toon, Relation between increasing methane and the presence of ice clouds at the mesopause, *Nature*, *338*, 490–492, 1989.
- Thomas, G. E., and J. Olivero, Noctilucent clouds as possible indicators of global change in the mesosphere, *Adv. Space Res.*, *28*(7), 937–946, 2001.
- Thulasiraman, S., and J. B. Nee, Further evidence of a two-level mesopause and its variations from UARS high-resolution Doppler imager temperature data, *J. Geophys. Res.*, *107*(D18), 4355, doi:10.1029/2000JD000118, 2002.
- Turnbull, D. N., and R. P. Lowe, Vibrational population distribution in the hydroxyl night airglow, *Can. J. Phys.*, *61*, 244–250, 1983.
- Turnbull, D. N., and R. P. Lowe, An empirical determination of the dipole moment function of OH(X<sup>2</sup>A), *J. Chem. Phys.*, *91*, 2763–2767, 1988.
- Turnbull, D. N., and R. P. Lowe, New hydroxyl transition probabilities and their importance in airglow studies, *Planet. Space Sci.*, *37*, 723–738, 1989.
- Weatherhead, E. C., A. J. Stevermer, and B. E. Schwartz, Detecting environmental changes and trend, *Phys. Chem. Earth*, *27*, 399–403, 2002.
- Weill, G., and J. Christophe, Long term variations of OH nightglow emission—Relation to stratospheric humidity?, in *Dynamical and Chemical Coupling*, pp. 85–90, D. Reidel, Norwell, Mass., 1977.
- Woods, T. N., and G. J. Rottman, Solar Lyman-alpha irradiance measurements during two solar cycles, *J. Geophys. Res.*, *102*, 8769–8779, 1997.
- World Meteorological Organization (WMO), Scientific Assessment of Ozone Depletion: 1994, *Rep. 37*, Global Ozone Res. and Monit. Proj., Geneva, 1995.
- World Meteorological Organization (WMO), Scientific Assessment of Ozone Depletion: 1998, *Rep. 44*, Global Ozone Res. and Monit. Proj., Geneva, 1999.
- Wuebbles, D. J., D. E. Kinnison, K. E. Grant, and J. Lean, The effect of solar flux variations and trace gas emissions on recent trends in stratospheric ozone and temperature, *J. Geomagn. Geoelectr.*, *43*, 709–718, 1991.
- G. Beig and S. Fadnavis, Indian Institute of Tropical Meteorology, Pune-411008, India. (beig@tropmet.res.in; suvarna@tropmet.res.in)
- J. Bremer and F. J. Lübken, Leibniz-Institute of Atmospheric Physics, Kühlunborn 18255, Germany. (bremer@iap-kborn.de; luebken@iap-kborn.de)
- B. R. Clemesha, Instituto Nacional de Pesquisas Espaciais, CP 515, S. J. dos Campos, 12245-970, SP, Brazil. (clem@laser.inpe.br)
- V. I. Fomichev, Department of Earth and Atmospheric Science, York University, Toronto, Ontario, Canada M3J 1P3. (victor@nimbus.yorku.ca)
- W. J. R. French, Atmospheric and Space Physics Group, Australian Antarctic Division, Kingston, Tasmania 7050, Australia. (john.french@aad.gov.au)
- P. Keckhut, Service d'Aéronomie, Institut Pierre Simon Laplace (IPSL), Verrieres-Le-Buisson 91 371, Cedex, France. (keckhut@aerov.jussieu.fr)
- R. P. Lowe, Centre for Research in Earth and Space Technology, University of Western Ontario, London, Ontario, Canada M7A 3K7. (lowe@physics.uwo.ca)
- M. G. Mlynczak, Radiation and Aerosol Branch, NASA Langley Research Center, Hampton, VA 23681, USA. (m.g.mlynczak@larc.nasa.gov)
- D. Offermann, Physics Department, University of Wuppertal, Wuppertal 42097, Germany. (offer@uni-wuppertal.de)
- E. E. Remsberg, Atmospheric Sciences Research, NASA Langley Research Center, Hampton, VA 23681, USA. (e.e.remsberg@larc.nasa.gov)
- R. G. Roble, High Altitude Observatory, National Center for Atmospheric Research, Boulder, CO 80307, USA. (roble@hoa.ucar.edu)
- J. Scheer, Instituto de Astronomía y Física del Espacio, Ciudad Universitaria, Buenos Aires 1428, Argentina. (jorgen@caerce.edu.ar)
- A. I. Semenov, Obukhov Institute of Atmospheric Physics, RAS, Moscow, 109017, Russia. (meso@omega.ifaran.ru)
- C. Y. She, Physics Department, Colorado State University, Fort Collins, CO 80523-1785, USA. (joeshe@lamar.colostate.edu)
- M. G. Shepherd, Centre for Research in Earth and Space Science, York University, Toronto, Ontario, M3J 1P3, Canada. (marianna@stpl.cress.yorku.ca)
- F. Sigernes, University Courses on Svalbard, Longyearbyen N-9171, Norway. (Fred.Sigernes@unis.no)
- J. Stegman, Meteorologiska Institutionen, Stockholms Universitet, S-106 91 Stockholm, Sweden. (jacek@misu.su.se)